Generation and characterization of mice lacking the α_4 nicotinic receptor subunit

A thesis submitted to the faculty of Medicine, Monash

University for the degree of Doctor of Philosophy

By

SHELLEY ROSS

Department of Medicine

Monash Medical Centre

Clayton, Victoria, 3168

Australia

January, 2001

Table Of Contents

Chapter Three: Generation Of An α_4 Nicotinic Acetylcholine Receptor Subunit

Chapter Four: Phenotypic Characterization Of An α_4 Nicotinic Acetylcholine

i

SUMMARY

Neuronal nicotinic acetylcholine receptors (nAChR) are present in high abundance in the nervous system and there are a large number of subunits expressed in the brain which combine to form multimeric functional receptors. The $\alpha_4\beta_2$ receptor subtype is involved in the mediation of a number of physiological processes, including anxiety, cognition and antinociception. However, because of the complex pharmacology of nicotinic receptors and the lack of receptor subtype specific ligands the functional role of these receptors *in vivo* remains unclear.

An α_4 nAChR subunit knockout line was generated to define the behavioural role of this subunit. Mutant (Mt) mice were normal in size, fertility and home cage behaviour and did not exhibit spontaneous epileptic seizures. *In situ* hybridization analyses using α_4 specific probes validated the knockout paradigm and ligand autoradiography confirmed the lack of high affinity binding to radiolabeled nicotine, cytisine and epibatidine in certain brain regions, although binding to a number of discrete nuclei remained. $[^{125}I]$-α-bungarotoxin (α-Bgt) high affinity binding was normal in Mt mice and there was no up-regulation of mRNA for α_3, α_5, α_6, α_7, β_2, β_3 and β_4 subunits.

Spontaneous unconditioned motor behaviour revealed an ethogram characterized by significant increases in several topographies of exploratory behaviour in Mt mice compared to Wt mice over the course of habituation to a novel environment. The behaviour of Mt mice in the elevated plus-maze assay was consistent with increased basal levels of anxiety-like behaviour. In response to nicotine, Wt mice exhibited early reductions in a number of behavioural topographies, under both unhabituated and habituated conditions; conversely, heightened levels of behavioural topographies in Mt

mice were reduced by nicotine, specifically in the late phase of the unhabituated condition. This study confirms the pivotal role played by the α_4 nAChR subunit in the modulation of a number of constituents of the normal mouse ethogram and in anxiety-like behaviour.

The genetic basis of a number of epilepsy syndromes has been identified but the precise mechanism whereby mutations produce seizures is unknown. Three mutations in the α_4 subunit have been identified in Autosomal Dominant Nocturnal Frontal Lobe Epilepsy (ADNFLE). *In vitro* studies have suggested an alteration of receptor function resulting in decreased flow. The response of the α_4 nAChR subunit knockout mice to the proconvulsants, pentylenetetrazol (PTZ) and kainic acid (KA) was investigated. Mt mice had a greater number of PTZ-induced major motor seizures and seizure related deaths. They also had a shorter latency to PTZ-induced hypokinetic and partial motor seizures. In contrast, KA significantly reduced the amount of normal behaviour in Mt mice and there was a significant increase in the number of hypokinetic and minor motor seizures. These results therefore suggest that the likely *in vivo* consequence of the missense mutation in ADNFLE is a global reduction in the function of the nAChR.

As part of my thesis, I also generated a knockin construct containing the missense mutation found in patients with ADNFLE. Analysis of this mutant model will help to address more directly the question of the relationship between the serine to phenylalanine mutation and enhanced seizure activity. The specific mutation was introduced into α_4 nAChR gene using site-directed mutagenesis and subsequently targeted into the J1 and R1 ES cell lines. The presence of the mutation in the genomic DNA of the targeted ES cells was confirmed using a PCR assay with primers designed

to detect the mutant allele. The blastocyst injections for the R1 targeted ES cell clones were undertaken in collaboration with Dr Peter G. Noakes in the Department of Physiology and Pharmacology at the University of Queensland. Currently, nine high grade male chimeras have been generated and matings are in progress to test for germline transmission.

DECLARATION

The work described in this thesis was performed by the author, except where acknowledged and has not been previously submitted for any other degree or diploma. The thesis is less than 100,000 words in length.

v

vi

PUBLICATIONS

Abstracts from Scientific Presentations

Shelley Ross and John Drago (1998) *An animal model for familial nocturnal frontal lobe epilepsy.* Abstract. Epilepsy Genetics Workshop, Marysville.

Ross, SA, Wong JYF, Clifford JJ, Waddington JL, Kola, T and Drago J (2000). *Phenotypic characterization of an α_4 neuronal nicotinic acetylcholine receptor subunit knockout mouse.* Australian Neuroscience Society, oral 6-5, 20th Annual meeting, 30/1/2000 to 2/2/2000.

Publications

J. Apostolopoulos, **S. Ross**, P. Davenport, A. Mutsukawa, M. Yoshinaga, P.J. Tipping (1996) *Interleukin-1 receptor antagonist: Characterization of its gene expression in rabbit tissues and large-scale expression in eucaryotic cells using a baculovirus expression system.* **Journal of Immunological Methods**, (199) 27-35.
Not relevant to this thesis.

Shelley A. Ross, John Y.F. Wong, Jeremiah J. Clifford, Anthony Kinsella, Jim S. Massalas, Malcolm K. Horne, Ingrid Scheffer, Ismail Kola, John L. Waddington, Samuel F. Berkovic and John Drago (2000) *Phenotypic characterization of an α_4 neuronal nicotinic acetylcholine receptor subunit knockout mouse.* **Journal of Neuroscience**, 20 (17) 6431-6441.

R.E. Ryan, **S.A. Ross**, J. Drago and R.E. Loiacono (2001). *Dose-related neuroprotective effects of chronic nicotine in 6-hydroxydopamine treated rats and loss*

of neuroprotection in α_4 *nicotinic receptor subunit knockout.* **British Journal of Pharmacology,** 132 (8):1650-1656.

Shelley A. Ross[Ψ], John.Y.F. Wong[Ψ], Jim S Massalas, Malcolm Clark, Malcolm.K. Horne, Samuel F. Berkovic and John Drago (2001) *Proconvulsant-induced seizures in* α_4 *neuronal nicotinic acetylcholine receptor subunit knockout mice.* [Ψ] Both authors made equal contribution.

ABBREVIATIONS

BIM	blastocyst injection media
bp	base pairs
Ci	Curie
DMEM	Dulbecco's modification Eagle medium
EB	electroporation buffer
EF	embryonic fibroblasts
ES	embryonic stem
FCS	fetal calf serum
2X FM	2X freezing medium
H/H	Hanks/Hepes
Hz	heterozygous
Kb	kilo base
LB	Luria-Bertani
LIF	Leukemia inhibitory factor
Mt	Mutant
%MPE	percentage of maximum possible effect
nAChR	nicotinic acetylcholine receptor
NEO	neomycin phosphotransferase resistance gene
PBS	phosphate buffer saline
PCR	polymerase chain reaction
SEM	standard error of mean
SM	suspension medium
TBE	Tris / borate / EDTA
TE	Tris / EDTA
Wt	wildtype

CHAPTER ONE

LITERATURE REVIEW

1.1 Introduction

Neuronal nicotinic acetylcholine receptors (nAChR) are important because of their postulated involvement in a number of physiological processes. However, because of a lack of receptor subtype specific ligands, it has proven difficult to validate the *in vivo* function of these receptors and hence their exact role remains speculative. Nicotinic agonists which bind to these receptors are known to have an effect on anxiety (Brioni et al., 1993; Gilbert et al., 1989; Pomerleau, 1986), cognition (Brioni et al., 1997) and antinociception (Damaj et al., 1998; Marubio et al., 1999; Tripathi et al., 1982). It has been suggested that nicotinic agonists are neuroprotective in Parkinson's disease and can improve cognitive function in Alzheimers's disease (Decker et al., 1995; Giacobini, 1991). Furthermore, three mutations in the α_4 nAChR subunit have been identified in Autosomal Dominant Nocturnal Frontal Lobe Epilepsy (ADNFLE) (Hirose et al., 1999; Steinlein et al., 1997; Steinlein et al., 1995). Several areas of research are starting to provide a clearer insight into the physiological function of nAChRs and their role in a number of disease states. This review outlines the structure, purification, distribution and pharmacology of nAChRs and also their contribution to normal behaviour and various disease states.

1.2   Structure Of Neuronal Nicotinic Acetylcholine Receptors

Acetylcholine receptors (AChR) found in the skeletal neuromuscular junction and in the *Torpedo* ray electric organ have been extensively studied. The *Torpedo* ray electric organ provides an exceptionally rich source of cholinergic synapses and possesses a receptor that closely resembles the AChR found in the neuromuscular junction (Nickel and Potter, 1973). Advances in molecular biology, immunology and neurophysiological

techniques have enabled growth in our knowledge of muscle AChRs paving the way for the study of neuronal nAChRs.

The first neuronal nAChR subunit was isolated using sequences based on proteins homologous to the α subunit of the mouse muscle AChR (Boulter et al., 1986). Since this first report, a gene family encoding 11 homologous genes of neuronal nAChR subunits have been identified and characterized in brain and pathways involved in sensory processing of the rat, chick and human (Boulter et al., 1987; Deneris et al., 1991; Nef et al., 1988; Papke, 1993; Sargent, 1993). The α subunit gene of muscle AChR is designated α_1 and the eight neuronal nAChR α subunits are designated α_2 to α_9. The neuronal non-α subunits are referred to as β subunits, of which there are three: β_2, β_3 and β_4 (Duvoisin et al., 1989; Elgoyhen et al., 1994; Wada et al., 1988). The α neuronal nAChR subunits possess adjacent cysteines analogous to cysteines 192 to193 of α subunit of the muscle AChR, which are believed to be intimately involved in acetylcholine binding. The β subunits do not have these cysteines, however they too contribute to the binding site and are important in conferring the pharmacological properties to the receptor complex (Luetje and Patrick, 1991).

Early studies suggested that the functional neuronal nAChR is a heteropentamer made up by assembly of α and β subunits, with a putative $2\alpha{:}3\beta$ subunit stoichiometry (Anand et al., 1991; Cooper et al., 1991). However a number of recent studies have revealed the existence of triplet receptors, which contain more than one α or β subunit (Conroy et al., 1992; Groot-Kormelink et al., 1998; Ramirez-Latorre et al., 1996; Wang et al., 1996).

Nicotinic receptors are members of a gene superfamily of ligand-gated ion channels (Galzi et al., 1991), which also includes glycine, γ-aminobutyric acid (GABA$_A$) and 5-hydroxytryptamine (5-HT$_3$) receptors (Betz, 1990). This superfamily represents a large, evolutionary related group of intrinsic membrane proteins that form multi-subunit complexes, whereby the binding of an agonist results in the transient opening of the channel.

Amino acid sequences of various cloned nAChR subunits appear to be strongly homologous and show similar hydrophobicity profiles (Galzi et al., 1991). The genes encode for a large hydrophilic amino-terminal domain (210 to 220 amino acids), a compact hydrophobic region (70 amino acids), which is subdivided into 3 segments of 19 to 28 uncharged amino acids (M1, M2 and M3), a short hydrophilic cytoplasmic domain of variable length and a carboxyl-terminal segment (20 hydrophobic amino acids) (M4) (Figure 1.1). The hydrophilic amino-terminal domain carries the acetylcholine binding site and faces the synaptic cleft (Devillers-Thiery et al., 1993). The subunits are arranged quasi-symmetrically around a central channel and experiments using site-directed mutagenesis have provided evidence that the M2 membrane-spanning region lines the ion channel pore of the receptor (Akabas et al., 1994; Leonard et al., 1988).
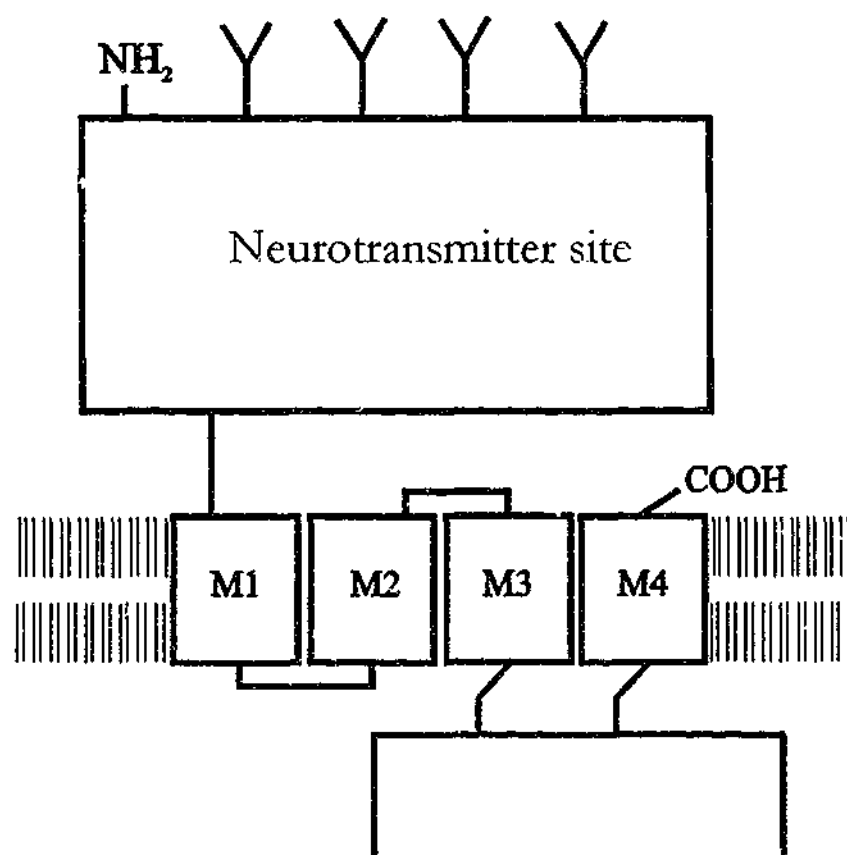
Figure 1.1 Model of transmembrane organization of the nAChR subunits based on the hydrophobicity profile of the primary amino acid sequence (adapted from Galzi et al., 1991).

1.3 Purification Of Neuronal Nicotinic Acetylcholine Receptors

Alpha-bungarotoxin (α-bgt) is a toxin isolated from the venom of Bungarus multicincyus (Hanley et al., 1977) and has proved to be an invaluable tool for characterizing nAChRs. Alpha-bgt was used to purify the first neuronal nAChRs, which appeared to be composed of two or more subunits (Betz et al., 1982; Conti-Tronconi et al., 1985; Whiting and Lindstrom, 1987). These studies revealed that there was a population of nAChRs that bind α-bgt (α-bgt-sensitive receptors) and a

population of nAChRs that do not bind α-bgt (α-bgt-insensitive receptors). The majority of α-bgt sensitive nAChRs in chicken brain were found to contain α_7 and/or α_8 subunits (Schoepfer et al., 1990).

In subsequent experiments using monoclonal antibody affinity chromatography, α-bgt-insensitive receptors were purified from chicken, (Whiting and Lindstrom, 1986), rat (Whiting and Lindstrom, 1987; Whiting et al., 1987) and human brain (Whiting and Lindstrom, 1988). This receptor species displayed high affinity for [^{3}H]-nicotine and other nicotinic agonists, but not for α-bgt. Immunoprecipitation experiments revealed that greater than 90% of the high-affinity [^{3}H]-nicotine binding sites in rat brain can be precipitated by antibodies raised against the α_4 and β_2 subunits (Flores et al., 1992). In summary, α-bgt binds α-bgt-sensitive α_7 and α_8 subunits, whereas nicotine binds α-bgt-insensitive α_4 and β_2 subunits.

1.4 Distribution Of Neuronal Nicotinic Acetylcholine Receptors

Radioligand techniques and immunolabelling, in combination with *in situ* hybridization studies have allowed a detailed characterization of the distribution of nAChRs in the central nervous system (CNS). In general, these complementary approaches have yielded similar results, in respect to relative protein levels and gene expression profiles.

1.5 Radioligand Techniques

The radioligands, [^{3}H]-acetylcholine (ACh), [^{3}H]-nicotine and ^{125}I-α-bgt have been commonly used to label putative nAChRs in the mammalian CNS (Clarke et al., 1985; Marks et al., 1986; Pauly et al., 1989). These studies have generated detailed maps of [^{3}H]-ACh, [^{3}H]-nicotine and ^{125}I-α-bgt labelling, revealing virtually identical binding

sites for [³H]-ACh and [³H]-nicotine, which were distinct from ^{125}I-α-bgt binding sites. High affinity [³H]-ACh and [³H]-nicotine binding was detected in the interpeduncular nucleus, thalamus, medial habenula and the superior colliculus. Moderate labelling was noted in the presubiculum, cerebral cortex, parts of the striatum and also in the dorsal tegmental nuclei. Weak labelling was noted in the cerebellum and a small amount of labelling was detected in the hypothalamus and hippocampus. In contrast, high affinity ^{125}I-α-bgt binding was detected in the cerebral cortex, hypothalamus, hippocampus, superior colliculus and inferior colliculus (Clarke et al., 1985).

The nAChR ligands, [³H]-epibatidine and [³H]-cytisine have also been mapped showing a similar binding profile to [³H]-ACh and [³H]-nicotine (Happe et al., 1994; Perry and Kellar, 1995). [³H]-Epibatidine binding differed from the general pattern seen with the other ligands in that [³H]-epibatidine binding selectively labelled the optic nerve and the fasciculus retroflexus nerve tracts, which are pathways involved in sensory processing (Perry and Kellar, 1995). Neuronal bungarotoxin (n-bgt) is a snake venom neurotoxin which selectively blocks nicotinic receptors in many peripheral and central neuronal preparations (Loring et al., 1989). ^{125}I-n-bgt binding has also been mapped, revealing a unique pattern, which was distinct from the other ligands (Schulz et al., 1991). High affinity ^{125}I-n-bgt binding was detected in the fasciculus retroflexus, medial habenula, inferior colliculus, superior colliculus, dorsal and ventral lateral geniculate nuclei and the interpeduncular nucleus (Schulz et al., 1991).

1.6   Immunolabelling

Studies using immunolabelling with a range of antibodies have provided information on the topographical distribution of neuronal nAChR protein subunits at the cellular and

subcellular levels and has been used to map neuronal nAChRs in the brain (Deutch et al., 1987; Mason, 1985; Schroder et al., 1989; Swanson et al., 1987). Immunolabelling in the rat, using the anti-β_2 nAChR subunit specific monoclonal antibodies revealed a pattern similar to that seen for [^{3}H]-ACh and [^{3}H]-nicotine binding (Deutch et al., 1987; Swanson et al., 1987). This correlated well with *in situ* localization of β_2 transcript in neuronal cell bodies (Hill et al., 1993). The pattern of α_4 immunoreactivity paralleled that of [^{3}H]-nicotine binding sites (Arroyo-Jim nez et al., 1999; Rogers et al., 1998) and also matched the distribution of the α_4 subunit transcripts observed previously by *in situ* hybridization (Wada et al., 1989). In chicken and rat brain, anti-α_7 immunostaining was shown to be consistent with radioligand studies of ^{125}I-α-bgt binding (Britto et al., 1992; Dominguez del Toro et al., 1994) and showed a similar pattern to that observed with *in situ* localization of the α_7 subunit.

1.7   *In Situ* Hybridization

In situ hybridization has been used to characterize the regional distribution of the various subunit mRNAs in the CNS and peripheral nervous system (PNS) in rat (Deneris et al., 1989; Dineley-Miller and Patrick, 1992; Elgoyhen et al., 1994; Le Novere et al., 1996; Seguela et al., 1993; Wada et al., 1989) (Table 1.1) and mice (Marks et al., 1992). (Refer to Chapter Four, Figures 4.1 and 4.2 for in situ hybridization images of the different nicotinic receptor subunits in mice). These experiments have demonstrated that the nAChR subunit distribution is strikingly different between subunits. The α_2 mRNA has a limited expression pattern, with moderate signal detected in certain interpeduncular nuclei, low levels detected in the dorsal tegmental nucleus, inferior colliculus, hippocampus and subiculum and very low levels in the cortex (Wada et al., 1989). The α_3 mRNA was most intensely expressed in

the medial habenula, entorhinal cortex, thalamus, hypothalamus and in the autonomic ganglia. A moderate to low signal was detected in the hippocampus, cortex and ventral tegmental area and a weak signal detected in the cerebellum (Wada et al., 1989). The α_4 mRNA is more widespread, with high levels detected in the thalamus, medial habenula, substantia nigra pars compacta, ventral tegmental area, piriform cortex, endopiriform nucleus, amygdala, subicular complex, septum, interpeduncular nucleus, somatosensory areas and the caudal linear raphe and moderate levels detected in the cerebral cortex and the hypothalamus. Expression was also detected in the cochlear and vestibular ganglia (Wada et al., 1989). The α_5 subunit mRNA has been detected in a small number of localized sites, with high levels detected in the subiculum, parasubiculum, substantia nigra pars compacta, ventral tegmental area, interpeduncular nucleus and in the brainstem. Lower levels were detected in the isocortex and olfactory cortex (Wada et al., 1990). The α_6 mRNA was found to be expressed at high levels in the substantia nigra pars compacta and ventral tegmental area and at low levels in the thalamus, medial habenula and the interpeduncular nucleus (Le Novere et al., 1996). Transcripts encoding the α_7 subunits were found in discrete neuronal populations throughout the rat brain. High levels were detected in the hippocampus, hypothalamus, amygdala, olfactory areas, endopiriform nucleus, claustrum and in the isocortex. Moderate levels were detected in the medial habenula, interpeduncular nucleus and in the superior and inferior colliculi. In the brainstem, moderate signals were expressed in the central gray, dorsal and median raphe nuclei, tegmental nuclei and in the lateral lemniscus. A weak signal was detected in the cerebellum (Seguela et al., 1993). The α_8 subunit has been identified in the chick brain (Keyser et al., 1993), however, the presence of this subunit in rodent or human brain is yet to be determined. The α_9 subunit has a very limited expression in the CNS, with signal only detected in the pars

tuberalis of the adenohypophysis. Signal was detected in the nasal epithelium, the hair cells of the cochlear and the skeletal muscle of the tongue (Elgoyhen et al., 1994).

The β_2 subunit mRNA was detected extensively in the nervous system, with highest levels in the thalamus, substantia nigra pars compacta, ventral tegmental area, piriform cortex, entorhinal cortex and in the somatosensory and motor areas of the brainstem and moderate levels in the medial habenula (Wada et al., 1989). In contrast, the β_3 subunit mRNA has a more limited expression pattern, with high levels detected in the medial habenula, substantia nigra pars compacta, ventral tegmental area, thalamus and the mesencephalic nucleus of the trigeminal (Deneris et al., 1989). The β_4 subunit was detected in a diverse number of loci, with the medial habenula having the greatest signal. Moderate signal was detected in the cortex, olfactory regions, hippocampus, hypothalamus, locus ceruleus, the pontine nucleus and the cerebellum. There was also isolated but intense hybridization in the interpeduncular nucleus and motor nucleus of the trigeminal nerve (Dineley-Miller and Patrick, 1992).

In summary, it appears that the α_4, β_2 and α_7 subunits are most widely expressed in the rodent brain, whereas α_2, α_3, α_5, α_6, β_3 and β_4 subunits have a somewhat limited expression, restricted to discrete cholinoceptive pathways. In addition, it was demonstrated that more than one type of α subunit was expressed in some brain regions such as the thalamus, which contains both α_3 and α_4 mRNAs (Wada et al., 1989). The distribution of α_4 mRNA was found to overlap with the β_2 mRNA (Wada et al., 1988), which showed a similar distribution pattern to $[^3H]$-nicotine autoradiographic studies. As expected, $[^3H]$-nicotine binding was absent from β_2 nAChR subunit gene knockout mice (Picciotto et al., 1995), confirming the selectivity of this ligand for the β_2 subunit.

The distribution of the α_7 gene transcript in rodent brain overlaps the pattern of ^{125}I-α-bgt binding sites (Clarke et al., 1985), suggesting that the α_7 subunit comprises most, if not all of the high affinity [^{125}I]-α-bgt-sensitive nAChRs. As expected [^{125}I]-α-bgt binding was absent in the α_7 knockout mice (Orr-Urtreger et al., 1997), confirming the selectivity of this ligand for the α_7 subunit.

Table 2.1. Expression of nAChR subunits in the rat brain.

Brain structure	α2 [1]	α3 [2]	α4 [3]	α5 [4]	α6 [5]	α7 [6]	α9 [7]	β2 [8]	β3 [9]	β4 [10]
Adenohyophysis							(++)			
Amygdala			(+++)			(+++)				
Autonomic ganglia		(+++)								
Brainstem			(+++)			(+++)		(+++)		
Caudal linear raphe			(+++)							
Cerebellum		(+)				(+)				(++)
Cochlear			(+)							
Coclear							(+++)			
Cortex	(+)	(++)	(++)	(+++)		(+++)		(+++)		(++)
Dorsal tegmental nuclei	(+)									
Endoporiform			(+++)			(+++)				
Enthorhinal cortex		(+++)						(+++)		
Hippocampus	(++)	(+)				(+++)				(++)
Hypothalamus	(+++)	(+++)	(++)			(+++)				(++)
Inferior colliculus	(+)					(++)				
Interpeduncular nucleus	(++)		(+++)	(+++)	(++)	(++)				(++)
Medial habenula		(+++)	(+++)		(++)	(++)		(++)	(+++)	(+++)
Nasal epithelium							(+++)			
Para/presubiculum				(+++)						
Pifiform cortex			(+++)					(+++)		
Septum			(+++)							
Skeletal muscle of the tongue							(+++)			

	1	2	3	4	5	6	7	8	9	10	11
Somatosensory areas			(+++)	(+++)					(+++)		
Subiculum	(+)		(+++)	(+++)							
Substantia nigra pars compacta			(+++)	(+++)	(+++)				(+++)	(+++)	
Superior colliculus						(++)					
Thalamus		(+++)	(+++)		(+)				(+++)	(+++)	
Vental tegmental area		(++)	(+++)	(+++)	(+++)				(+++)	(+++)	
Vestibular ganglia			(++)								

[1] Wada et al., 1988; Wada et al., 1989

[2] Wada et al., 1988; Wada et al., 1989

[3] Wada et al., 1988; Wada et al., 1989

[4] Wada et al., 1990

[5] Le Novere et al., 1996

[6] Seguela et al., 1993

[7] Elgoyhen et al., 1994

[8] Wada et al., 1988; Wada et al., 1989

[9] Deneris et al., 1989

[10] Dineley-Miller and Patrick, 1992

1.8   Heterologous Expression And Functional Diversity Of Neuronal Nicotinic Acetylcholine Receptor Genes

Experiments using *Xenopus* oocytes have provided a powerful means of assessing the neurophysiology of ligand-gated ion channels. *Xenopus* oocytes are large cells that translate exogenous mRNA into functional proteins. In the case of nAChR subunits, mRNA is injected and a functional protein is synthesized and incorporated into the membrane. This preparation can then be used to study the cell as a whole or to analyse the behaviour of single receptor molecules. The net effect of all the channels in a cell can be determined by intracellular recordings, whereas the behaviour of single receptor molecules can be determined by patch-clamping techniques. Heterologous expression studies in *Xenopus* oocytes have provided valuable insight into the pharmacology and electrophysiology of the nAChRs.

Although the nAChR subunits are highly homologous at the protein level, a large number of studies using recombinant rat and chicken nAChRs expressed in *Xenopus* oocytes have revealed a substantial degree of diversity among the different subunit combinations (Luetje and Patrick, 1991). This diversity of pharmacological properties may account for the diversity of these receptors observed *in vivo*. Expression of pairwise combinations of rat α and β subunits and α subunits alone in oocytes has demonstrated the existence of two subfamilies of neuronal nicotinic receptors. The first subfamily consists of α_2, α_3 and α_4 subunits that can combine with either β_2 or β_4 subunits to form functionally distinct heterooligomeric receptors (Boulter et al., 1987; Couturier et al., 1990b; Wada et al., 1988). The second subfamily consists of the α_7, α_8 and α_9 subunits that can form functional ligand-gated ion channels when expressed in the oocyte in the absence of β subunits, presumably functioning as homooligomeric

receptors (Elgoyhen et al., 1994). These homooligomeric receptors are pharmacologically different from the heterooligomeric receptors, in that the α_7, α_8 and α_9 homooligomeric receptors are blocked by α-bgt, whereas none of the α/β heterooligomeric receptors are sensitive to this toxin (Corringer et al., 1995; Couturier et al., 1990b; Sargent, 1993).

Because of the failed attempts of expressing the α_6, α_5 and β_3 subunits in *Xenopus* oocytes, these subunits have long been considered orphans, incapable of forming functional receptors either alone or with any other available subunits (McGehee and Role, 1995). However, recent studies have demonstrated that these subunits can assemble with other subunits to form functional receptors, thus adding further members to the large family of nAChRs. Early studies of heterologous expression in oocytes of the rat α_5 subunit, either alone or in combination with β_2, β_3 or β_4 subunit failed to yield functional receptors (McGehee and Role, 1995). However, a recent study has shown that the chick α_6 subunit can form functional α/β pair receptors if expressed with β_2 or β_4 subunits in a human cell line (Fucile et al., 1998). This study also demonstrated that the α_6 subunit can coassemble with $\alpha_3\beta_4$ combinations, forming unique functional triplet receptors consisting of two different α subunits and a β subunit. Sequence comparison indicates that α_6 subunit belongs to the subfamily of nAChRs insensitive to α-bgt (Le Novere and Changeux, 1995).

Earlier studies suggested that the α_5 subunit does not form functional α/β pair receptors when expressed in combination with another β subunit (Deneris et al., 1991; McGehee and Role, 1995). However, recent studies have demonstrated that like the α_6 subunit,

the chick α_5 subunit participates in nAChRs expressed in oocytes and primary neurons when coexpressed with another α and β subunit. The α_5 subunit has been shown to coassemble with $\alpha_4\beta_2$ combinations (Ramirez-Latorre et al., 1996) and also with $\alpha_3\beta_2$ and $\alpha_3\beta_4$ combinations (Wang et al., 1996), forming unique functional triplet receptors, which are pharmacologically distinct from the α/β pair receptors, $\alpha_4\beta_2$, $\alpha_3\beta_2$ and $\alpha_3\beta_4$.

The β_3 subunit is also incapable of forming α/β pair receptors when expressed with a single α subunit (McGehee and Role, 1995). The β_3 subunit has 80% amino acid homology to the α_5 subunit (Le Novere and Changeux, 1995) and a recent study has concluded that, like the α_5 subunit, the β_3 subunit can form functional receptors only when coexpressed with both α and β subunits. The β_3 subunit was shown to be incorporated into an $\alpha_3\beta_4$ receptor complex, forming a functional $\alpha_3\beta_4\beta_3$ nicotinic receptor (Groot-Kormelink et al., 1998). In a recent study, the transfection of a mammalian cell line with α_4, β_2, β_3 and β_4 subunits showed that all four subunits coassembled in these cells forming a functional receptor consisting of four receptor subunits (Forsayeth and Kobrin, 1997).

Expression studies in *Xenopus* oocytes have confirmed that both α and β subunits contribute to the binding properties of nAChRs (Luetje and Patrick, 1991). The presence of the α_2, α_3 or α_4 subunits has an effect on the responsiveness of the receptor to nicotine, which is a weak agonist on the $\alpha_3\beta_2$ receptor subtype, but a potent agonist on the $\alpha_2\beta_2$ and $\alpha_4\beta_2$ receptor subtypes. The presence of the β_2 or β_4 subunit determines the responsiveness of the receptor to the nicotinic agonist, cytisine. Receptors containing the β_2 subunit have a low affinity for cytisine, whereas β_4-containing subunit

combinations have a high affinity for cytisine (Luetje and Patrick, 1991). The $\alpha_3\beta_2$ subtype is sensitive to n-bgt, whereas the $\alpha_3\beta_4$ subtype is insensitive to n-bgt (Duvoisin et al., 1989; Luetje and Patrick, 1991), indicating that the β subunit is responsible for determining the sensitivity of nAChRs to n-bgt.

With the recent discoveries of functional triplet receptors and receptors consisting of four subunits, it is clear that the potential for functional diversity is very broad. A large number of examples have been documented to date. It has been shown that the $\alpha_3\beta_4$ and $\alpha_3\beta_4\beta_2$ receptors have similar agonist pharmacology, whereas the $\alpha_3\beta_2$ and $\alpha_3\beta_4\beta_2$ have different agonist pharmacology (Colquhoun and Patrick, 1997). The presence of the β_4 subunit in $\alpha_3\beta_4\beta_2$ receptor affects the sensitivity of the receptor to cytisine. The $\alpha_3\beta_2$ receptor is blocked by cytisine, whereas the $\alpha_3\beta_4\beta_2$ is sensitive to cytisine (Colquhoun and Patrick, 1997). The response to nicotine is nearly doubled by the incorporation of the β_3 subunit into the $\alpha_3\beta_4$ receptor subtype (Groot-Kormelink et al., 1998), whereas the incorporation of the α_5 subunit into the $\alpha_3\beta_4$ receptor has little effect on the response to nicotine (Conroy et al., 1992). The response to nicotine is also doubled by the incorporation of the α_5 subunit into the $\alpha_3\beta_2$ receptor (Conroy et al., 1992).

Heterologous expression techniques have provided much insight into the diverse single channel properties of nAChRs. Each class of channels, expressed after injection of oocytes with β_2 mRNA from rat in combination with the α_2, α_3, and α_4 mRNA genes, could be distinguished by its distribution of channel open times (Papke et al., 1989). For example, two distinct populations of open channel conductances were observed after injection of rat $\alpha_2\beta_2$ and $\alpha_3\beta_2$ subunit combinations into oocytes (Papke, 1993;

Papke et al., 1989). Neuronal nAChRs containing the β_2 subunit generated brief synaptic currents, suggesting that these subunits have the potential for rapid signal processing. In contrast, synaptic currents for nAChRs containing the β_4 subunit had a smaller conductance and did not desensitize as rapidly. The α_7 subunit homooligomer desensitized more rapidly than other nicotinic receptors (Couturier et al., 1990a; Seguela et al., 1993) and displayed a permeability to calcium ions that was significantly greater than those observed for other ligand-gated ion channels (Seguela et al., 1993; Vernino et al., 1992). The α_8 subunit exhibited significant permeability to calcium ions similar to α_7 and also desensitized rapidly when expressed in oocytes. The α_9 subunit is an unusual member of the nAChR family, because unlike other neuronal α subunits which share sequence homologies ranging from 48% to 70% identity, the sequence identity between α_9 and all known subunits was found to be less than 39% (Brioni et al., 1997). The α_9 subunit injected into oocytes displayed unique pharmacological properties, similar to muscarinic and glycine receptors. Nicotine, which normally acts as an agonist of nAChRs, functioned as an antagonist at the α_9 homooligomer subtype (Elgoyhen et al., 1994). Among new pharmacological tools are subtype selective agonists and antagonists, such as α-conotoxins, which will permit a more comprehensive pharmacological characterization of the nAChRs (Favreau et al., 1999).

So far, most of the studies using expression of nAChR subunits in *Xenopus* oocytes have been performed using rat or chicken cDNA, however recently, recombinant human nAChRs have been used in expression systems. These studies have revealed that recombinant human nAChRs expressed in *Xenopus* oocytes display unique sensitivities to nAChR agonists and antagonists, and the pharmacology of some of these human nAChRs differs from their rat homologs. For example, nicotine was shown to act as a

full agonist on rat $\alpha_3\beta_2$ receptor, whereas it was a partial agonist on chick and human $\alpha_3\beta_2$ receptors (Chavez-Noriega et al., 1997; Hussy et al., 1994). Therefore, in the discovery of nAChR-directed therapeutic agents for humans, it is preferable to use human nAChRs as primary targets.

The different agonist and antagonist sensitivities and single-channel properties are consistent with the existence of multiple subpopulations of nicotinic receptors being expressed *in vivo*. *In vitro* experiments provide significant insight into the unique pharmacology and electrophysiology of different receptor configurations, which suggests that these receptors may have very specific functions *in vivo*. However, some caution is required in interpreting these results because of the atypical nature of the oocyte membrane environment. In recent studies, nAChR subunit combinations have been expressed in a number of mammalian cell lines (Gopalakrishnan et al., 1995; Gopalakrishnan et al., 1996; Wong et al., 1995), revealing differences in channel properties between receptors expressed in mammalian preparations and those expressed in oocytes (Fucile et al., 1997). These cell lines will be a valuable tool for the identification of subtype-selective compounds and they will also allow a more comprehensive analysis of the structure, function and regulation of nAChR subtypes. The uncertainty of which heterologous expression system resembles the native neurons for the different receptor combinations makes it difficult to ascertain true results. The weakness inherent in *in vitro* studies may be overcome to an extent by complementary studies conducted using overexpressing conventional transgenic mice and gene knockout and knockin mice.

Despite this detailed characterization of nAChR subunits *in vitro*, the precise function of the individual subunits *in vivo*, particularly with respect to complex behaviours, still remains unknown.

1.9   Anxiety

A large body of clinical data has shown that nicotine reduces anxiety in both smokers (Gilbert, 1979; Gilbert et al., 1989; Pomerleau, 1986) and nonsmokers (Hutchinson and Emley, 1973), but despite this knowledge, the effect of nicotine on emotional behaviour has not been extensively investigated. A number of studies have suggested that the $\alpha_4\beta_2$ receptor configuration plays a major role in anxiety-like behaviour (Brioni et al., 1993; Gilbert et al., 1989; Pomerleau, 1986).

Anxiety is characterized by feelings of apprehension, uncertainty and fear. Although often not attributable to a real or appropriate threat, it can paralyze the individual into inaction or withdrawal. In addition, anxiety can result in heightened motor activity, depending on the individual and the specifics of the environment (Kandel, 1991). Benzodiazepines, which exert anxiolytic, anticonvulsant and hypnotic actions, have been the drugs of choice for the treatment of anxiety (Shader and Greenblatt, 1993). However, this method of treatment is not ideal as it is associated with side effects including amnesia, sedation and the potentiation of alcohol related adverse effects (Lader, 1990), hence the search for clinically useful anti-anxiety agents lacking such side effects.

In smokers, nicotine has been shown to reduce anxiety provoked by a stress-producing movie (Gilbert et al., 1989). This anxiolytic effect of nicotine in smokers is unlikely to

be due to reduction of withdrawal as it is seen in smokers under minimal deprivation (Gilbert, 1979). The anxiolytic-like effects of nicotine and a number of nicotinic agonists have been documented in experimental animals. These studies utilized the ethologically based behavioural paradigms such as the elevated plus-maze (Brioni et al., 1993), the light-dark transition test and the mirrored chamber test (Cao et al., 1993; Costall et al., 1989). Unlike a number of other paradigms, these tests rely on ethological or more naturalistic situations, such as fear of novelty and avoidance of lightened areas and social interaction (Crawley and Goodwin, 1980; File et al., 1979).

The elevated plus-maze is a pharmacologically validated test for anxiety, in which the exposure of an animal to an elevated open arm leads to an avoidance response considerably stronger than that evoked by exposure to an enclosed arm. Avoidance of the open arm is therefore assumed to reflect an enhanced anxiety-like state. The elevated plus-maze has been validated using drugs which are known to be anxiolytic and anxiogenic in humans. Cocaine and picrotoxin, which accentuate anxiety in humans, caused a reduction in the exploration, number of entries and time spent in the open arms. Benzodiazepines, ondansetron (a $5-HT_3$ antagonist) and nicotine, which are known to reduce anxiety in humans, resulted in an increase in the exploration, number of entries and the time spent in the open arms (Lister, 1987).

Nicotine and the nicotinic receptor agonists, ABT-418 and lobeline are anxiolytic, whereas cytisine (Brioni et al., 1993), anabasine and epibatidine are devoid of these anxiolytic-like properties (Decker et al., 1995). This differential behavioural profile of nicotinic agonists implies that the anxiolytic actions may be mediated by a specific subunit configuration of the neuronal nicotinic receptor.

Using the elevated plus-maze, the anxiolytic-like effect of nicotine was blocked by mecamylamine, a central blocker of the nicotinic receptor, whereas hexamethonium, a peripheral blocker, showed no effect. This indicates the central nature of the anxiolytic effect of nicotine and suggests that it involves the activation of nAChRs (Brioni et al., 1993). The blockade of these receptors by mecamylamine did not result in an anxiogenic response, thus indicating that a tonic cholingeric activation of the nAChRs does not modulate the emotional status of the animal (Brioni et al., 1993). The benzodiazepine receptor antagonist, flumazenil, blocked the anxiolytic-like effect of nicotine in the elevated plus-maze, suggesting that the reduction in anxiety induced by nicotine occurs indirectly via the release of endogenous substances that can activate the benzodiazepine receptor (O'Neill and Brioni, 1994). Mecamylamine did not block the anxiolytic-like effects of diazepam confirming that GABA receptor activation occurs downstream of nAChR stimulation (O'Neill and Brioni, 1994).

In summary, central nicotinic receptors participate in emotional behaviour, such as anxiety. Unlike benzodiazepines, which induce amnesia and potentiate adverse effects of alcohol, the activation of nicotinic receptors does not seem to be associated with any of these liabilities (Brioni et al., 1993). Pharmacological intervention through the nAChR system may provide a novel therapeutic approach for the treatment of anxiety. For this to be done, the identity of nAChR subunits involved in the modulation of anxiety-like behaviour needs to be defined at the specific molecular level in the whole animal.

1.10 Analgesia

Analgesic agents are primarily classified into two groups: opioids and nonsteroidal anti-inflammatory drugs. However both of these classes are associated with side effects and prolonged use can result in dependence and tolerance (Sachin et al., 1986). Despite this, systemic administration of opioid analgesics such as morphine remains the most effective means of alleviating severe pain across a wide range of conditions (Yaksh, 1997). Morphine has a broad spectrum of analgesic actions, however its clinical use is limited by side effects such as respiratory depression, constipation and physical dependence (Cherny, 1996). This has encouraged research in the quest for other potential analgesics without the associated side effects and the potential for dependency.

The analgesic effect of nicotine has been widely documented in a large number of studies (Damaj et al., 1994; Sullivan et al., 1994; Damaj et al., 1998) and recently, considerable interest has focused on nAChR agonists as potential analgesics. An extremely potent nAChR agonist, epibatidine, which was first isolated from the skin of the Ecuadoran poisonous frog (Spande et al., 1992), was recently reported to have a very potent analgesic property in a number of studies (Qian et al., 1993; Badio and Daly, 1994; Rao et al., 1996). Epibatidine has a non-opioid mechanism of action and was found to be greater than 100-times more potent than either nicotine or morphine in the hot-plate assay (Badio and Daly, 1994) and 350-times more potent than nicotine in the tail flick assay (Rao et al., 1996). Administration of mecamylamine prior to epibatidine prevented the antinociceptive effect (Badio and Daly, 1994; Rao et al., 1996), indicating a central site of action for epibatidine.

Although epibatidine and nicotine do not show the withdrawal and physical dependence associated with opioids, these are not suitable for therapeutic use in man. Epibatidine and nicotine display toxic effects such as reduced activity, laboured respiration and at high doses can cause convulsions (Rupniak et al., 1994). Therefore, research is now focusing on novel nAChR agonists, which have analgesic actions, but do not have the associated toxicity. A recent study has shown that the novel nicotinic agonist, ABT-594, has antinociceptive properties equal in efficacy to those of morphine and repeated treatment does not appear to elicit opioid-like withdrawal or physical dependence (Bannon et al., 1998), thus highlighting the importance of this area of research. In mouse models of acute and persistent pain, ABT-594 has a broader spectrum of activity than that displayed by nicotine and has an improved safety profile relative to both nicotine and epibatidine (Bannon et al., 1998; Decker et al., 1998).

A number of studies have investigated the mechanisms underlying the antinociceptive action of nicotine and evidence suggests that there is more than one site of action. These studies have emphasized either brain (Iwamoto, 1989; Tripathi et al., 1982; Rogers and Iwamoto, 1993) or spinal sites for the action of nicotine (Aceto et al., 1986; Christensen and Smith, 1990). There are several lines of evidence that implicates the brain as a site of nicotine action. Firstly, peripheral administration of quaternary derivatives of nicotine, which do not penetrate the CNS, failed to induce antinociception in mice and rats, whereas nicotine which can penetrate the CNS induced antinociception (Aceto et al., 1983). Secondly, centrally acting nicotinic blockers blocked nicotine induced antinociception, whereas quaternary blockers failed to prevent nicotine-induced antinociception (Sahley and Berntson, 1979). Many of the studies above have used the tail flick method of assessing antinociception and as shown in a recent study, different

methods of assessing antinociception may engage different neural mechanisms (Iwamoto, 1989; Caggiula et al., 1995). In the study by Caggiula et al., (1995), the peripheral blocker, chlorisondamine, failed to block nicotine-induced antinociception in the hot-plate assay, whereas mecamylamine produced total blockade, thus suggesting that this is a centrally mediated effect (Caggiula et al., 1995). In comparison, chlorisondamine and mecamylamine completely blocked nicotine-induced antinociception in the tail flick assay. This result implicates peripheral nicotinic-sensitive pathways in nicotinic-induced antinociception in the tail flick assay, however does not rule out the possibility that central peripheral sites could also be involved. Therefore in summary, the hot-plate assay involves nAChRs in the CNS only, whereas the tail flick assay involves both peripheral and centrally located nicotinic receptors.

Evidence suggests that nicotine produces antinociception through different mechanisms in rats and mice (Tripathi et al., 1982). In rats, brain levels of nicotine did not correlate with antinociception, therefore suggesting that nicotine is acting peripherally, whereas in mice, a correlation was seen between antinociception and nicotine brain levels, suggesting a central site of action.

In a recent study, using α_4 and β_2 nAChR subunit knockout mice, the role of these subunits in antinociception was investigated (Marubio et al., 1999). Using the hot-plate and tail flick assays, this study evaluated the analgesic responses of the knockout mice to nicotine, epibabtidine and morphine. The α_4 knockout mice showed no antinociceptive response to nicotine in the hot-plate assay, while the β_2 knockout mice showed a reduced response. Epibatidine showed no antinociceptive effect in the α_4 knockout mice. These results suggest that the α_4 subunit is required for nicotine

antinociception in the hot-plate assay and the β_2 subunit is important, but not as pivotal as the α_4 subunit. The hot-plate assay involves nAChRs in the CNS only and therefore this study implicates the $\alpha_4\beta_2$ receptor subtype in the CNS in the modulation of pain. In support of these findings, the antinociceptive action of the ABT-594 has been shown to be partly mediated by activation of α_4 containing nAChRs located on the serotonergic neurons of the nucleus raphe magnus (Bitner et al., 1998).

Nicotine had a reduced analgesic response in the α_4 and β_2 nAChR subunit knockout mice compared to Wt mice when tested by the tail flick assay, thus suggesting that these subunits are not exclusive components in tail flick analgesia (Marubio et al., 1999). Hexamethonium almost completely blocked nicotine-induced antinociception in α_4 knockout mice in the tail flick assay, thus indicating that in the periphery the α_4 subunit is not involved in nicotine-induced antinociception. There is evidence that the principal neuronal nAChR subtype in sensory ganglion is composed of α_3 and β_4 subunits (Flores et al., 1996), suggesting that the $\alpha_3\beta_4$ nAChR subtype could mediate the peripheral effects of nicotine in the tail flick assay.

The descending pathway that modulates pain is an inhibitory pathway that originates in the periaqueductal gray matter and terminates on nociceptive neurons in the spinal cord (Kandel et al., 1991). Neurons in the periaqueductal gray matter make excitatory connections with the rostroventral medulla, which is a region that includes the serotonergic nucleus raphe magnus (Cross, 1994). These areas are highly sensitive to morphine and administration of the narcotic antagonist, naloxone, has been shown to block analgesia produced by morphine (Azami et al., 1982). The nucleus raphe magnus is also sensitive to nicotine, whereby the administration of nicotine produced

antinociception in mice and rat models of thermal pain (Iwamoto, 1991; Damaj et al.,

1994). The expression of nAChR subunits in various brainstem regions (Wada et al.,

1989) supports findings of a nAChR-mediated mechanism of antinociception in a

supraspinal site. However, it should be emphasized that the nucleus raphe magnus may

be only one of several nuclei that represent potential sites of antinociception action

produced by nicotine and ABT-594, and other subunits beside or in addition to the α_4

and β_2 may also be involved (Bitner et al., 1998).

The mechanism by which nicotine produces antinociception remains unclear. Some

investigators have suggested that the nicotinic effect is mediated through the release of

acetylcholine (Sahley and Berntson, 1979) and others suggest that some of the analgesic

effects of nicotine are mediated through the activity of endogenous opioids (Balfour,

1982; Tripathi et al., 1982; Davenport et al., 1990; Malin et al., 1993). There is

evidence that suggests nicotine is acting through an opiate receptor mechanism in mice,

as shown by the ability of naloxone to block the antinociceptive response of nicotine in

the tail flick assay. However this was not the case in rats, as naloxone failed to block

the analgesic effect of nicotine in the tail flick assay (Tripathi et al., 1982). In a

conflicting study, there is evidence that nicotine is acting through an opiate mechanism

by releasing endogenous opioids (Davenport et al., 1990). In this study, nicotine

pretreatment prevented the ability of β-funaltrexamine, an irreversible opioid receptor

antagonist, to block morphine analgesia (Davenport et al., 1990).

In another study, using the tail flick assay, a small dose of nicotine, which exerts no

antinociception on its own, increased morphine antinociception (Zarrindast et al., 1996),

thus supporting the involvement of the opiate system in nicotine antinociception. In this

study, the antimuscarinic agent, atropine, decreased the response of nicotine plus morphine, whereas mecamylamine and hexamethonium had no effect on this response, thus implicating the involvement of muscarinic receptors and not the nicotinic receptors. However in a conflicting study by the same authors, nicotine could attenuate naloxone-induced jumping behaviour in morphine-dependent mice and this effect of nicotine could be blocked by mecamylamine, but not by atropine, thus implicating central nAChRs rather than muscarinic receptor involvement (Zarrindast and Farzin, 1996). Another study highlighting the cross talk between nAChRs and opioid systems showed that the opiate antagonist naloxone was able to precipitate an abstinence syndrome in nicotine-dependent rats and that morphine administration was able to reduce spontaneous abstinence signs seen following cessation of nicotine (Malin et al., 1993).

1.11   Cognition

Alzheimers's disease (AD) is a degenerative brain disorder characterized by profound and progressive cognitive deficits (Kandel et al., 1991). There are several lines of evidence which implicate the involvement of the cholinergic system in cognitive disorders. Physostigmine, a drug that potentiates central cholinergic function, was shown to significantly enhance long-term memory (Davis et al., 1978). Patients with AD were found to have a reduction in the cholinergic enzymes, choline acetyltransferase (the enzyme which synthesizes ACh) and acetylcholinesterase (the enzyme which hydrolyses ACh) (Bowen et al., 1976; Davies and Maloney, 1976). Early studies failed to find a reduction in muscarinic receptors in the cortex of patients with AD (Bowen et al., 1976; Perry et al., 1978), however a more recent study demonstrated a decrease in presynaptic M_2 muscarinic receptors in these patients (Mash et al., 1985).

Recently, a number of findings have implicated nicotinic receptors in cognitive disorders. In some clinical trials, nicotine has shown to improve memory and learning in healthy volunteers and AD patients (Jones et al., 1992; Newhouse et al., 1988). In addition, high affinity nicotine binding sites are reduced by 80% in patients suffering from AD (Nordberg and Winblad, 1986; Whitehouse et al., 1986) and a more recent study identified the selective loss of the $\alpha_4\beta_2$ nAChR subtype (Warpman and Nordberg, 1995). Experiments in animals have also revealed the importance of nAChRs in memory and learning and their overall importance in cognitive function (Levin et al., 1992; Brioni and Arneric, 1993). Mecamylamine impairs memory performance in a variety of cognitive tasks in rats, whereas hexamethonium had no such effect (Decker and Majchrzak, 1992), indicating that the effects of mecamylamine on cognitive function are mediated centrally.

Surprisingly, β_2 knockout mice performed better than non-mutant littermates in a passive avoidance test, a paradigm used to examine learning and memory (Picciotto et al., 1995). The more predictable result was the failure of nicotine-induced improvement in avoidance learning in these mice (Picciotto et al., 1995). The performance of the β_2 knockout mice on the Morris water maze, a paradigm used to evaluate spatial orientation learning, did not differ from that of non-mutant littermates (Picciotto et al., 1995). However, aged β_2 knockout mice showed a significant impairment as compared to their non-mutant littermates (Zoli et al., 1999), suggesting that the β_2 subunit plays a more significant role in the aged brain with the baseline cognitive function being closer to what would be expected given the extensive literature on cognitive enhancement with nicotine.

GTS-21 and ABT-418 are novel nicotinic agonists that were reported to improve cognitive performance in experimental animals and appeared to be less potent than nicotine in producing many adverse side effects (Decker et al., 1994; Decker et al., 1995; Meyer et al., 1997). GTS-21 is an anabaseine analog that is a functionally potent partial agonist for the α_7 subtype and was found to improve both avoidance and spatial memory (Meyer et al., 1997). ABT-418 is an isoxazole analog that is selective for the $\alpha_4\beta_2$ receptor subtype and was shown to improve retention of avoidance learning in mice (Decker et al., 1994). Both GTS-21 and ABT-418 have reduced peripheral side effects as compared to nicotine and thus may be improved agents for the treatment of the cognitive deficits in AD patients (Brioni et al., 1997; Nanri et al., 1998).

1.12   Locomotor Activity

Nicotine has been shown to produce a wide range of behavioural changes in mice, such as the depression or stimulation of locomotor activity. A number of studies on nicotine-induced locomotor changes in rats suggest that nicotine causes an initial depressant effect of locomotor activity, followed by a stimulant effect (Stolerman et al., 1973; Battig et al., 1976). The effect of nicotine on locomotion depends on the drug dosage. This was demonstrated by a study in which a low dose of nicotine caused an increase in activity 15 mins post injection, whereas a high dose of nicotine reduced activity within 5 mins of the injection and then caused an increase in activity 15 mins later (Freeman et al., 1987). Both the locomotor depressant and stimulant effects of nicotine are antagonized by mecamylamine but not hexamethonium, suggesting that the effects are mediated by central nicotinic receptors (Clarke and Kumar, 1983; Martin et al., 1990). The stimulant effect of nicotine on locomotion has been thoroughly investigated and several lines of evidence suggest that these effects are due to an interaction between

central nicotinic and dopaminergic systems (Clarke, 1990). Amphetamine causes the release of dopamine and like nicotine has a stimulant effect on locomotion (Robinson and Becker, 1986), therefore it is not surprising that a compound that increases dopamine release might stimulate activity. There is evidence that suggests the depressant effects of nicotine on locomotor activity are not due to altered dopamine levels, but may be related to changes in acetylcholine metabolism. This was shown in a study in which acute nicotine administration caused a reduction in acetylcholine utilization in the brain (Freeman et al., 1987).

1.13   Nicotine-Induced Neurotransmitter Release

Neuronal nAChRs at presynaptic sites can modulate synaptic transmission by regulating the extent of neurotransmitter release (Role and Berg, 1996). This has been demonstrated for a number of neurotransmitters, including ACh, dopamine, norepinephrine, serotonin, GABA and glutamate (Role and Berg, 1996). The striatum receives dopaminergic innervation from the substantia nigra and lesioning studies with 6-hydroxydopamine have shown that some high affinity [^{3}H]-nicotine binding sites have a presynaptic location on dopaminergic nerve terminals of the nigrostriatal and mesolimbic systems (Schwartz et al., 1984; Clarke and Pert, 1985). One of the best characterized presynaptic actions of nicotine is its ability to stimulate the release of [^{3}H]-dopamine from the striatum. This has been shown *in vivo* using microdialysis (Damsma et al., 1989) and *in vitro* using both tissue slices (Damsma et al., 1989; Giorguieff et al., 1976; Westfall and Perry, 1986) and synaptosomes (de Belleroche and Bradford, 1980; Sakurai et al., 1982; Rapier et al., 1990). Most studies have demonstrated that nicotine-induced release of [^{3}H]-dopamine from striatal synaptosomes or tissues slices is dependent on calcium (Westfall, 1974; Giorguieff-

Chesselet et al., 1979; Rapier et al., 1988; Schulz and Zigmond, 1989; Grady et al., 1992) and can be blocked by mecamylamine and hexamethonium (Westfall, 1974; Schulz and Zigmond, 1989; Grady et al., 1992). Calcium independent release of [^{3}H]-dopamine in response to nicotine has also been reported (Arqueros et al., 1978; Marien et al., 1983; Takano et al., 1983), however it appears that this type of release only occurs with high concentrations of nicotine. This release was not blocked by mecamylamine or hexamethonium indicating the lack of involvement of nicotinic receptors (Marien et al., 1983). At these higher concentrations of nicotine, it has been suggested that nicotine is acting in an amphetamine-like manner and displacing dopamine from vesticular stores (Fischer and Cho, 1979; Raiteri et al., 1979). From these experiments, it appears that the concentration of nicotine used to evoke dopamine release is critical in determining the type of release.

The presynaptic nicotinic modulation of dopamine release from striatal nerve terminals is now well established (for review see (Role and Berg, 1996; Wonnacott, 1997). *In vitro* experiments have shown that nicotine and cytisine stimulate the release of [^{3}H]-dopamine, but the selective nicotinic agonist, lobeline, has no such effect (Westfall and Anderson, 1967; Grady et al., 1992). This differential behavioural profile of nicotinic agonists implies that specific nAChR subtypes mediate the release of dopamine, however the subtype or subtypes underlying this response remain unidentified.

Nigrostriatal neurons express a number of nAChR subunits, such as α_3, α_4, α_5, α_6, β_2 and β_3 (Deneris et al., 1989; Wada et al., 1989; Wada et al., 1990; Dineley-Miller and Patrick, 1992; Seguela et al., 1993), suggesting a number of subtypes are possible. Neuronal-bgt, which is specific for the $\alpha_3\beta_2$ receptor subtype (Luetje et al., 1990), was

shown to block nicotine-induced [^{3}H]-dopamine release from rat striatal slices (Schulz and Zigmond, 1989; Grady et al., 1992), therefore implicating the $\alpha_3\beta_2$ receptor subtype in mediation of nicotine-induced [^{3}H]-dopamine release. The involvement of the β_2 subunit in this process has been supported by studies using the β_2 knockout mice which demonstrated that nicotine-induced [^{3}H]-dopamine release requires an intact β_2 subunit (Picciotto et al., 1998). A major obstacle in identifying these receptor subtypes has been the lack of subtype-specific ligands. Alpha conotoxin-MII is a newly characterized nAChR antagonist that selectively blocks the $\alpha_3\beta_2$ receptor subtype and in a recent study, this toxin was shown to partially block nicotine-induced [^{3}H]-dopamine release from rat striatal synaptosomes (Kulak et al., 1997). The partial block of [^{3}H]-dopamine release indicates that there are at least two different receptor complexes that mediate striatal dopamine release and the $\alpha_3\beta_2$ receptor subtype is one of these receptors. Alpha-bgt failed to inhibit nicotine-stimulated [^{3}H]-dopamine release from mouse striatal synaptosomes, suggesting that the α_7 subtype does not appear to be involved in mediating this response (Grady et al., 1992).

1.14   Autosomal Dominant Nocturnal Frontal Lobe Epilepsy (ADNFLE)

Epileptic seizures are classified as to whether their onset is focal (partial seizures) or generalized. Partial epilepsy, which does not normally disrupt consciousness, is a form of seizure that begins in a restricted brain region and either remains localized or can spread to the adjacent cortex (Kandel et al., 1991). The clinical manifestations of a partial seizure reflect the region of the brain involved, for example, a discharge in the motor area can induce rhythmical uncontrolled motor activity in the contralateral face or limbs. In contrast, generalized epilepsy simultaneously involves large parts of the brain and is classified into tonic-clonic, clonic, atonic and absence forms. The tonic-clonic

form is the most common type of generalized epilepsy. It is characterized by abrupt loss of consciousness and postural control, whereby the patient falls to the ground and suffers initially rigid posturing followed by rhythmic limb and body movements. Absence seizures, which begin in childhood, are accompanied by a transient loss of consciousness and present as a few seconds of staring with rapid return to awareness (Kandel et al., 1991).

Epilepsy is a common condition that affects 2 to 3% of the population at some time in their lives (Hauser et al., 1993). Epilepsy is divided into a large number of clinical syndromes, which are grouped into two aetiological categories, namely symptomatic and idiopathic epilepsies. Symptomatic epilepsies are associated with obvious brain lesions that disturb neuronal structure and function. The causes of these include brain tumours, perinatal brain injury, postnatal head injury, postencephalitic injury and progressive neuronal degeneration. In contrast, in idiopathic epilepsies there is no evidence of underlying neuronal damage (Shin and McNamara, 1994).

Genetic factors have been identified in both symptomatic and idiopathic epilepsies. In contrast to symptomatic epilepsies in which genetic factors play a small role, genetic factors are believed to be paramount in idiopathic epilepsies (Andermann, 1982). Because most idiopathic epilepsies appear to be inherited in a complex manner, linkage studies and the identification of specific gene defects have been quite difficult. However, recently a number of idiopathic epilepsies with single gene inheritance have been successfully identified (Scheffer et al., 1994; Scheffer et al., 1995a; Scheffer et al., 1995b; Berkovic et al., 1996; Berkovic and Scheffer, 1997).

ADNFLE is a recently characterized idiopathic familial partial epilepsy, in which brief partial seizures occur during light sleep which are often misdiagnosed as nightmares (Scheffer et al., 1994; Scheffer et al., 1995a). ADNFLE was the first form of partial epilepsy to be defined at the DNA level. Three mutations in the α_4 nAChR subunit have been identified in ADNFLE, two of which result from amino acid substitutions and the other resulting from an amino acid insertion (Steinlein et al., 1995; Steinlein et al., 1997; Hirose et al., 1999). The first mutation was found in affected members of a large Australian family, in which a C was changed to a T in amino acid position 248 in the fifth exon of the α_4 subunit (Steinlein et al., 1995). This mutation thereby resulted in the replacement of the highly conserved small hydrophilic amino acid, serine, with the large hydrophobic amino acid, phenylalanine, in the second transmembrane (M2) domain. In a subsequent study, a second mutation was identified in a Norwegian family, in which an amino acid was inserted into the α_4 subunit. Three nucleotides (GCT) were inserted at amino acid position 259 into the coding region of the C-terminal end of the M2 domain resulting in the insertion of an additional leucine amino acid (Steinlein et al., 1997). The most recent mutation, described in a Japanese family, was an amino acid substitution in the fifth exon of the α_4 subunit. This missense mutation resulted in a nucleotide change from a C to a T in the M2 domain, causing a serine to be replaced with a leucine at amino acid position 252 (Hirose et al., 1999).

Site-directed mutagenesis studies have revealed that the M2 domain lines the nAChR cation channel near the channel gate at the cytoplasmic surface (Akabas et al., 1994). The functional importance of serine at amino acid position 248 in the M2 domain has been highlighted by site-directed mutagenesis experiments of the $\alpha 1$ subunit of the mouse muscle nAChR and the *Torpedo* ray electric organ (Changeux et al., 1992;

Devillers-Thiery et al., 1992; Leonard et al., 1988). These experiments suggest that this position lines the pore and affects a number of electrophysiological parameters including the affinity for ACh, desensitization properties and ion currents (Leonard et al., 1988; Devillers-Thiery et al., 1992).

The site and nature of these mutations in ADNFLE suggest that they may have major adverse functional effects on receptor activity. This has been demonstrated for the Ser248Phe substitution and 259Leu insertion mutation by *in vitro* examination of *Xenopus* oocytes expressing mutated α_4 nAChR subunits. These studies revealed that the mutations have diverse effects on the receptor properties. However, they both result in reduced permeability to calcium and enhanced desensitization (Weiland et al., 1996; Kuryatov et al., 1997; Bertrand et al., 1998). Studies of the Ser252Leu substitution mutation are yet to be reported. In summary, these results therefore argue that the net effect of the α_4 nAChR mutations causing ADNFLE may be to reduce nAChR activity.

Epilepsy is caused by excessive neuronal activation and a considerable amount of research has focused on the hypotheses that excessive glutamate (the major excitatory neurotransmitter) or deficient GABA (the major inhibitory neurotransmitter) causes epilepsy (Bradford, 1995; Armijo et al., 2000). The involvement of the GABAergic system in seizure induction is highlighted by the fact that many proconvulsant drugs appear to block CNS GABA activity and a number of anti-convulsants enhance its activity (Olsen, 1981; White, 1999). It would not be envisaged that a mutation affecting the cholinergic system, which causes a net reduction in receptor activity, would cause epilepsy. The β_2 nAChR knockout mice do not have spontaneous seizure activity (Picciotto et al., 1995) and there is little evidence linking the inhibition of nicotinic

receptors to paroxysmal neuronal bursting and hence epilepsy. Recent evidence suggests that the principle function of nicotinic receptors may be to modulate presynaptic release of other neurotransmitters, including glutamate, GABA, dopamine, acetylcholine and noradrenaline (Role and Berg, 1996). There are a number of studies describing nicotine-induced release of the inhibitory neurotransmitter GABA either from isolated synaptosomes or in-slice preparations (Lena et al., 1993; Kayadjanian et al., 1994; McMahon et al., 1994). Therefore, a possible explanation for the seizures observed in ADNFLE could be that the mutation results in impaired GABA release.

Given the complexity of nAChRs in the brain and in particular the presynaptic location of the abundantly expressed α_4 subunits, heterologous expression studies in *Xenopus* oocytes are unlikely to give the definitive word on the mechanism of epilepsy in ADNFLE. Mouse models that replicate the disease *in vivo* are the key to understanding the relationship between the loss of α_4 nicotinic receptor subunits and paroxysmal EEG patterns, which are the defining features of epilepsy (Noebels, 1996). Understanding the rare single gene inherited epilepsies such as ADNFLE will ultimately provide vital links in understanding the more genetically complex epilepsies.

A number of animal models of epilepsy exist providing insight into the basic neuronal dysfunction underling human epilepsies and a means for discovery of potential new effective antiepileptic drugs. Mouse models of primary generalized epilepsy are exemplified by several single gene mutations including stargazer (Noebels et al., 1990), tottering (Noebels and Sidman, 1979) and lethargic (Hosford et al., 1992). Genetically more complex models for epilepsy also exist, including the EL/Suz (EL) mouse, which is considered a model for human temporal lobe epilepsies or complex partial seizures

with secondary generalization (Seyfried and Glaser, 1985). *In vivo* electrical recordings from the EL mouse suggest that seizures initiate in the parietal cortex and then spread to the hippocampus from where they generalize to other brain areas (Ishida et al., 1993). Spontaneous seizures occur with routine handling at about 80 to 100 days old and can be evoked at an earlier age by repeated sensory stimulation such as tail twisting, tossing or rocking (Suzuki, 1976; Sugaya et al., 1986; Flavin et al., 1991; Ishida et al., 1993). The predisposition of EL mice to seizures is inherited as a complex genetic trait and several seizure frequency loci have been chromosomally mapped, including loci on chromosomes 9, 2, 14, 10 and 11 (Rise et al., 1991; Frankel et al., 1995).

Several lines of inbred mouse strains have been selectively bred for increased susceptibility to seizures induced by sound (Kurokawa et al., 1966), chemical stimulation (Marley et al., 1986; Freund et al., 1987; Marley and Wehner, 1987) and handling (Crabbe et al., 1980). The most popular model of generalized epilepsy is the inbred mouse with sound-induced seizures. Several strains of these inbred mice exist, including the DBA/2J and the SJL/J strains (Purpura, 1972). The nature of inducing noise is not critical, but is typically loud (120 dB), sudden and contain frequency components in the 12 to 16 kHz range (Purpura, 1972). These mouse models have no direct correlation with clinical epilepsy, however are important in determining seizure susceptible genes (Seyfried et al., 1980).

The administration of proconvulsant drugs in animals has been widely used as animal models for epilepsy. For example, pentylenetetrazol (PTZ) is a proconvulsant that induces convulsions by blocking the Cl^- ionopore of the $GABA_A$ receptor complex (Squires et al., 1984; Corda et al., 1990) and has been widely used in the study of

epilepsy (Purpura, 1972). Drugs that are effective in preventing PTZ-induced convulsions are also effective in preventing human generalized absence seizures, thus these models are integral components in the identification of clinically useful anticonvulsants (Porter et al., 1984). In addition, these models are important in identifying genes involved in determining sensitivity to PTZ (Ferraro et al., 1999).

The administration of the proconvulsant, kainic acid (KA) has also been wildly used to study epilepsy in animal models. KA is a glutamate agonist and causes a well characteristic seizure syndrome that is associated with excitotoxic generation in selected neurons in the hippocampus (Olney et al., 1974; Ben-Ari, 1985). Mice lacking the kainate receptor, GluR6, are much less susceptible to administration of kainate, suggesting that kainate receptors located on CA3 hippocampal neurons are important in the primary epileptogenic effects of kainate (Mulle et al., 1998).

Another example of an animal model in which the seizures are induced experimentally is the kindling model. Kindling is a phenomenon by which repeated shocks to various parts of the brain result in enhanced electrical excitability of the brain (Fisher, 1989) and is suggested to be a viable model of complex partial seizure disorders. Kindling is usually initiated by electrical stimulation of the amygdala, but most regions of the forebrain can be kindled (Goddard et al., 1969). To produce the model, bipolar stimulating wires are implanted in the amygdala or elsewhere in the brain and daily electrical stimulus trains are applied via the electrodes. After a few days of stimulation, a train of shocks begins to induce electrical afterdischarges, resulting in full bilateral motor seizures. The electrical afterdischarges then become progressively more complex and prolonged with each kindling stimulus (Croucher et al., 1988). At this time, the

animal is said to be 'kindled' and the effect seems to be permanent and seizures can be evoked by a single electrical pulse (Croucher et al., 1988). If the stimulus is continued for a few weeks, rodents exhibit spontaneous epileptic seizures (Pinel and Rovner, 1978). Repeated stimulation by excitatory chemicals can also produce kindling (Mason and Cooper, 1972). Kindling induced in experimental animals shares many features with human epilepsy, including similar EEG changes, changes in behaviour patterns during the seizure and responsiveness of the seizures to anticonvulsants (Adamec, 1990). The kindling model relates to partial epilepsy with secondary generalization.

1.15   Knockout Mice

The lack of nAChR subunit selective antagonists has been a major obstacle in defining the biological role of nAChR subunits *in vivo*. The ability to manipulate genes in mammals is providing insights into many facets of biology, including the function and regulation of genes and the mechanisms of developmental and pathological processes. In addition, this technology has enabled the creation of animal models to study the pathophysiology of disease and to assess therapy. Conventional transgenic and gene targeting technology provides the means whereby the genome can be altered and the *in vivo* consequences of the induced mutation determined at the molecular level of the whole animal.

When a fragment of genomic DNA is introduced into a mammalian cell, it undergoes homologous recombination, which is the ability of the foreign fragment of DNA to locate and recombine with the endogenous homologous DNA sequences. Gene targeting through homologous recombination in embryonic stem (ES) cells is a commonly used method of genome manipulation (Capecchi, 1989b; Koller and

Smithies, 1992) and was the method adopted in this study to create an α_4 nAChR subunit knockout.

ES cells can be expanded and maintained as stable diploid cell lines by culturing similar to other cells. However the ES cells must be prevented from differentiating by growing them on a substratum of embryonic fibroblasts and in some lines of ES cells (eg J1 and R1) by adding leukemia inhibitory factor to the culture medium (Smith et al., 1988; Williams et al., 1988). Under these conditions, ES cells can be grown for many weeks and retain totipotency when introduced into recipient blastocysts.

A targeting vector is designed to recombine with and mutate a specific chromosomal locus and is introduced into the ES cell genome by either electroporation or single cell microinjection (Robertson, 1987). Electroporation is technically simple making it the most commonly used method for introducing DNA into ES cells. Electroporation involves the application of a high voltage electrical pulse into a suspension of cells and DNA (Potter et al., 1984). Single cell microinjection on the other hand is more efficient, although this method has been limited applicability because of technical constraints (Robertson, 1987). A targeting vector contains homologous sequences with the desired chromosomal integration site and a plasmid backbone. Homologous recombination events are rare and to select for these events, the targeting vector contains selection markers. Two types of targeting vectors can be designed, such as a sequence replacement targeting vector ('knockout') or an insertion targeting vector ('knockin'). A number of experiments have revealed that the greater the length of homologous sequences the greater the targeting frequency (Thomas and Capecchi, 1987; Hasty et al., 1991). For optimal targeting frequency each of these two vectors

should ideally contain between 5 and 10 kb of DNA homologous to the target gene (Joyner, 2000). In the example in Figure 1.2, a gene containing four exons (black boxes) is mutated, so that one exon (exon 2) is deleted, thus rendering the gene product non-functional.

Random integration is the random insertion of the entire targeting vector into the chromosome and occurs at a much higher rate than homologous recombination. ES cells carrying the targeted mutation are enriched by a positive and negative selection procedure in culture (Capecchi, 1989a; Mansour et al., 1988). The vector usually contains two selectable markers, such as the bacterial neomycin-resistance (NEO) gene and the herpes simplex virus thymidine kinase (HSV-TK) gene (see Figure 1.2). The targeting vector is constructed so that it contains two regions of sequences identical to the chromosomal DNA (large boxed areas). These homologous regions flank the (NEO) gene, which replaces one of the exons (thick black lines) and the intronic DNA, thereby serving as a mutagen as well as a selectable marker. The HSV-TK gene lies outside these two regions of homology. Thin lines denote surrounding DNA derived from the plasmid DNA used in cloning. Prior to electroporation, the vector is linearized and subsequent homologous recombination results in DNA being exchanged (large 'X') between the targeting DNA and the chromosome at the regions of homology.
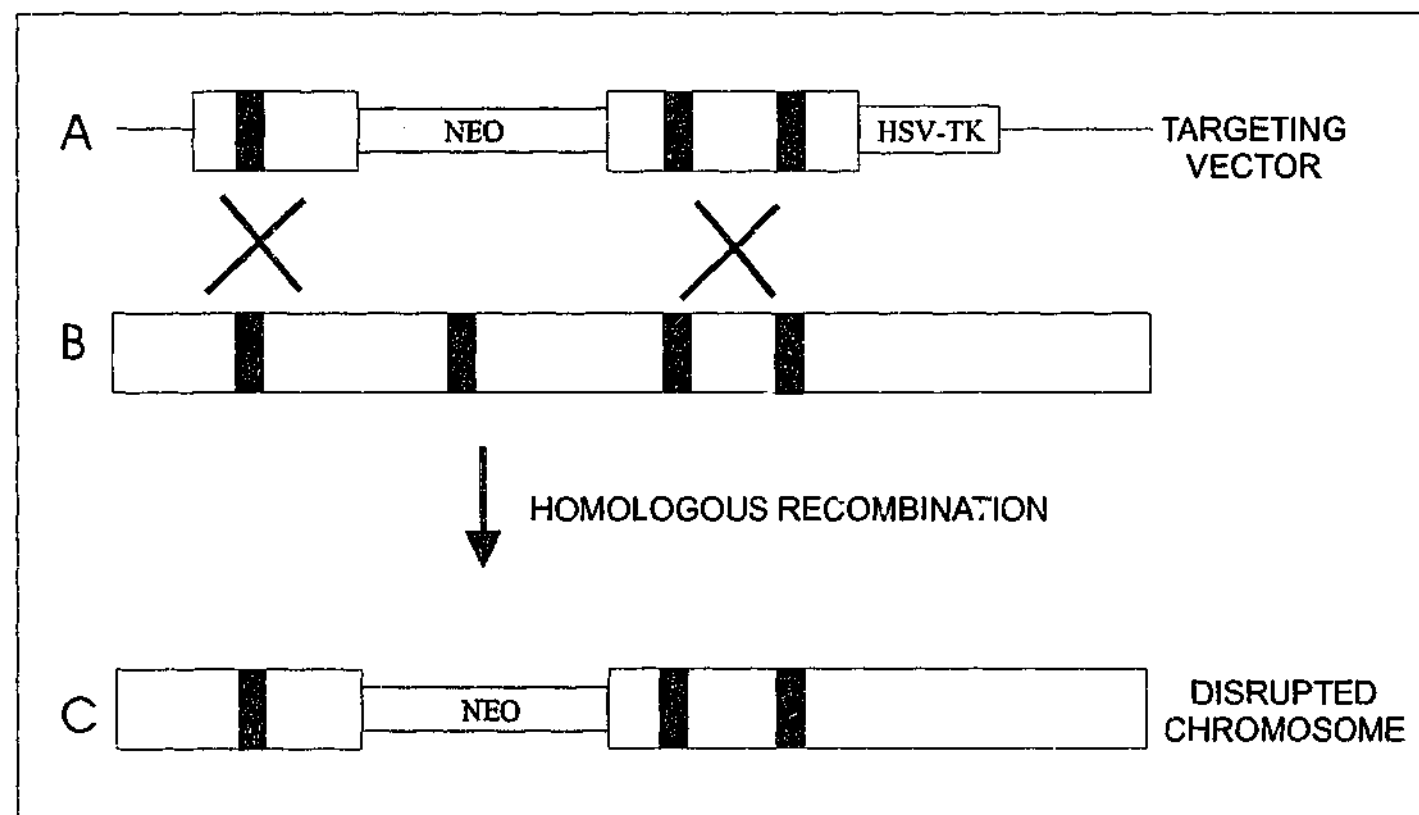
Figure 1.2 Genetic mutation via homologous recombination.

Panel A represents the targeting construct containing the two homologous flanks, the NEO selection cassette and HSV-TK gene. Panel B represents the normal chromosomal configuration at the gene locus to be targeted and panel C represents the chromosomal architecture following successful homologous recombination (note that the HSV-TK cassette has been spliced out).

The positive selection is based on the resistance of the ES cells to a drug, such as neomycin and ensures that the disrupted copy of the gene has been integrated into the chromosome. The negative selection is used to decrease the number of drug-resistant cells that have integrated randomly. The most commonly used negative marker is the HSV-TK, which is cloned into the vector outside the region of homology. Random integration generally inserts the entire DNA fragment, including the toxic HSV-TK gene into the chromosome. The TK gene is involved in the utilization of thymidine

from the medium and is found in all species, excluding some fungi. The cellular and viral enzymes have different substrate specificites and a number of antivirals have been developed based on this fact, including gancyclovir, which is a toxic thymidine analog (Sedivy, 1992). Toxic thymidine analogs are utilized by viral enzymes much more efficiently than by cellular enzymes, thus cells containing the HSV-TK will be killed in a medium containing gancyclovir. In correctly targeted clones, the HSV-TK gene is spliced out and clones are therefore insensitive to gancyclovir. Thus, positive and negative selection enrich for the cells that have the desired homologous recombination event. Enrichment strategies other than HSV-TK have been used, such as the diphtheria toxin, which has been used particularly for genes which target with a very low frequency (McCarrick et al., 1993).

Clones surviving the positive and negative selection process are then expanded and screened by PCR and/or Southern blot analysis. The clones identified as having the correct targeting event are subsequently expanded and maintained as a pure population. Ideally, a minimum of two targeted clones, isolated from separate plates, are selected for transfer into embryos. This is to control for functionally significant random mutations, which may occur in individual clones during the tissue culture periods. The other valid option is to confirm preservation of the phenotype following backcrossing. Introduction of the cloned cells into embryos is accomplished by either microinjection into blastocysts or by morula aggregation (Robertson, 1987). The ES cell-containing embryos are then surgically implanted into the uterus of a surrogate mother, where development proceeds to term. The resulting chimeric mice therefore contain cells derived from both the donor ES cells and the host blastocyst. The donor ES cells are most often derived from the 129 strain and the host blastocyst from the C57BL/6 strain,

however some successful C57BL/6 ES cell lines have been produced (Auerbach et al., 2000). Chimeras are identified by coat colour, in which they have patches of the colour of the blastocyst strain (black, if C57BL/6 blastocysts are used), as well as the colour from the ES cell donor (Agouti, if 129 strain ES cells are used). The breeding of chimeras with wildtype mice tests for germline transmission and generates heterozygotes, which are mice containing one mutant allele and one normal allele. Interbreeding of heterozygotes generates animals homozygous for the mutation.

Gene targeting in ES cells therefore ultimately allows the production of mice that contain a functional inactivation in a predefined gene of interest. Gene knockout techniques, such as those described above, provide animals that will inherit genetic deletions in all cell types and throughout the life of the animal. Considerable information regarding the functional role of the altered gene and its regulation by other genes can be obtained using this technique. However, this regionally and temporally unrestricted genetic deletion may lead to severe developmental defects or premature death (Joyner and Guillemot, 1994) and therefore prevent analysis of postdevelopmental gene functions.

Recently two exciting technical advances have been developed which should override this problem and also make it possible to control the time and site of a gene knockout. A major step towards cell type-specific restriction of targeted gene disruption has come with the use of regulated expression of Cre recombinase, an enzyme that recognizes Lox P motifs and excises the intervening DNA (Tsien et al., 1996; Marshall, 1997; Nebert and Duffy, 1997). In this procedure, which is outlined in Figure 1.3, the cloned gene to be disrupted is flanked by Lox P recognition sequences and introduced by homologous

recombination in ES cells. Transgenic mice bearing the Lox P-mediated gene are then crossed with transgenic mice expressing Cre recombinase under the control of a cell-type specific promoter. The second major advance involves the discovery of promoters whose temporal activity can be directly manipulated in transgenic animals providing a tool for the study of gene functions *in vivo*. The advent of promoters that are inducible with exogenously added drugs (eg tetracycline antibiotic derivatives) is emerging as the most promising approach to temporal control of targeted inactivation (Kuhn et al., 1995; Chambon, 1998).

In summary, transgenic animals are produced using molecular genetic techniques to add functional genes, alter gene products, delete genes, insert reporter genes into regulatory sequences, replace/repair genes and to make tissue/lineage-specific alteration of gene expression. These genetically altered animals provide unique tools for studying a wide range of problems *in vivo* and thereby allowing for the result of specific genetic changes in a variety of biological systems to be investigated. Pharmacological studies rely largely on animal systems but significant progress has been hindered because of the lack of selective or functional pharmacological tools and suitable animal models.
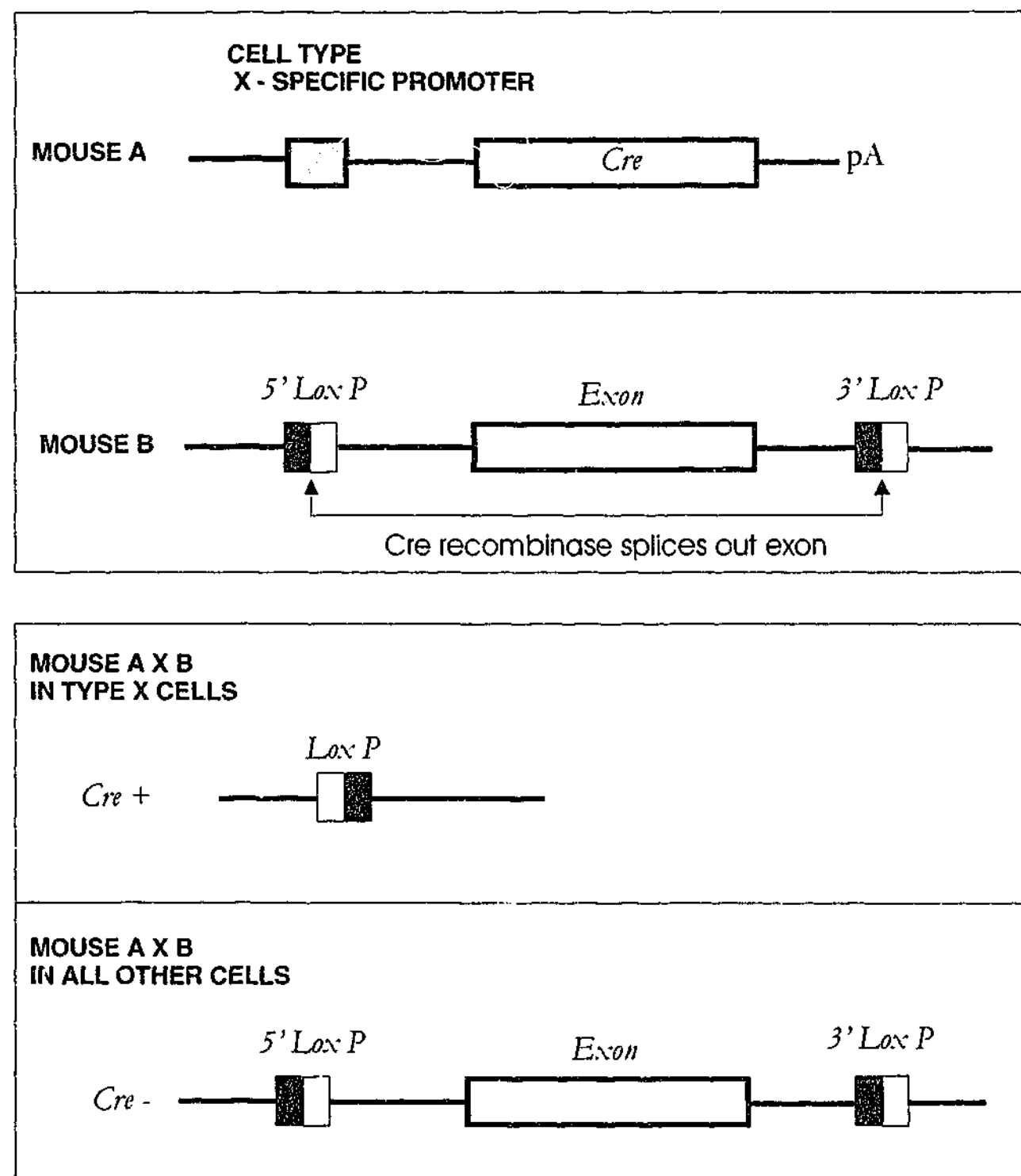
Figure 1.3 Strategy for cell type-restricted gene knockout.

Mouse A is transgenic mouse expressing Cre recombinase under the control of the cell type X-specific promoter and mouse B is a transgenic mouse bearing the Lox P-mediated gene. Mouse A is mated with mouse B and in cells containing the type X-specific promoter the Cre recombinase excises the exon, whereas in all other cells, the exon remains in the genome.

In classical gene targeting studies, ES cells are derived from the 129 strain and chimeric mice are mated to C57BL/6, however these two strains have been associated with unusual behaviours (Crawley, 1996; Gerlai, 1996). A possible confounding factor when using the transgenic approach is the background strains of the animals, which might complicate the interpretation of the behavioural analysis. The 129 strain is one of the most unique strains, in that these animals are severely impaired in spatial-learning tasks, they are considered passive (Gerlai, 1996) and the development of the corpus callosum is defective (Wahlsten and Bulman-Fleming, 1994; Wahlsten and Schalomon, 1994). Whereas the C56BL/6 strain, which is a more robust strain, performed well in the spatial-learning tasks (Upchurch and Wehner, 1988). Due to strain-dependent differences in behaviour, it is therefore uncertain whether the phenotypical changes observed in the mutant animals are due to the absence of the gene of interest or in fact due to genetic differences in the background genes of the strains used.

To overcome this problem, the most obvious solution would be to generate mutant mice with an isogenic background. Theoretically this could be achieved by targeting C57BL/6 ES cells and then backcrossing germline transmitting chimeras directly with C57BL/6 mice. Heterozygous progeny would be detected by Southern blotting. Initially this seemingly simple solution proved too difficult to accomplish due to the difficulty in isolating ES cells from the C57BL/6 strain (Ledermann and Burki, 1991; Wiles and Keller, 1991), however recently, ES cells have been successfully isolated from the C57BL/6 strain (Kawase et al., 1994; Auerbach et al., 2000). An alternative solution is to decrease the probability of the contribution of background genes by backcrossing the mutant hybrid mice to the strain of choice, such the C57BL/6 strain and thus create a congenic strain that carries the mutation on the desired genetic

background. The degree of congenicity therefore relates directly to the number of backcrosses.

The generation of a congenic mouse strain by backcrossing to eliminate the background genes is a simple and effective technique, however is very timely. F1 males and females heterozygous for the desired mutation are mated with wildtype C57BL/6 mice. By selecting animals heterozygous for the desired mutation, an F2 generation having a 50% decrease in undesired genes is effectively generated. Repeating this strategy will result in the production of animals having a cumulative 50% reduction in the undesired genes for each backcross performed (Crusio, 1996; Gerlai, 1996, Lathe, 1996 #266). Unfortunately this backcrossing approach will never remove 129 derived genes closely linked to the mutated allele.

CHAPTER TWO

MATERIALS AND METHODS

2.1 MATERIALS

2.1.1 General chemicals and reagents

Acrylamide (cat# 161-0101), *Biorad (NSW)*

Agarose (DNA grade) (cat# 200-0011), *Progen (QLD)*

Agar (Bacteriological grade) (cat# 150-178), *ICN Biomedicals (NSW)*

Ammonium acetate (cat# 27-500G), *AJAX CHEMICALS (VIC)*

Ammonium persulphate (cat# A3426), *Sigma (NSW)*

Ampicillin (100 mg/ml) (cat# 835242), *Roche Molecular Biochemicals (NSW)*

5-Bromo-4-chloro-3-indolyl-β-D-galactoside (X-Gal) (cat# V3941), *Promega (NSW)*

Bromophenol blue (cat# 161-0404), *BioRad (NSW)*

Bovine serum albumin (BSA) (5% solution) (cat#A4628), *Sigma (NSW)*

Calcium chloride (CaCl$_2$) (cat# 127500G), *AJAX CHEMICALS (VIC)*

Dextran sulphate (cat# 17-0340-02), *Pharmacia Biotech (VIC)*

Dithiothreitol (DTT) (cat# 95690), *Research Organics (USA)*

Ethidium bromide (cat# 806808). *ICN Biomedicals (NSW)*

Ethylenediaminetetraacetic acid (EDTA) (cat# E5134), *Sigma (NSW)*

Ficol (cat# F4375), *Sigma (NSW)*

Formamide (cat# F7503), *Sigma (NSW)*

Gelatin (cat# G2500), *Sigma (NSW)*

Glucose (cat# 0188), *Astral (NSW)*

Glycerol (cat# 242 500ML), *AJAX CHEMICALS (VIC)*

Herring sperm DNA (cat# 223646), *Roche Molecular Biochemicals (NSW)*

Isopropyl-1-thio-α-D-galactoside (IPTG) (cat# V3951), *Promega (NSW)*

Isopropanol (cat# 425-215L GL), *AJAX CHEMICALS (VIC)*

Maltose (cat# 1126 100G), *AJAX CHEMICALS (VIC)*

MOPS (3-[N-morpholino] propane-sulphonic acid) (cat# 1124684), *Roche Molecular*

Biochemicals

Manganese chloride (MnCl$_2$) (cat# M3634), *Sigma (NSW)*

Magnesium sulphate (MgSO$_4$) (cat# 1548 500G), *AJAX CHEMICALS (VIC)*

MgSO$_4$.7H$_2$O (cat# 29117 2L), *BDH (VIC)*

MgSO$_4$.6H$_2$O (cat# 302 500G), *AJAX CHEMICALS (VIC)*

NZ Amine N,N,N`,N`-Tetramethylethylenediamine (TEMED) (cat# T9281), *Sigma (NSW)*

Polyvinylpyrollidone (cat# PVP 360), *Sigma (NSW)*

Potassium acetate (CH$_3$COOK) (cat# P3542), *Sigma (NSW)*

Potassium chloride (KCl) (cat# 104874S), *BDH (VIC)*

Rubidium chloride (RbCl) (cat# R2252), *Sigma (NSW)*

Salmon sperm DNA (cat# 113456), *Roche Molecular Biochemicals (NSW)*

Sarkosyl (N-lauroylsarcosine) (cat# L5125), *Sigma (NSW)*

Sodium dodecyl sulphate (SDS) (cat# 0027), *Astral (NSW)*

Sodium chloride (NaCl) (cat# X190), *Astral (NSW)*

Sodium hydroxide (NaOH) (cat# 482 500G), *AJAX CHEMICALS* (NSW)

Sucrose (cat# 530 500G), *AJAX CHEMICALS (NSW)*

Trisborate (cat# 1002), *Astral (NSW)*

Tri sodium citrate (Na$_3$citrate.2H$_2$O) (cat# 0101), *Astral (NSW)*

Tris (tris hydroxymethyl-aminomethane) (cat# 708968), *Roche Molecular*

Biochemicals (NSW)

Tryptone (cat# P3278), *OXOID (VIC)*

Urea (cat# 817 5KG), *AJAX CHEMICALS (VIC)*

Yeast extract (cat# 0127-01), *DIFCO Laboratories (USA)*

2.1.2 Other materials

Nick column, Sephadex G-50 (cat# 6854), *Pharmacia Biotech (VIC)*

Hybond N (cat# RPN 132 N), *Amersham Life Sciences (NSW)*

X-ray film (cat# 03E220), *FUJI*

X-ray film (Kodak Scientific Imaging film) (cat# 165 1512), *Integrated Sciences (NSW)*

X-ray Hyperfilm (cat# RPN12), *Amersham (NSW)*

2.1.3 Radiochemicals

$[\alpha^{32}P]$ dCTP (250 µCi) (cat# ADC-2), *Bresatec (SA)*

$[S^{35}]$ dATP (125 µCi) (cat# SDA-2), *Bresatec (SA)*

$[^3H]$-nicotine (81.5 Ci/mmol) (cat# NET 827), *NEN, Life Science Products (USA)*

$[^3H]$-epibatidine (33.8 Ci/mmol) (cat# NET 1102), *NEN, Life Science Products (USA)*

$[^3H]$-cytisine (32 Ci/mmol)(cat# NET 1054) , *NEN, Life Science Products (USA)*

$[I^{125}]$-α-bungarotoxin (2000 Ci/mmol), *a gift from Professor Bevyn Jarrott,*

Department of Pharmacology, Monash University

2.1.4 Plasmids

pBluescript SK +/- phagemid (cat# 212205), *Stratagene (USA)*

PGem-T vector system (cat# A3600), *Promega (NSW)*

2.1.5 Enzymes

Proteinase K (cat# 1092 766), *Roche Molecular Biochemicals (NSW)*

Taq DNA polymerase (cat# N801-0060), *Perkin Elmer (VIC)*

Polynucleotide kinase (PNK) (cat# 2015), *New England Biolabs (QLD)*

DNA ligase (cat# 481220), *Roche Molecular Biochemicals (NSW)*

2.1.6 Kits

Random primed labelling kit (cat# 1004 760), *Roche Molecular Biochemicals (NSW)*

Maxi Plasmid Preparation (cat# 12163), *Qiagen (VIC)*

Wizard plus mini prep DNA purification system (cat# A7510), *Promega (NSW)*

Lambda Phage Maxi Preparation (cat# 12562), *Qiagen (VIC)*

Sequenase Version 2.0 DNA Sequencing Kit (cat# 70770), *Amersham (NSW)*

QuikChange Site-Directed Mutagenesis Kit (cat# 200518), *Stratagene (USA)*

Agarose Gel DNA Extraction Kit (cat# 1696 505), *Roche Molecular*

Biochemicals (NSW)

2.1.7 Synthetic oligodeoxyribonucleotides

Oligodeoxyribonucleotides were synthesized using DNA synthesizer by Life Technologies custom primers, (Life technologies, Gibco BRL) (VIC). All oligonucleotides used in this study are shown in Table 2.1.

Table 2.1 Sequence information of oligonucleotides used.

nAChR Subunit Target	Probe code	Accession number	Probe position	Sequence of oligonucleotide	% GC	Experiment
α_4	E1	131620	485	TATAAGAGCTCCTGCAGCATCGACG	52	PCR
α_4	E3	131620	1476	GTGCGTGGCGAGCGGTGGTGCAC	73	PCR
α_4	E4	131620	1004	GTGCGTGGCGAGCGGTGGTGCAC	74	PCR
α_4	M1			ACGCTGTCAATCTCG	53	PCR
α_4	ISACh1			CGAGGTCGGGATGATCTCGGTGATGAGCAGCAGGAAGACGGTGAGAG	60	In situ
α_4	ISACh2			TGGAGAGGGTGACGAAGATCAGGTGAAGAGCAGGTACTCGCCGATGAGCG	58	In situ
α_4	ISACh3			GCTGTGCATGCTCACCAAGTCAATCTTGGCCTTGTCGTSGGTCCAGGACC	56	In situ
α_4	ISACh4			CATAATGACCCACTCCCCACTTTCCCAGAAGTCCAGTTGGTCCACACGGC	54	In situ
α_3	$\alpha 3$	L31621	1038	CCCAAGTGGGCATGGTGTGTGTGGTTGGAGTTCTATAGTGCACAT	51	In situ
α_6	$\alpha 6\#1$	L08277	325	TCAAAGTGCACCGTGACGGGATCAGAAACGTTTTCCACTGGCCGG	55	In situ
α_6	$\alpha 6\#2$	L08277	1575	GCCCCACAGTTCCAAACACACAGACGATTATAAACACCCAGAGGA	48	In situ
α_7	$\alpha 7$	L37663	197	TCCATGATCTGCAGGAGGCTCAGGGAGAAGTACACGGTGAGCGGC	60	In situ
β_2	$\beta 2\#1$	L31622	1455	TCGCATGTGGTCCGCAATGAAGCGTACGCCATCCACTGCTTCCCG	60	In situ
β_2	$\beta 2\#2$	L31622	1341	AGCCAAGCCCTGCACTGATGCAGGGTTGACAAAGCAGGTACATGG	55	In situ
β_3	$\beta 3\#1$	J04636	1315	CAGAACTCTTTCTCCATCGCTGGCGGGAGTCTGTTTCCTTTTGCC	53	In situ
β_3	$\beta 3\#2$	J04636	440	ATTCTTCCGGATTCCAGCGTAATTTTTGGTCTGTCCATTCCTGCT	44	In situ
β_4	$\beta 4\#1$	U42976	1322	AGCTGACACCCTCTAATGCTTCCTGTAGATCTTCCCGGAACCTCC	53	In situ

2.1.8 Media and solutions for the routine culture of embryonic stem (ES) cells and embryonic fibroblasts (EF)

Dulbeccos's Modification of Eagles Medium (DMEM) (cat# 12100-046), *Sigma (NSW)*

Dulbeccos's Modification of Eagles Medium (DMEM) with Hepes (cat# 23700-040), *Sigma (NSW)*

10 X Hanks (cat# 14180-053), *Sigma (NSW)*

1 M Hepes Buffer (cat# 15630-080), *Sigma (NSW)*

Non essential amino acids (cat# 11140-050), *Sigma (NSW)*

2-β-Mercaptoethanol (cat# 21985-023), *Sigma (NSW)*

Penicillin : streptomycin (cat# 15140-122), *Sigma (NSW)*

Trypsin (0.05%) - EDTA (cat# 15305-014), *Sigma (NSW)*

Trypsin (0.25%) - EDTA (cat# 25200-056), *Sigma (NSW)*

Fetal Calf Serum (FSC) (cat# 10099-141), *Sigma (NSW)*

Geneticin (G418) (cat# 11811-023), *Sigma (NSW)*

Gelatin(cat# 6541), *Sigma (NSW)*

Mitomycin C (2mg ampoule) (cat# 1210), *Sigma (NSW)*

Gancyclovir, *Syntex Corporation*

Leukemia Inhibitory Factor (LIF), *a gift from Dr Surrinda Cheema, Department of Anatomy, Monash University*

Dimethyl sulphoxide (DMSO) (cat# D8779), *Sigma (NSW)*

NaCl (cat# X190), *Astral*

$Na_2HPO_4.2H_2O$ (cat# 0348), *Astral*

$NaHPO_4.2H_2O$ (cat# 0823), *Astral*

NaOH (cat# 0583), *Astral*

All serum was batch tested to ensure its ability to support the growth of ES cells.

Serum was heat inactivated at 57°C for 30 mins prior to use and stored at 4°C following

inactivation.

2.2 PREPARATION OF SOLUTIONS AND BUFFERS FOR MOLECULAR BIOLOGICAL TECHNIQUES

2.2.1 Luria-Bertani (LB) medium

Per Litre

LB medium consisted of 10 g tryptone, 5 g yeast extract and 5 g NaCl, supplemented

with 0.2% maltose and 10 mM $MgSO_4$.

2.2.2 Suspension medium (SM) buffer

SM buffer consisted of 0.1 M NaCl, 8.1 mM $MgSO_4.7H_2O$, 50 ml 1 M Tris- HCl pH 7.5

and 2 ml of 2% gelatin.

2.2.3 Top agar

Per Litre

Top agar consisted of 85.6 mM NaCl, 8.1 mM $MgSO_4.7H_2O$, 5 g yeast extract, 10 g NZ

Amine (casein hydrolysate) and 0.7 % of bacterial grade agarose and was sterilized by

autoclaving.

2.2.4 NZY plates

Per Litre

NZY plates consisted of 85.6 mM NaCl, 8.1 mM $MgSO_4.7H_2O$, 5 g yeast extract, 10 g

NZ Amine (casein hydrolysate) and 1.5 % bacterial grade agarose. This solution was

autoclaved and poured into plates.

2.2.5 1 X Sodium chloride / Sodium Citrate solution (SSC)

0.15 M NaCl and 0.015 M sodium citrate at pH 7.0.

2.2.6 Hybridization buffer

10% dextran sulphate, 1 M NaCl and 1 % sodium dodecyl sulfate (SDS).

2.2.7 Tris borate EDTA (TBE) buffer

45 mM Tris-borate and 1 mM EDTA, pH 8.0.

2.2.8 Tris EDTA (TE) buffer

19 mM Tris.Cl and 1 mM EDTA, pH 8.0

2.2.9 Loading dye

38% (w/v) sucrose, 0.1% (w/v) bromophenol blue and 67 mM EDTA.

2.2.10 SOB medium

2 % bacto tryptone, 0.5 % bacto yeast extract, 10 mM NaCl, 2.5 mM KCl, 10 mM

$MgCl_2$ and 10 mM $MgSO_4$.

2.2.11 RF1 buffer

0.01 mM RbCl, 0.068 mM $MnCl_2$, 0.03 M CH_3COOK, 0.01 mM $CaCl_2.H_2O$ and 15 %

v/v glycerol, pH 5.8.

2.2.12 RF2 buffer

4.14 μM RbCl, 5 mM MOPS, 0.037 mM $CaCl_2.H_2O$ and 7.5 % v/v glycerol, pH 6.8.

2.2.13 SOC solution

33 μl 1M $MgCl_2$ and 66 μl 20% glucose.

2.2.14 2 X Glycerol solution

65% v/v glycerol, 0.1 M $MgSO_4$, 0.025 M Tris.Cl, pH 8.

2.2.15 10 X PCR reaction buffer

50 mM KCl, 15 mM Tris pH 8.4, 1 mM $MgCl_2$ and 0.1 mM dNTPs.

2.3 PREPARATION OF MEDIA AND SOLUTIONS FOR ROUTINE CULTURE OF ES CELLS AND EF

The following consists of a list of solutions used in tissue culture

2.3.1 Phosphate buffered saline (PBS)

17.4 g NaCl (149 μM), 1.1 g $Na_2HPO_4.2H_2O$ (4 μM) and 5.7 g $NaHPO_4.2H_2O$ (36.5 μM) in 2 litres.

2.3.2 0.2% gelatin in PBS

0.2% gelatin was made by diluting a 10 % stock (10 g of gelatin was added to 100 ml of PBS and autoclaved).

2.3.3 Mitomycin C

Contents of one ampoule (2 mg) was dissolved in 10 ml of autoclaved milli Q water, filtered through a 0.2 μM filter (Sartorius) and stored at 4°C wrapped in foil and used for only 10 days.

2.3.4 400 μg/ml Geneticin selective antibiotic (G418)

To make the stock solution, 1 g of G418 powder was dissolved in 10 ml of sterile PBS and filter sterilized through a 0.2 M filter. 2.4 ml of stock was added to 600 ml of ESM for 400 μg/ml of G418.

2.3.5 2 μM Gancyclovir

12.8 mg of gancyclovir powd. was dissolved in 10 ml of autoclaved milli Q water and filter sterilized through a 0.2 μM filter.

2.3.6 0.25 % Hepes-trypsin-EDTA

2 ml of 1 M Hepes was added to 100 ml of 0.25% Trypsin.

2.3.7 ES cell culture medium (ESM)

ES cell complete culture medium consisted of 500 ml 1 X DMEM, 90 ml 15 % FCS, 3 ml penicillin/streptomycin, 1 ml 2-β mercaptoethanol, 6 ml non-essential amino acids and 6.7 μl LIF (100 μg/ml).

2.3.8 EF culture medium (EFM)

EF cell complete culture medium consisted of 500 ml 1 X DMEM, 50 ml 10 % FCS and 5 ml penicillin/streptomycin.

2.3.9 Hanks / Hepes (H/H)

H/H buffer contained 50 ml of 10 X Hanks, 10 ml of 1 M Hepes, 1.25 ml of 1 M NaOH and 438.75 ml autoclaved milli Q water.

2.3.10 Electroporation buffer (EB)

EB contained 5 ml 10 X Hanks, 1 ml 1M Hepes, 0.1 ml 2-β mercaptoethanol, 50 μl 1 M NaOH and 44 ml of autoclaved milli Q water.

2.3.11 Blastocyst injection media (BIM)

BIM contained 1 X DMEM, 1 M Hepes, 1 M NaOH and 10 % FCS.

2.3.12 2 X Freezing medium (2X FM)

2 X FM contained 2ml of DMSO, 2 ml of FCS and 6 ml of ESM.

2.4 IN SITU HYBRIDIZATION AND LIGAND BINDING

2.4.1 Hybridization buffer

50% deionised formamide, 4 X SSC, 1 X Denhardt's solution, (2 % of each of Ficol, Bovine Serum Albumin and Polyvinylpyrolidone in 0.1 % Sarcosyl), 10 % dextran sulphate and 0.5 mg/ml Herring Sperm DNA.

2.4.2 Krebs-Ringers HEPES

118 mM NaCl, 4.8 mM KCl, 2.5 mM CaCl$_2$, 1.3 mM MgSO$_4$7H$_2$O, 20 mM HEPES, pH to 7.5 with NaOH.

2.5 MOLECULAR BIOLOGICAL METHODS

2.5.1 Screening a library

The α_4 nAChR subunit gene was isolated from a 129/*Sv* lambda genomic library (Lambda Fix II vector, Strategene). The titre of the library was determined so that accurate concentrations of the phage could be plated out. A single colony of XL1-Blue MRA cells (Stratagene) was inoculated in 50 ml of LB medium and the culture then incubated at 30°C overnight with moderate shaking. This temperature ensures that the cells do not overgrow, as phage can adhere to dead as well as live cells and thus lower the titer. The cells were then centrifuged in sterile conical tubes for 10 min at 2000 rpm. The supernatant was carefully removed and the cell pellet gently resuspended in 15 ml of 10mM MgSO$_4$. The cells were then diluted in 10 mM MgSO$_4$ to obtain OD$_{600}$ = 0.5. The phage DNA was serially diluted by 100 fold starting with 2 μl in 198 μl SM buffer. In a sterile 12 ml Falcon tube, 200 μl of host cells was added to 10 μl of each phage dilution and incubated at 37°C for 15 min. Three ml of melted top agar, pre-heated to 48°C, was added to infected bacteria and spread evenly over prewarmed 100 mm diameter NZY plates. The plates were dried for 10 min at room temperature and incubated overnight at 39°C. Following this incubation, plaques were visible as clear areas (1-2 mm) on a bacterial lawn. The number of plaques were counted and the concentration of the library was determined in plaque forming units (pfu) / ml.

2.5.2 Screening process

Phage was diluted to give 8×10^4 pfu / 100 mm diameter plate and added to 600 µl of cells (cells prepared as above $OD_{600} = 0.5$). This was incubated at 37°C for 15 min and added to 6.5 ml of top agar (pre-heated to 48°C) and spread evenly over prewarmed 150 mm diameter NZY plates. The plates were dried at room temperature for 10 min and incubated overnight at 39°C. Following this incubation, plates were chilled at 4°C for 2 hs to prevent top agar sticking to the membrane. Optimal phage concentration resulted in the plates having a characteristic lace mesh-like appearance. Phage DNA was transferred onto hybond nylon membranes (Amersham, Life Sciences) for 2 min. Filter orientation was established by random needle holes through the membrane when in contact with the plates. Duplicates were made and the second transfer was carried out for 4 min. Filters were denatured by submerging in 1.5 M NaCl, 0.5 M NaOH for 5 min, then neutralized by submerging in 0.2 M Tris-HCl pH 7.5, 2 X SSC and then blotted onto Whatmann 3MM paper. The DNA was then crosslinked to the filters for 30 sec using an autocrosslink setting on the Stratalinker UV crosslinker. The agar plates were routinely stored at 4°C during processing of membranes.

2.5.3 cDNA probes

A random primed labelling kit (Roche Molecular Biochemicals) was used to [32] P-label cDNA probes. Twenty five ng of DNA was added to water in a final volume of 9 µl, denatured for 7 min at 96°C and then chilled on ice for 2 min. Three µl of nucleotide mix (dATP, dGTP, dTTP), 2 µl of reaction mix, 5 µl of α-[32]P dCTP (270 µCi) (Bresatec) and 1 µl of Klenow fragment of DNA Polymerase I was added and the reaction incubated at 37°C for 30 min. The reaction was stopped by adding 4 µl of 0.1 M EDTA. Labelled cDNA was separated from unincorporated nucleotides by using a

nick column (Sephadex G-50, Pharmacic Biotech). The column was emptied and washed once with TE pH 8, refilled and the solution allowed to drip through. Thirty μl of TE pH 8 was added and the final volume of labelled cDNA (54 μl) was added to the prepared nick column and the mixture allowed to flow through. The column was washed twice with 400 μl of TE, pH 8, and the second wash collected into an Eppendorf tube. The radioactivity of the probe was estimated by placing 1 μl next to the Geiger counter (series 900 mini monitor). Only labelled probes with counts greater than 50 counts per sec were used.

2.5.4 Hybridization of probes to filters

Filters were prehybridised at 65°C in 10 ml of hybridization buffer for a minimum of 3 hr. Following this initial prehybridization period, filters were hybridized in fresh buffer with the addition of heat denatured probes. Twenty μl of labelled cDNA probe was added to 20 μl of salmon sperm DNA (Roche Molecular Biochemicals) (100 μg / ml) and denatured by boiling at 100°C for 7 min and chilling on ice for 2 min. The filters were routinely hybridised at 65°C for approximately 16 hr. The membranes were then washed under high stringency conditions in the following order: 30 min in 2 X SSC at 65°C, 30 min in 2 X SSC, 1% (w/v) SDS at 65°C (pre-heated to 65°C) and 30 min in 0.1 X SSC at room temperature. The samples were agitated throughout all washing steps.

2.5.5 Autoradiography

Autoradiography of filters that had been hybridised to ^{32}P-labelled probes was carried out by exposing to X-ray film (FUJI) with an intensifying screen (Roland Scientific) at -70°C. Film was subsequently developed for 3 min at room temperature in Kodak D-19

Photo Developer, dipped in Kodak indicator Stop Bath for 1 min, then immersed for 3 min in Ilford Hypam Paid Fixer and washed in running water for 20 min.

2.5.6 Secondary screening

The autoradiographs were aligned with the orientation dots and the strongest "putative" clones selected. The plaques were cut out using a pasteur pipette and placed into 1 ml of SM buffer. The phage was then diluted and added to host cells as above and added to the 100 mm NZY plate so that one plate had approximately 50 plaques and the second had approximately 450 plaques. Phage DNA was then transferred to nylon membranes (section 2.5.2), probed, (section 2.5.4) and the film exposed and developed (section 2.5.5).

2.5.7 Tertiary screening

Tertiary screening was only required if phage was not a pure isolate (not all "dots" on film correspond to lytic plaques). The autoradiograph was lined up as before and an isolate cut from the plate. An isolate in 1 ml of SM represents approximately 1×10^6 pfu's. These "cored" putatives were stored at 4°C in SM buffer with 2% chloroform. After a true isolate was obtained, a large scale phage preparation was performed.

2.5.8 Large scale phage preparation

The phage was plated out on 100 mm diameter plates at an appropriate titer to obtain confluency. A single colony of XL-blue bacteria (Stratagene) was inoculated in 200 ml of LB containing 2 ml of 1 M $MgSO_4$ and 50 µl of 1 M $CaCl_2$ and then incubated overnight in a bacterial shaker. Following the incubation, 10 ml of cell suspension was pelleted at 2000 rpm for 10 min and resuspended in 10 ml of LB containing 10 mM

MgSO$_4$. The phage was collected from the plate by rocking the plate in 4 ml of SM buffer for 4 hrs and was then added to the bacteria. The cell suspension was incubated for 10 min at 37°C to inoculate the phage. One hundred and ten ml of LB containing 10 mM MgSO$_4$ was added and incubated at 37°C for about 4 hrs or until the cells had lysed. Chloroform (1.2 ml) was then added and incubated again for 15 min at 37°C. The phage was then purified using a Qiagen Lambda maxi kit. All buffers described in this precedure were supplied in the kit. Four hundred μl of Buffer L1 was added to 250 ml of phage preparation and incubated at 37°C for 30 min. Following the incubation, 50 ml of ice-cold Buffer L2 was added, mixed gently and incubated on ice for 60 min. This was then centrifuged at >10,000 x g for 10 min and the supernatant discarded. The pellet was then resuspended in 9 ml of Buffer L3 by pipetting up and down. Three ml of Buffer L4 was then added, mixed gently, incubated at 70°C for 20 min and then chilled on ice. Nine ml of Buffer L5 was then added, mixed gently and centrifuged at 4°C for 30 min at ≥15,000 x g. The supernatant was removed promptly and then centrifuged again at 4°C for 10 min at ≥15,000 x g to obtain a particle free lysate. A Qiagen-tip 500 was equilibrated with 10 ml of Buffer QBT and the supernatant added and flowed through by gravity. The Qiagen-tip 500 was washed with 30 ml of Buffer QC and the DNA eluted with 15 ml of Buffer QF. The phage DNA was then precipitated using 0.7 volumes of isopropanol and centrifuged at room temperature or 4°C for 30 min at ≥15,000 x g. The DNA was then washed with 70 % ethanol and air dried.

2.5.9 Restriction enzyme digests

Plasmid DNA was digested for cloning using restriction enzymes purchased from Roche Molecular Biochemicals. One μg of DNA was digested in a 20 μl reaction

digest, containing 0.5 µl of restriction enzyme, 2 µl of 10 X reaction buffer and distilled H_2O (dH_2O). The reaction was incubated for 1 hr at the optimal temperature for the restriction enzyme (as recommended by Roche Molecular Biochemicals). For genomic DNA digests, 30 µl was digested in a 50 µl reaction digest, containing 5 µl of restriction enzyme, 5 µl of 10 X reaction buffer and dH_2O. The reaction was incubated overnight at the optimal temperature for the restriction enzyme (as recommended by Roche Molecular Biochemicals)

2.5.10 Agarose gel electrophoresis

DNA in the size range 0.1 – 20 kb was resolved by electrophoresis at 30 – 100 V in 0.8 – 2.5% agarose gels containing 0.5 µg / ml ethidium bromide (ICN Biomedicals) and run in 1 X TBE. Samples were prepared for loading by adding 1/6 volumes of loading dye. The DNA was detected by fluorescence using a UV light box (312 nm Spectroline TVC-312A) and gels photographed using a polaroid camera.

2.5.11 Purification of DNA from agarose gels

DNA was recovered from agarose gels using an Agarose Gel DNA Extraction Kit (Roche Molecular Biochemicals). A gel slice containing the DNA (~100 mg) was excised from a 1.0 % agarose gel and placed in an Eppendorf tube. Three hundred µl of agarose solubilisation buffer and 10 µl of silica suspension was added and incubated for 10 min at 56°C - 60°C (vortexing every 2-3 min). Following the incubation, the mixture was spun in a microcentrifuge (Eppendorf centrifuge 5415C) at 14,000 rpm for 30 sec, the supernatant discarded and the matrix containing the DNA was then resuspended in 500 µl of nucleic acid binding buffer. The mixture was centrifuged again as before and the supernatant discarded. The pellet was washed two times with

500 µl of washing buffer and then air dried for 15 min. The DNA was eluted by adding 20 µl of TE to the pellet, vortexing and then incubating at 56°C - 60°C for 10 min (vortexing every 2-3 min). This was then centrifuged as above and the DNA containing supernatant transferred to a new tube. To increase the efficiency, 2 elution cycles were performed.

2.5.12 Competent cells

Competent cells were used for transformation of plasmids. A single colony of XL1 Blue cells was inoculated into 10 ml of SOB medium and incubated at 37°C overnight in a bacterial shaker. Following the incubation, 1 ml of cells was inoculated in 100 ml of SOB and incubated at 37°C with moderate agitation until the cell density was 4-7 x 10^7 viable cells / ml (OD_{600} = 0.55). The cells were centrifuged in 50 ml polypropylene centrifuge tubes at 2000 – 3000 rpm for 12 – 15 min at 4° C and then chilled on ice for 10 - 15 min. The cell pellet was resuspended by moderate vortexing in a volume of RF1 buffer that is 1/3 of the volume collected (i.e. 33 ml) and incubated on ice for 1 h. The cells were centrifuged as above and the pellet resuspended in a volume of RF2 buffer equal to 1/12.5 of the original volume of cells (i.e. 7ml) and incubated on ice for 15 min. RF1 buffer and RF2 buffer were made up fresh on the day, filter sterilized and chilled on ice. Following the incubation, the cells were aliquoted into chilled autoclaved screw-capped tubes or 1.5 ml microcentrifuged, flash frozen in a solid CO_2 / ethanol bath or in liquid nitrogen and then stored at -70°C.

2.5.13 Ligation

Cohesive termini ligations and blunt ended ligations were both commonly used. Ligation reactions were carried out using T4 DNA ligase and T4 DNA ligase buffer

(Roche Molecular Biochemicals). Reactions were designed to contain between 3:1 and 10:1 molar ratios of insert to vector. Reactions were performed in 10 µl reaction volumes and incubated at 14°C for 3 hrs (cohesive termini) or overnight (blunt ended).

2.5.14 Transformation

Ligation mixes and plasmid DNA were transformed into competent cells by the following method. Fifty ng of the plasmid DNA or 5 µl of ligation mix was added to a pre-chilled 12 ml falcon tube containing 200 µl of thawed competent cells. The cells were gently mixed with the DNA and incubated on ice for 30 min. Following the incubation, the cells were heat shocked in a 45°C water bath for 45 sec and then placed immediately back on ice. Eight hundred µl of prechilled SOC solution was added to the cells and incubated at 37°C for 1 hr in a bacterial shaker at maximum speed. The cells were then plated onto a 90mm diameter LB plate containing ampicillin (50 µg/ml) and incubated at 37°C overnight.

2.5.15 Blue / white selection

Blue / white selection was used to identify positive clones for cloning into pBluescript. One hundred µl of 0.1 M IPTG (Promega) stock and 16 µl (50 mg / ml) X-Gal (Promega) was spread over a 90 mm diameter LB / ampicillin plates and dried at room temperature. Positive colonies containing an insert were clear, indicating the disruption of the β-galactosidase gene and colonies without the insert were blue.

2.5.16 Small scale plasmid preparation

Small scale plasmid preparations were performed using the Wizard Plus Mini Prep DNA Purification System (Promega). Following transformation reactions, single

colonies were inoculated in 3 ml of LB medium containing ampicillin (50 μg/ml) and incubated overnight at 37°C in a bacterial shaker. Following the incubation, 1.5 ml of the cells were isolated by centrifugation for 2 min at 14,000 rpm in a microcentrifuge. The pellet was resuspended in 200 μl of resuspension buffer and then 200 μl of cell lysis buffer was added and mixed by inverting the tube several times. Two hundred μl of neutralization buffer was added, mixed and centrifuged as above for 5 min. The supernatant was transferred to a new Eppendorf tube and 1 ml of wizard minipreps DNA purification resin added and mixed by inversion. The plasmid DNA was purified by adding the contents to a wizard minicolumn and attaching the column to the luer-lock extension of each minicolumn. This was then assembled onto the vacuum manifold and a vacuum applied until all the solution had been sucked through the column. The column was washed by adding 2 ml of column wash solution and then reapplying the vacuum. Once the solution had been sucked through, the vacuum was applied for an additional 1-2 min. The filters were removed and transferred to Eppendorf tubes. The Eppendorf tubes were then centrifuged at 14,000 rpm in a microcentrifuge and the minicolumn transferred to a new Eppendorf tube. To elute the plasmid DNA, 50 μl of TE buffer pH 8 was added to the minicolumn and incubated for 1 min. For plasmids greater than 10 kb, the TE was pre-heated to 65°C. The Eppendorf tubes were then centrifuged at 14,000 rpm for 20 sec to elute the plasmid, which was subsequently stored at 4°C for short term storage and at -20°C for long term storage.

2.5.17 Large scale plasmid preparation

For large scale preparation of plasmid DNA, the Qiagen Maxi Plasmid Preparation Kit was used. All buffers used were supplied in the kit. One hundred μl of mini prep bacterial stock was inoculated in 200 ml of LB medium, containing 100 μg/ml of

ampicillin. The cells were incubated at 37°C overnight in a bacterial shaker at maximum speed. Following this incubation, the cells were added to 5 centrifuge tubes (50 ml) and centrifuged at 4,000 rpm. The supernatant was discarded and the cell pellet resuspended in 8 ml of buffer P1. Eight ml of P2 buffer was then added, mixed gently by inverting the tubes 5 times and then incubated at room temperature for 5 min. Following this incubation, 8 ml of chilled P3 was added, mixed again by inversion and then incubated on ice for 20 min. The mixture was then centrifuged at 13,000 x g for 30 min at 4°C and the supernatant transferred to a new 50 ml tube. This centrifugation step was repeated to further purify the supernatant. The kit column was equilibrated with 10 ml of QBT buffer and the supernatant added and allowed to flow through. The column was washed twice with 30 ml of QC buffer and the DNA eluted using 15 ml of QF buffer. The DNA was precipitated using 0.7 volumes of isopropanol and mixed by inversion. This solution was then centrifuged at 14,000 x g at 0°C and the supernatant quickly removed. The pellet was then dissolved in 300 µl of TE buffer pH 8 and transferred to an Eppendorf tube. Ethanol precipitation was performed using 1/10 volume sodium acetate pH 5.2 and 2.5 volume ice-cold 100% ethanol and incubating at -70°C freezer for 15 min. The DNA solution was then centrifuged for 5 min in a microcentrifuge at 14,000 rpm. The supernatant was removed and the pellet washed twice with 1 ml of 70% ethanol. The pellet was air-dried and then resuspended in 300 µl of TE buffer, pH 8. An aliquot of DNA was restriction mapped and stocks stored at -70°C. In all cases, frozen stocks of bacteria were made by adding 20µl of mini prep stock to 200 µl of 2 X glycerol solution and storing at -70°C.

2.5.18 DNA sequencing

DNA sequencing was performed using the Amersham Sequenase Version 2.0 DNA sequencing kit. Two μl of freshly prepared 2 M NaOH, 1 mM EDTA solution was added to 4 μg of DNA in 18 μl of dH$_2$O, incubated at 65°C for 5 min and then immediately chilled on ice. Two μl of 2 M ammonium acetate pH 4.6, was added to the solution and vortexed. Seventy five μl of 100% ethanol was then added, the solution vortexed again and incubated at -20°C for 15 min. This was then centrifuged at 12,000 x g for 10 min. The pellet was then washed in 60 μl of 70% ethanol and air dried for 5 to 10 min. Two μl of 5 x sequenase buffer, 1 μl primer and 7 μl dH$_2$O was added to the pellet and incubated at 37°C for 15 min. While incubating, the labelling mixture was diluted 1:4 with dH$_2$O and the sequenase was diluted 1:7 with dilution buffer. Following the incubation, 1 μl of DTT, 2 μl of labelling mixture, 0.5 μl [^{35}S] dATP (125 μCi) (Bresatec) and 2 μl sequenase was added and 3.5 μl of this was added to 4 Eppendorf tubes pre-filled with either 2.5 μl ddA, ddT, ddC, or ddG, pre-warmed to 37°C for 1 min. This was incubated at 37°C for exactly 3 min and then chilled on ice. Four μl of stop solution was added to each tube and the samples stored at -20°C until loading.

Sequencing reactions were resolved by electrophoresis at 2000 V in a 30% acrylamide gel. The gel was prepared by dissolving 42 g of urea in 10 ml of 10 x TBE, 16.7 ml 30% Acry/Bis and 42 ml H$_2$O and then degassing for 5 to 10 min. One hundred μl of 25% ammonium persulphate and 75 μl TEMED was added and the gel cast as per manual instruction. The samples were heated at 75°C for 2 min and then 4 μl loaded when the temperature of the gel reached 50°C. After electrophoresis, the gel was dried

onto 3MM Whatman paper using a Slab Gel Drier GD40/50 (Gibco BRL), then exposed to Kodak Scientific Imaging film (Integrated Sciences) for 36 h and developed (section 2.5.5).

2.5.19 Site-directed mutagenesis

A two base pair mutation was created using a QuikChange Site-Directed Mutagenesis Kit (Stratagene). This method is performed using *Pfu* DNA polymerase, which replicates both plasmid DNA strands with high fidelity. The basic procedure utilizes a supercoiled double stranded vector with an insert of interest and two synthetic oligonucleotide primers containing the desired mutation, which are complementary to opposite strands of the vector. The oligonucleotide primers extend during temperature cycling by means of *Pfu* DNA polymerase. On incorporation of the oligonucleotide primers, a mutated plasmid containing staggered nicks is generated. Following temperature cycling, the product is treated with *Dpn* I, which is specific for methylated and hemimethylated DNA and is used to digest the parental DNA template and to select for mutation-containing synthesized DNA. Mu1 and Mu2 oligonucleotides were designed to contain the 2 base change in the middle of the oligonucleotide. In a polymerase chain reaction (PCR) tube, 50 ng of plasmid DNA, 5 μl of 10 X reaction buffer, 125 ng of oligonucleotide Mu1, 125 ng of oligonucleotide Mu2 and 1 μl of 10 mM dNTP mix (2.5 mM each NTP) were added to a final volume of 50 μl. One μl of *Pfu* DNA polymerase (2.5 U / μl) was added and the reaction cycled in a Gene Amp PCR system (Perkin - Elmer Model 2400) using the recommended cycling parameters as indicated by the instruction manual. Following the PCR reaction, 1 μl of the *Dpn* I restriction enzyme (10 U / μl) was added, mixed thoroughly, spun in a microcentrifuge for 1 min and then incubated at 37°C for 1 h to digest the parental supercoiled DNA.

The 1 µl of the *Dpn* I-treated DNA was then transformed (section 2.5.14) into 50 µl of Epicurian Coli XL1-Blue Supercompetent Cells (Stratagene).

2.5.20 Colony hybridization

For colony hybridization, the ligation mixture was plated onto 150 mm diameter LB / ampicillin plates and incubated overnight to give single colonies. Transfer of colonies onto nitrocellulose was carried out as per section 2.5.2. Appropriate cDNA probes were made (section 2.5.3), the filters hybridized (section 2.5.4), exposed to X-ray film and developed as per section 2.5.5. The plates were re-incubated at 37°C until the colonies had grown to a suitable size for picking (6 hr). The plates and film were aligned using orientation marks and positive colonies identified. Positive clones were picked and plasmid DNA purified by mini plasmid preparation (section 2.5.16).

2.5.21 Polymerase chain reaction (PCR)

PCR was used to amplify DNA. One µg of DNA was used in the PCR reaction to amplify genomic DNA and 1 ng was used to amplify plasmid DNA. All PCR reactions contained the correct concentration of DNA, 10 µM of primers, 5 µl of 10 X PCR reaction buffer and 0.5 µl of 1.25 U Taq polymerase (Perkin Elmer) in a final volume of 50 µl. The reaction mix was then heated at 94°C for 5 min in a Gene Amp PCR system. For all PCR reactions undertaken in this thesis, strand separation was carried out for a further 20 sec at 94° C followed by 35 cycles consisting of annealing at 58°C for 20 sec and extension at 72°C for 1 min. The PCR products were analyzed by agarose gel electrophoresis (section 2.5.10) on a 1.0 % TBE gel.

2.6 TISSUE CULTURE METHODS

2.6.1 Routine culture of ES cells

ES cells (both J1 and R1 lines) grew as colonies and were trypinized every 2 to 3 days to avoid differentiation. All reagents were pre-warmed to 37°C before use and cells were trypinized as follows. The culture medium was aspirated and the layer of cells washed twice with 4 ml of H/H per 6 cm petri dish. The cells were then trypsinized by the addition of 1 ml of 0.25% hepes-trypsin-EDTA, 1 M Hepes per 6 cm dish and incubated at 37°C for 2.5 min. The was then gently swirled until the cells started to detach from the bottom of the dish and were then incubated for a further 2.5 min. A single cell suspension was obtained by pipetting the mixture, approximately 10 times, using a 1 ml plastic pipette and the trypsin then inactivated by the addition of 4 ml of ESM. The suspension was pipetted 16 times and centrifuged at 1300 rpm for 3 min. The supernatant was then removed and the cell pellet gently resuspended in 1 ml of ESM. A 1 in 10 dilution of a confluent plate of ES cells in a volume of 1 ml was usually replated onto Mitomycin C treated feeder layer of embryonic fibroblasts (section 2.6.5), an additional 3 ml of ESM was added and the cells incubated at 37°C with 5% CO_2 in air.

2.6.2 Freezing ES cells and EF

ES cells (section 2.6.1) and EF (section 2.6.4) were grown to subconfluency and harvested as normal. The cells were centrifuged at 1300 rpm and resuspended at a density of 2×10^6 cells / ml in ESM. For freezing, 0.4 ml of cells were dispensed into a freezing ampoule containing 0.4 ml of 2X FM. The freezing ampoule was then placed inside a polystyrene box, sealed with tape and then placed in a -70°C freezer overnight.

The polystyrene box allowed slow freezing of the ES cells and EF. The next day, the ampoules were transferred to liquid nitrogen storage unit for long term storage.

2.6.3 Isolation of primary mouse embryo fibroblasts

In order to be able to use selection medium containing G418 to select for targeting vector incorporation, it was necessary to use a feeder layer of neomycin resistant embryonic fibroblasts (EFN). We derived EFN from mice homozygous for the D3 dopamine targeted allele (Accili, et al., 1996). Each cell therefore had 2 copies of the neomycin phosphotransferase (NEO) gene under the influence of the phosphoglycerokinase promoter. The method of isolating embryonic fibroblasts was identical for both routine culture of ES cells (grown on embryonic fibroblasts derived from CBA mice) and ES cells under G418 selection (neomycin resistant fibroblasts). A 14 to 16 day pregnant D3 knockout mouse was killed by cervical dislocation. The pregnant uterus was dissected out using sterile forceps and iris scissors and placed in a petri dish of sterile PBS. The dish was swirled around to remove the maternal blood and the embryo containing uterus was transferred to a second petri dish of sterile PBS and into a class II biohazard cabinet. The embryos were dissected out of the uterus and the head, feet, hands, heart and the liver removed and discarded. The embryo bodies were placed in another petri dish containing sterile PBS and the bodies chopped using a scalpel blade. The embryos were then transferred to a 50 ml Falcon tube containing 25 ml of 0.05% trypsin-EDTA. The contents were gently triturated using a 10 ml pipette several times to disperse the tissue and then incubated at 37°C in a water bath for 30 min, with inversion of the tube every 5 to 10 min. Five ml of FCS and 20 ml of EFM was added to the aspirated supernatant to inactivate the trypsin. Another 5 ml of 0.05% trypsin-EDTA was added to the remaining clumps and this was then incubated at 37°C

transferred to a 10 ml tube and then centrifuged at 1300 rpm for 3 min. The cells were resuspended in 1 ml of EFM and seeded into pre-gelatinized 6 cm petri dishes of appropriate concentration. The feeders were routinely used within 2 hs and up to one week after plating.

2.6.6 Electroporation of ES cells

ES cells were expanded to 5 confluent 6 cm petri dishes. This gave approximately 1.6 x 10^7 cells for electroporation. The cells were harvested and the cell pellet resuspended in 10 ml of EB. The cells were then transferred to a 50 ml Falcon tube and washed again with 30 ml of EB. The cells were centrifuged at 1300 rpm for 3 min and resuspended at 1.5 x 10^7 cells / ml in 0.8 ml of EB and placed in a 0.4 cm electrode cuvette (BioRad 165-2088). The targeting construct was linearized with the restriction enzyme Not I and 50 μg of DNA resuspended in dH_2O added to the cuvette containing the ES cells. Using a Bio-Rad gene pulser, a pulse of 0.4 kV and 25 μF (McMahon and Bradley, 1990) was delivered to the cells. Before the cells were plated out, they sat at room temperature for 10 min and were then plated onto thirty 6 cm petri dishes at 2.5 x 10^5 cells / plate. Twenty four hs later, 28 of the plates received ESM containing 400 μg / ml G418 (Gibco BRL) and 2 μM gancyclovir (Syntex corporation). Of the remaining 2 plates, 1 received ESM only, as it was used to assess colony survival after electroporation and the remaining plate received ESM containing 400 μg / ml of G418, without gancyclovir, as it was used to assess the degree of enrichment by gancyclovir. The medium was changed each day on all plates for approximately 7 days and negative selection was stopped after day 5.

2.6.7 Harvesting of neomycin resistant ES cells

ES cells proliferated and formed tight colonies after plating. Cell death started after 3 days and progressed over the culture period with discrete ES colonies becoming apparent to the naked eye after 7 days in culture. Gancyclovir enrichment resulted in a 10 fold decrease in the number of colonies per late. Plates treated with G418 and gancyclovir resulted in an average of 2 colonies per plate, whereas plates treated with G418 alone had about 20 colonies. The medium was removed and fresh ESM containing G418 was added several hours before picking. The plates were washed twice with H/H and the colonies aspirated one at a time into a pulled-pasteur pipette by mouth suction and transferred to a well of a 96 well U-bottom plate containing 30 µl of a 1:10 dilution of 0.25 % trypsin-EDTA with H/H. Sixteen colonies were picked in succession (i.e. 2 vertical rows) and incubated for 5 min at 37°C. Using a Gilson multichannel pipette, the colonies were dispersed by pipetting 2 to 3 times and then 50 µl of ESM containing G418 was added to the wells. The colonies were pipetted aggressively a further 10 times and the cells dispensed onto a 24 well plate containing EFN feeder cells. ES cells were grown in 0.5 ml of ESM containing G418.

2.6.8 Harvesting and freezing clones

A large proportion of the cells within the clones died after individual clones were dispersed. Confluent ES cells were established within 24 wells between 3 and 7 days after plating. Individual clones were harvested as soon as they became 50% confluent. The cells were washed with H/H and then 200 µl of 0.25 % trypsin-EDTA was added and the cells incubated at 37°C for 5 min. Four hundred µl of ESM was added to each well and agitated 10 times with a P-1000 Gilson pipette. Four hundred µl of each cell suspension was then transferred into a freezing ampoule containing 400 µl of 2X FM

and frozen (section 2.6.2). The remaining cells were transferred to a pre-gelatinized 24 well plate containing 0.5 ml of ESM for DNA preparation.

2.6.9 Isolation of genomic DNA from 24 well plates for Southern blot analysis

The 24 well cultures were harvested when they were confluent. Confluent wells were washed with H/H and then 0.5 ml of lysis buffer containing 0.1 mg / ml of proteinase K (Roche Molecular Biochemicals) was added. The next day, the contents were transferred to an Eppendorf tube and 0.5 ml of isopropanol added and the tubes mixed by inversion to precipitate the DNA. Using a blue tip, the precipitated DNA was scooped out and transferred to a new tube containing 70% ethanol. The tubes were then centrifuged for 10 min and the DNA washed with 70% ethanol. The ethanol was removed and the pellet air dried for 10 min. Two hundred μl of TE was added and the tubes incubated overnight at 37°C. The following day, the DNA was resuspended completely by pipetting up and down several times.

2.6.10 Southern blot transfer

After digestion, ES cell genomic DNA was transferred from agarose gels onto nitrocellulose membrane (GeneScreen Plus, Biotechnology Systems NEN Research Products) by capillary action in 10 X SSC (Sambrook, 1989). Following the transfer process, the filter was UV cross linked using a UV light box for 5 min. The filter was then baked at 60°C for 30 min prior to hybridization.

2.6.11 Hybridization of probes to filters

Filters were prehybridized at 65°C in 10 ml of hybridization buffer for a minimum of 3 hr. Following this initial prehybridization period, filters were hybridized in fresh buffer

with the addition of heat denatured probes. One hundred μl of the labelled cDNA

probes and 100 μl of 100 μg / ml salmon sperm DNA (Roche Molecular Biochemicals)

were denatured by heating at 100°C for 7 min and chilling on ice for 2 min. The filters

were routinely hybridized at 65°C for approximately 16 hr. The filters were then

washed as follows: 30 min in 2 X SSC at 65°C; 30 min in 2 X SSC containing 1% (w/v)

SDS (pre-heated to 65°C) at 65°C; 30 min in 0.1 X SSC at room temperature.

Autoradiography was carried out as per section 2.5.5.

2.6.12   Harvesting ES cells for blastocyst injection to produce chimeras

Positive clones were validated for both 5' and 3' recombination events and also proven

to have a single insertion with a NEO cDNA probe. Clones were thawed into a 24 well

plate containing EFN and grown to confluency in ESM containing G418. The cells

were then harvested and transferred into 6 cm diameter plates for expansion prior to

blastocyst injection. The cells were harvested as described in section 2.6.8, washed

twice with 30 ml of BIM and then resuspended in 1 ml of BIM. The cells were then

counted using a haemocytometer and resuspended in BIM cell medium at a

concentration of 2×10^5 cells / ml, which was found to be optimal for blastocyst

injection.

2.6.13   Microinjection of ES cells into blastocysts

Microinjection of ES cells was kindly performed by Professor Imail Kola's team at the

Institute of Reproduction and Development, Monash University.

The Materials and Methods for *in situ* hybridization, receptor autoradiography and

behavioural studies are detailed in the subsequent chapters.

in a water bath for a further 5 min. Again the supernatant was removed and EFM added to inactivate the trypsin. The cell pellet from each of the two 50 ml Falcon tubes was then isolated by centrifugation for 12 min at 1200 rpm. The cells from each tube were then resuspended in 45 ml of EFM, the total cell suspension pooled and 15 ml plated onto 10 cm petri dishes. The cells were then transferred to an incubator at 37°C with 5% CO_2 in air. This primary culture was left undisturbed for 6 hr, at which point cell clumps not attached to the substratum were aspirated and discarded. About 3 days later confluent monolayers were washed 2 X with 10 ml of PBS. Then 2 ml of 0.05% trypsin-EDTA was added and a single cell suspension obtained and divided between 3 large tissue culture flasks (175 cm^2) per 10 cm petri dish. The cells were then cultured for a further 3 to 4 days until confluent after which time the fibroblasts were harvested for freezing and stored at 3×10^6 cells per 1 ml ampoule.

2.6.4 Routine culture of EF

For routine use, 1 ampoule of frozen EF (containing 3×10^6 cells) were recovered from liquid nitrogen and seeded into a medium tissue culture flask (75 cm^2) in 15 ml of EFM. When confluent, the cells were passaged into large flasks (150 cm^2).

2.6.5 Mitomycin C treatment of EF for use as feeder layers

Cultures to be treated were selected when sub-confluent (actively growing). Twenty ml of EFM containing 200 μg/ml Mitomycin C (Gibco BRL) was added to a large flask of EF and incubated at 37°C for 3 hr. After incubation, the medium was removed and the monolayer washed twice with 30 ml of PBS. The cells were trypsinized by the addition of 3 ml of 0.05% trypsin-EDTA for 1 min at 37°C. The cells were swirled to make sure they were completely detached. Seven ml of EFM was added to the trypsinized cells,

CHAPTER THREE

GENERATION OF AN α_4 NICOTINIC

ACETYLCHOLINE RECEPTOR SUBUNIT GENE

KNOCKOUT MOUSE.

4

3.1 RESULTS

Cloning the α_4 nAChR subunit gene

Most ES cells are derived from the 129/*Sv* strain of mouse and the use of targeting constructs made with isogenic (129) DNA has been found to be important to achieve optimal targeting efficiency (Waldman and Liskay, 1988). A lambda mouse 129/*Sv* genomic ES cell library (Stratagene) was screened using a 1 kb cDNA probe encoding part of the fifth exon of the α_4 nAChR. This cDNA encodes the putative second transmembrane domain of this receptor subunit. The 1 kb α_4 nAChR cDNA probe was cloned by PCR amplification of ES cell genomic DNA using a forward primer, E1, and a reverse primer, E3. E1 and E3 were designed based on conserved regions between the human (accession #135901) and rat (accession #131620) published cDNA sequences (for sequences of E1 and E3 refer to chapter 2, section 2.1.7). The identity of the amplified cDNA fragment was validated by partial sequencing (data not shown).

Three lambda clones were obtained and the largest clone, which was 11.2 kb in length, was subcloned into pBluescript SK +/- phagemid (pBS). The identity of the lambda clone was confirmed by partial sequencing and was characterized by restriction mapping (Figure 3.1). Comparison of this sequence with the published human and rat sequences demonstrated a 90% homology at the nucleotide level.
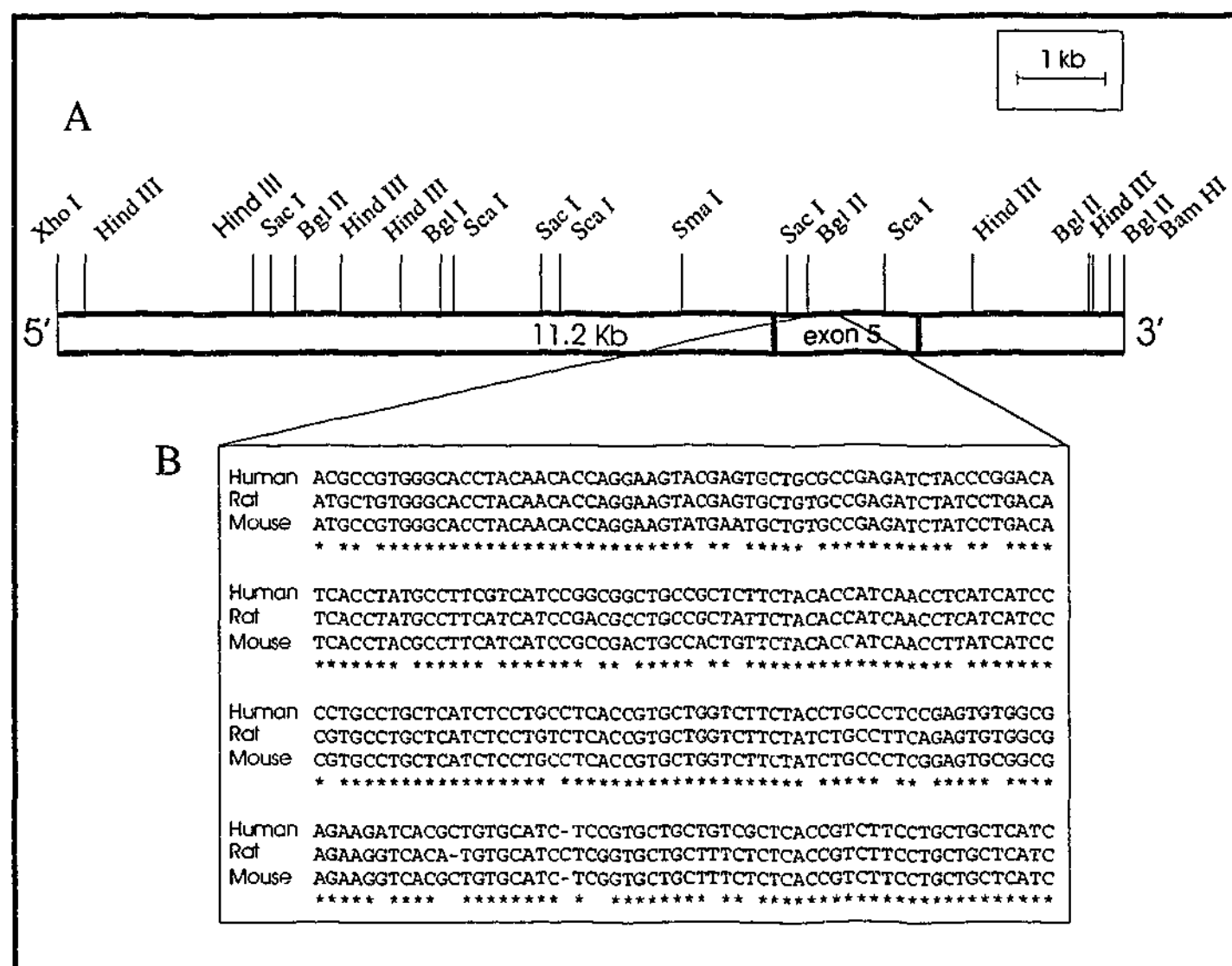
Figure 3.1 Characterization of lambda genomic clone.

(A) Represents the restriction enzyme map of the 11.2 kb lambda genomic clone and

(B) represents partial sequencing of exon 5 to confirm identity of clone.

* Indicates sequence homology between human, rat and mouse.

Knockout construct design

The knockout targeting construct was made using the pPNT neomycin-thymidine kinase-1 gene containing plasmid (Tybulewicz et al., 1991) as a base. The construct was designed to create a non-functioning allele by removing a 750 bp Bgl II / Sca I fragment from the fifth exon and replacing it with a neomycin phosphotransferase (NEO) gene (Tybulewicz et al., 1991) which is driven by the phosphorglycerokinase (PGK) promoter (Mori et al., 1986). This fragment encodes the putative first, second and third hydrophobic transmembrane domains, the first hydrophilic intracytoplasmic loop and the extracytoplasmic loop. It also encodes part of the second hydrophilic intracytoplasmic loop (Figure 3.2). The second hydrophobic transmembrane (M2) domain is involved in formation of the ion channel (Leonard et al., 1988) and it would be expected that removal of this part of the protein would functionally inactivate the molecule, although the most likely outcome of removing such a large stretch of gene close to the N-terminal region of the protein was to produce no protein at all.

To maximize the likelihood of a homologous recombination event, both 5' and 3' flanks were selected on the basis of their size and the lack of repetitive sequence. The lack of repetitive sequence was determined by using the DNA as probes in genomic Southern blots. DNA not containing a large number of repeats identified discrete bands whereas DNA with excessive repetitive sequence gave heavy smears on genomic Southern blots. This strategy was empirical and based on the successful targeting of at least 20 genes in the laboratory of Dr Heinen Westphal (NICHD, NIH, Bethesda). The cloning strategy used to generate the knockout construct is outlined in Figure 3.3.
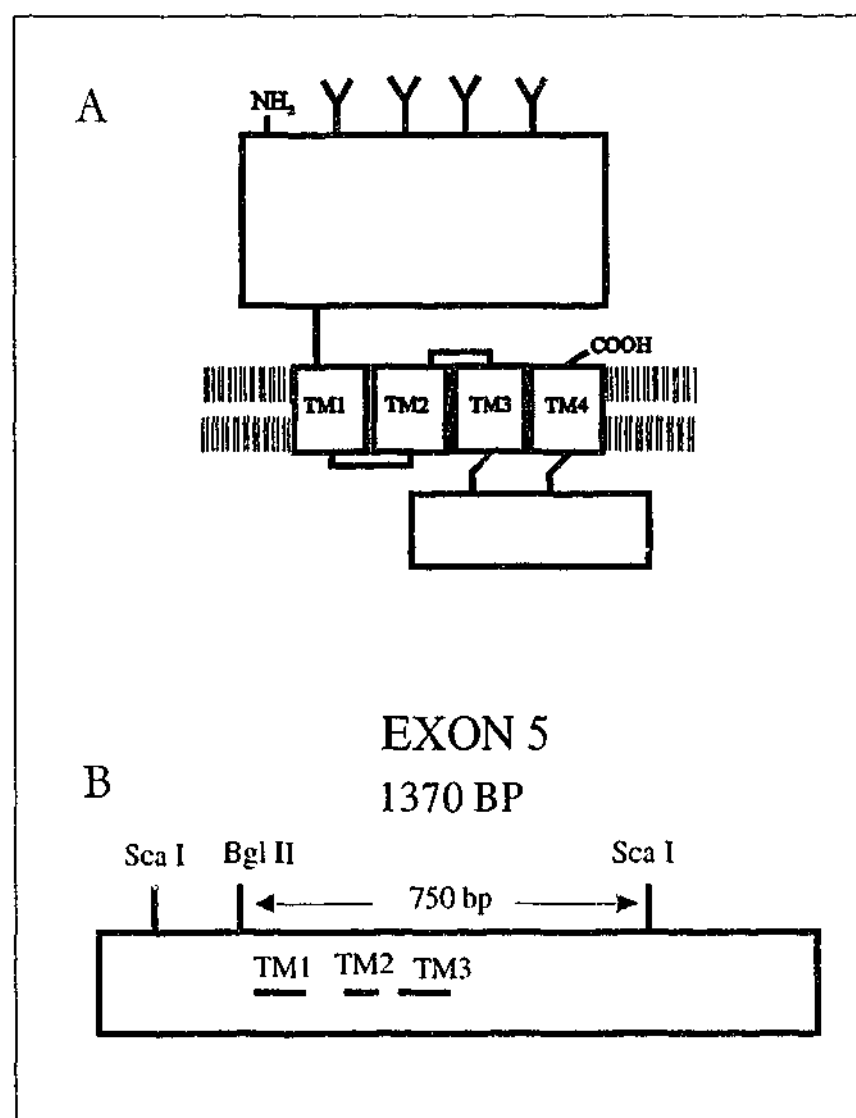
Figure 3.2 Knockout construct design.

(A) Represents a model of transmembrane organization of the nAChR subunits based

on the hydrophobicity profile of the primary amino acid sequence (adapted from Galzi,

et al., 1991). (B) Represents exon 5 and indicates the encoded transmembrane domains

(TM1, TM2 and TM3). A 750 bp Sca I / Bgl II fragment was spliced out in the

knockout construct.

Strategy for cloning the 5' flank

The 5' Lox P site was subcloned into pPNT targeting vector by inserting the oligonucleotide pair encoding the sequence Not I Hind III Xho I Lox P Sal I into the Not I / Xho I site of pPNT, generating pPNT.KO (5' Lox P) (Figure 3.3). The 5' flank (4.0 kb Bgl II / Bgl II fragment) was isolated from the lambda genomic clone (pBS.genomic.clone) and subcloned into the Bam HI site of pBS. This fragment was then excised with Not I and Xho I and ligated into the Not I / Xho I site of pPNT.KO (5' Lox P), generating pPNT.KO (5' Lox P 5' flank) (Figure 3.3).

Strategy for cloning the 3' flank

The 3' Lox P site was first subcloned into pBS by inserting the oligonucleotide pair Bam HI Lox P Sca I Sma I, generating pBS.KO (3' Lox P). To generate appropriate cloning sites in pBS.KO (3' Lox P), the oligonucleotide pair Sma I Bgl II Eco RI Xho I was subcloned into the Sma I / Xho I site, generating pBS.KO (3'LoxP.SX). The 3' flank (2.0 kb Sca I / Bgl II fragment) was isolated from the lambda genomic clone (pBS.genomic.clone) and subcloned into pBS.KO (3' Lox P.SX), generating pBS.KO (3' Lox P 3' flank). To isolate the Sca I / Bgl II fragment from pBS.KO (3' LoxP.SX) a partial digest was performed, as this plasmid has two Sca I sites. The 3' flank was excised using Bam HI and Eco RI and subcloned into pPNT.KO (5' Lox P 5' flank).

In summary, the 5' flank was a 4.0 kb Bgl II / Bgl II genomic fragment and the 3' flank was a 2.0 kb Sca I / Bgl II genomic fragment. The final knockout targeting construct was called pEP.KO (Figure 3.3) and all restriction sites were confirmed by restriction digests (data not shown). The modifications to the original pPNT plasmid of flanking the NEO gene with Lox P sites was performed to permit the removal of the NEO

cassette. This avoids the potential problem of the PGK promoter influencing neighbouring genes.

Figure 3.3 **Cloning strategy for generating the knockout construct.**

Strategy for subcloning 5' Lox P into pPNT

1. Ligate oligonucleotide (Not I Hind III Xho I Lox P Sal I)
   into pPNT digested with Not I and Xho I
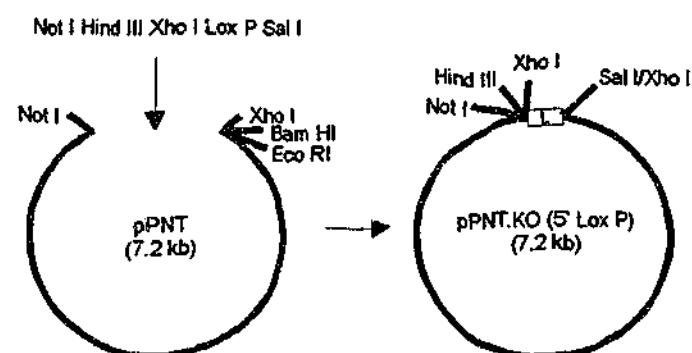
Strategy for subcloning 5' flank into pPNT.KO (5' Lox P)

1. Ligate 5' flank (4.0 kb Bgl II/Bgl II fragment) into
   pBS digested with Bam HI
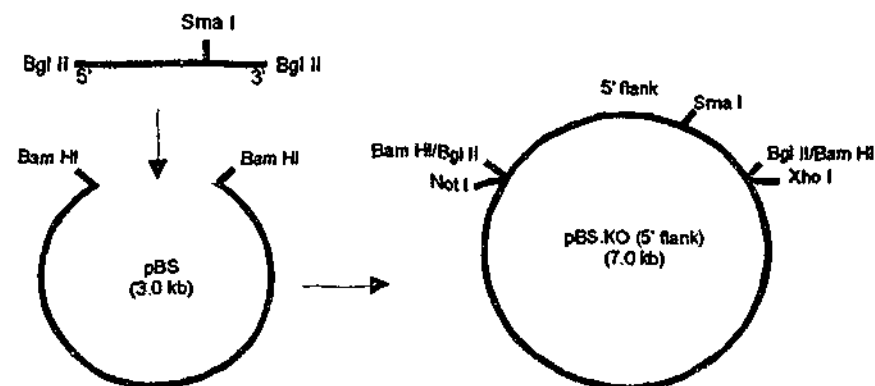
2. Excise 5' flank using Not I and Xho I

3. Ligate 5' flank into pPNT.KO (5' Lox P) digested with Not I and Xho I
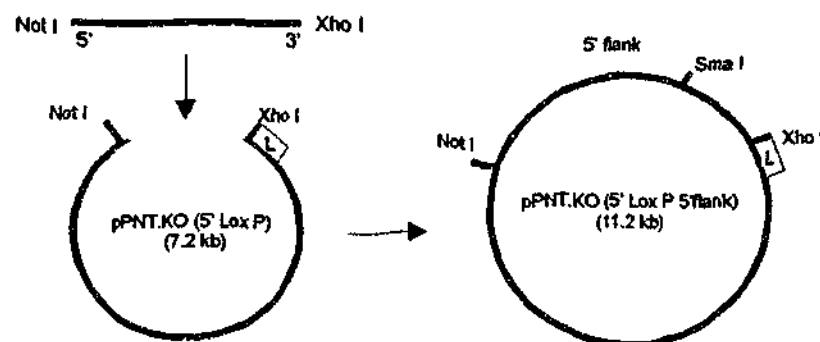
Strategy for subcloning 3' Lox P and 3' flank
into pPNT.KO (5' Lox P 5' flank)

1. Ligate oligonucleotide (Bam HI Lox P Sca I Sma I) into pBS
   digested with Bam HI and Sma I
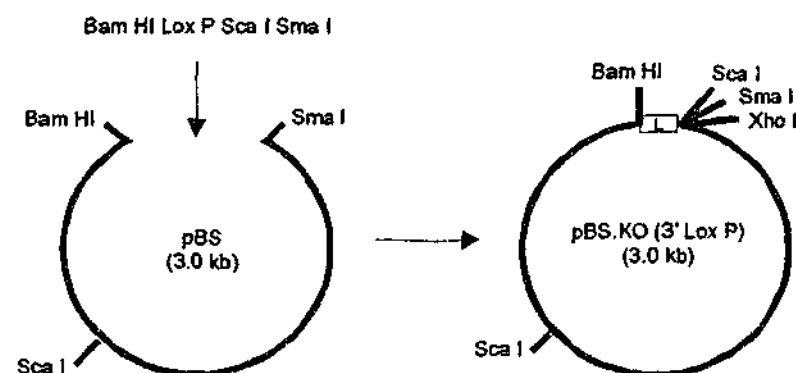
2. Ligate oligonucleotide (Sma I Bgl II Eco RI Xho I) into
   pBS.KO(3' Lox P) digested with Sma I and Xho I
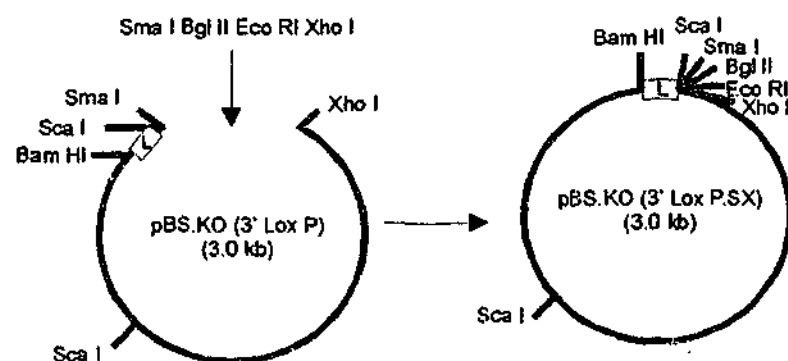
3. Ligate 3' flank (2.0 kb Sca I/ Bgl II fragment) into
   pBS.KO (3' Lox P.SX) digested with Sca I and Bgl II
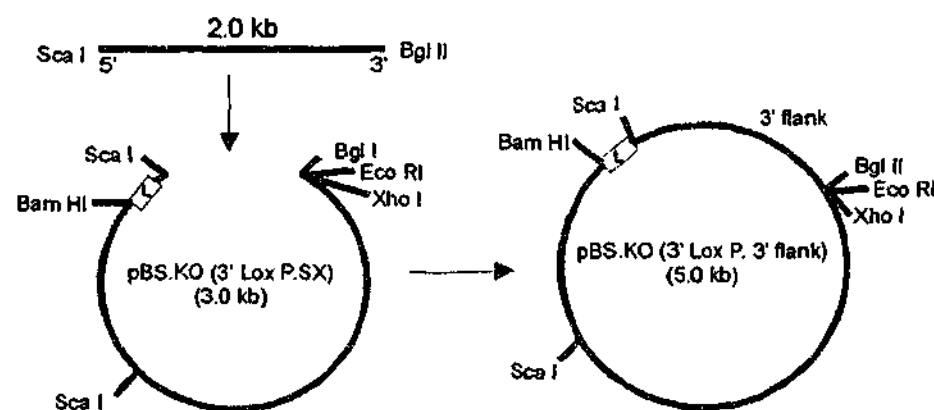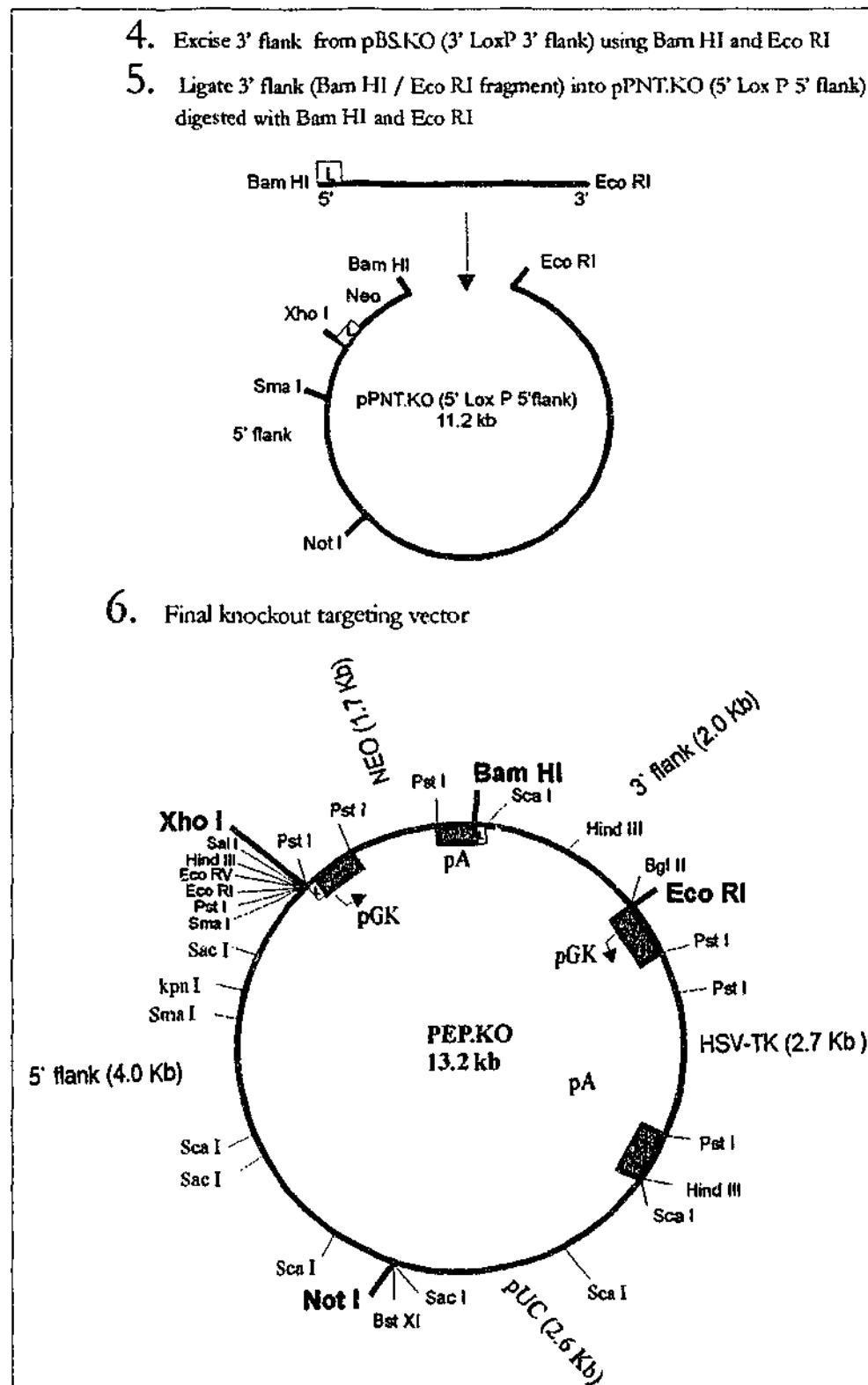
Figure 3.3 Cloning strategy for generating knockout targeting construct, pEP.KO.

The 5' flank is a 4.0 kb *Bgl* II / *Bgl* II fragment and the 3' flank is a 2.0 kb *Sca* I / *Bgl* II fragment. pUC represents the plasmid backbone, NEO represents the neomycin phosphotransferase resistant gene and HSV-TK represents the thymdine kinase gene from the herpes simplex virus. The sequential cloning steps are described in detail in the text.

A strategy of simultaneous positive selection with Geneticin (G418) and negative selection with gancyclovir was used to target the J1 line (a gift from Dr. R. Jaenisch, MIT) of ES cells. The J1 ES cell line had been successfully used to create germline transmitting chimeras (Drago et al., 1994; Drago et al., 1998). Flanking probes were identified to validate accurate 5' and 3' homologous recombination (Figure 3.4 A, B C).

Culture of ES cells

ES cells were grown using standard techniques (Drago et al., 1994) on an EF feeder and the ESM medium was supplemented with LIF. The cells under these conditions showed morphology most typical of undifferentiated ES cells. The fibroblasts were rendered mitotically inactive by treatment with the drug Mitomycin C (Sigma).

Targeting experiments using J1 ES cell line

The targeting construct was linearized with the restriction enzyme Not I and purified by ethanol precipitation. J1 ES cells (passage 12) from an actively growing two day culture were electroporated with 50 µg of the linearized targeting construct, pEP.KO. The electroporated cells were plated onto fifty-five 6 cm dishes at a concentration of 2.5 x 10^5 cells per 6 cm dish. Nine days later, 240 colonies were picked and cells dispersed into 24 well plates on Mitomycin C treated EFN feeders. Of these colonies, 111 grew to give undifferentiated ES cell colonies which were harvested 2 to 4 days later for freezing (section 2.6.8) and DNA isolation (section 2.6.9). A Southern blot of Hind III digested ES cell genomic DNA was probed with pE1 and used to verify 5' recombination. Four clones (C3, C44, C55 and C59) had undergone homologous recombination as indicated by the presence of 2 bands. The normal allele was 6 kb and the recombinant allele 4.2 kb. C67, which was a non-targeted clone, was used as a

negative control (Figure 3.4 D). To verify 3' recombination, a Southern blot of Bam HI digested ES cell genomic DNA was probed with pE2. All 4 clones had also undergone accurate homologous recombination at the 3' end as indicated by the presence of 2 bands. The normal allele was 12 kb and the recombinant allele 2.5 kb (Figure 3.4 E). To confirm single insertion of the targeting construct into the genome of targeted clones, a Southern blot of Bam HI digested ES cell genomic DNA was probed with a NEO probe (Figure 3.4F). An expected single band at 8 kb was identified in all 4 clones. Four positive homologous recombination events out of 111 positive clones corresponded to a targeting efficiency of 3.6%.

Injection

The blastocyst injections were undertaken in collaboration with Professor Ismail Kola at the Institute of Reproduction and Development, Monash University. Of the 4 recombinant clones, C3 was chosen for injection as the cells were rapidly growing and appeared to have an undifferentiated morphology. The cells were injected into Balb/C blastocysts and 12 chimeras were generated of which 4 were female and 8 male. All were mated with CF1 mice. However, none of them were capable of transmitting the mutated allele to their progeny, indicating that the introduced ES cells containing the mutated allele were not contributing to the germ cells in these chimeras.

Figure 3.4 Construction of the knockout targeting vector (pEP.KO) and Southern blot analysis of J1 targeted ES clones.

Panel A represents the genomic map of the α_4 nAChR gene, panel B represents the targeting vector pEP.KO and panel C represents the expected allelic disruption after homologous recombination. The restriction sites shown are abbreviated as follows: N, *Not* I; H, *Hind* III; Bg, *Bgl* II; Sc, *Sca* I; X, *Xho* I; E, *Eco* RI; B, *Bam* HI. NEO represents the neomycin phosphotransferase resistance gene and TK represents the thymidine kinase gene. The origin of the probes used for homologous recombination screening are also shown. Probe pE1 is a *Hind* III - *Bgl* II fragment and was used to confirm 5' recombination. Probe pE2 is a *Hind* III - *Bam* HI fragment and was used to confirm 3' recombination. Panel D shows the Southern blot of *Hind* III digested ES cell genomic DNA probed with pE1, showing correctly targeted clones C3, C44, C55, C59 and a randomly selected non-targeted, C67. The Wt allele is 6 kb and the recombinant allele 4.2 kb. Panel E shows the Southern blot of *Bam* HI digested ES cell genomic DNA probed with pE2, showing correctly targeted clones C3, C44, C55 and C59. The Wt allele is 12 kb and the recombinant allele 2.5 kb. Panel F shows a Southern blot of a *Bam* HI digest probed with a NEO specific probe. Clones C3, C44, C55 and C59 have a single band at the expected size of 8 kb confirming a single insertion event in all the clones examined.

A — B — C maps with Probe pE1, Probe pE2; restriction sites B, H, H, H, H Bg, Bg, Sc, H, Bg, H, B; Wt (Hind III) (6.0 kb); Wt (Bam HI) (12.0 kb); EX.5.

B — N, H, X, B, Sc, H, E; NEO; TK

C — Mt (Hind III) (4.2 kb); B H, H, H H, H X, B Sc H Bg E H B; NEO; Mt (Bam HI) (2.5 kb); Mt (Bam HI) (NEO, 8.0 kb)

D (C3 C44 C55 C59 C67): ◄ 6 kb; ◄ 4.2 kb — Hind III probed with pE1

E (C3 C44 C55 C59 C67): ◄ 12 kb; ◄ 2.5 kb — Bam HI probed with pE2

F (C3 C44 C55 C59 C67): ◄ 8 kb — Bam HI probed with NEO
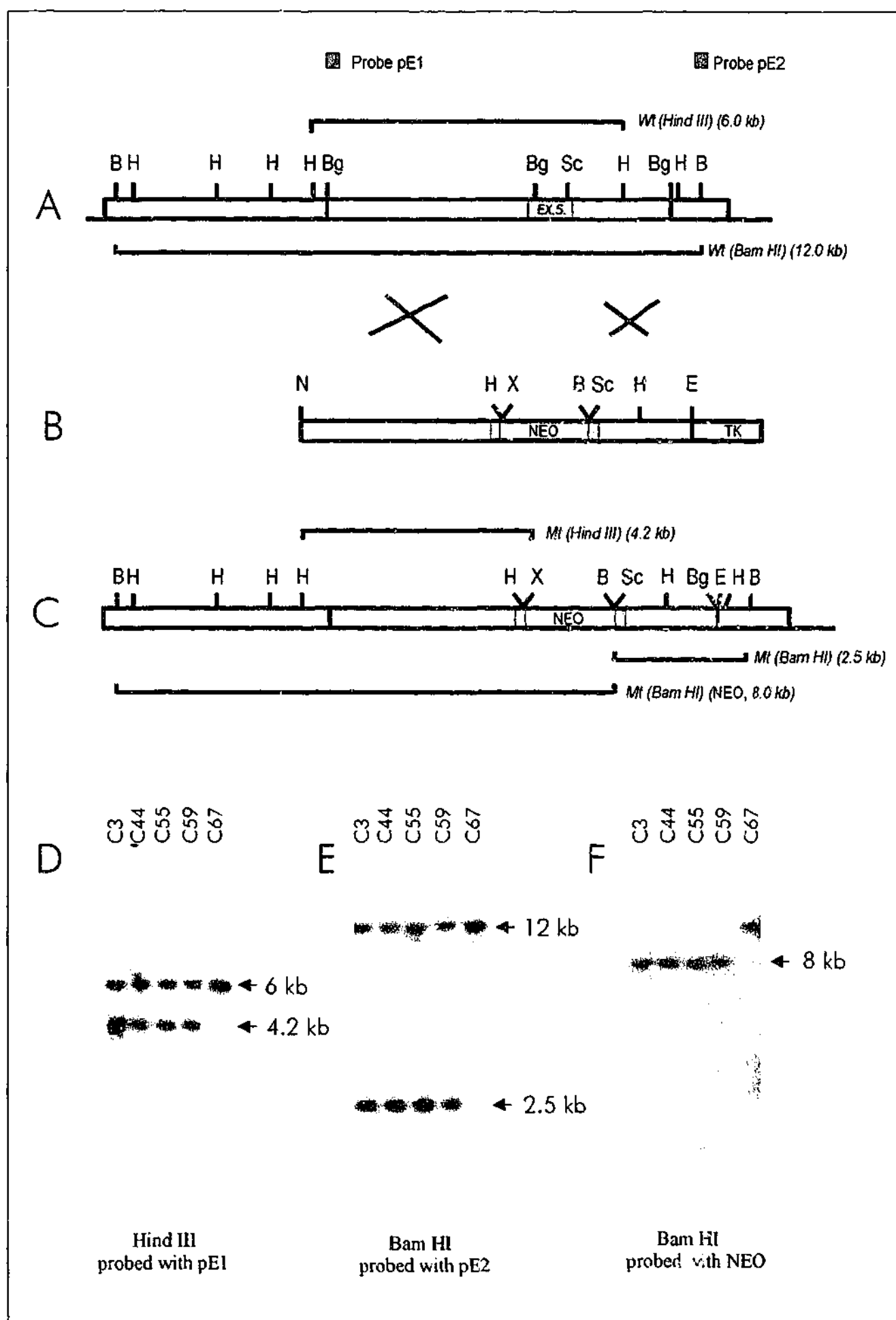
The cells were injected for a second round, however this time all 4 positive clones were pooled and injected. Four chimeras were generated, 1 female and 3 male. A female chimera of 5% coat chimerism gave germline transmission. Southern blot analysis of tail genomic DNA digested with Hind III and probed with pE1 identified a heterozygous (Hz) mouse by the presence of 2 bands. The normal allele was 6 kb and the recombinant allele 4.2 kb. The Hz founder was used to generate the entire colony by subsequent crossing with C57/BL6 mice. Hz progeny, obtained after two backcrosses with C57/BL6 mice were mated to establish a number of mutant (Mt) mating pairs and wildtype (Wt) mating pairs (Figure 3.5). All Mt mice used in this study were therefore derived from Mt mice intermatings and all Wt mice were derived from Wt intermatings.

A possible confounding factor when using a transgenic approach is the effect of the genetic background of the mice used in generating the mutant. This is particularly problematic, as 129 mice are known to have structural brain changes that may result in behavioural change. In an effort to overcome this problem, we decided to eliminate as many 129-type genes as possible by backcrossing Mt mice with C57BL/6 mice thereby creating a C57BL/6 congenic strain. A complete backcross would take up to 12 generations that may occupy approximately two years of breeding. Because of this time factor all experiments in this thesis were performed using Mt mice from two C57BL/6 backcrosses. The colony has since been backcrossed to 7 generation. Maximal diversity in the genetic background was maintained by randomly interchanging breeders within a given genotype. All mice were routinely genotyped by Southern blotting. Every mouse used in behavioural, pharmacological or *in situ* hybridization studies had its genotype determined by Southern blotting.
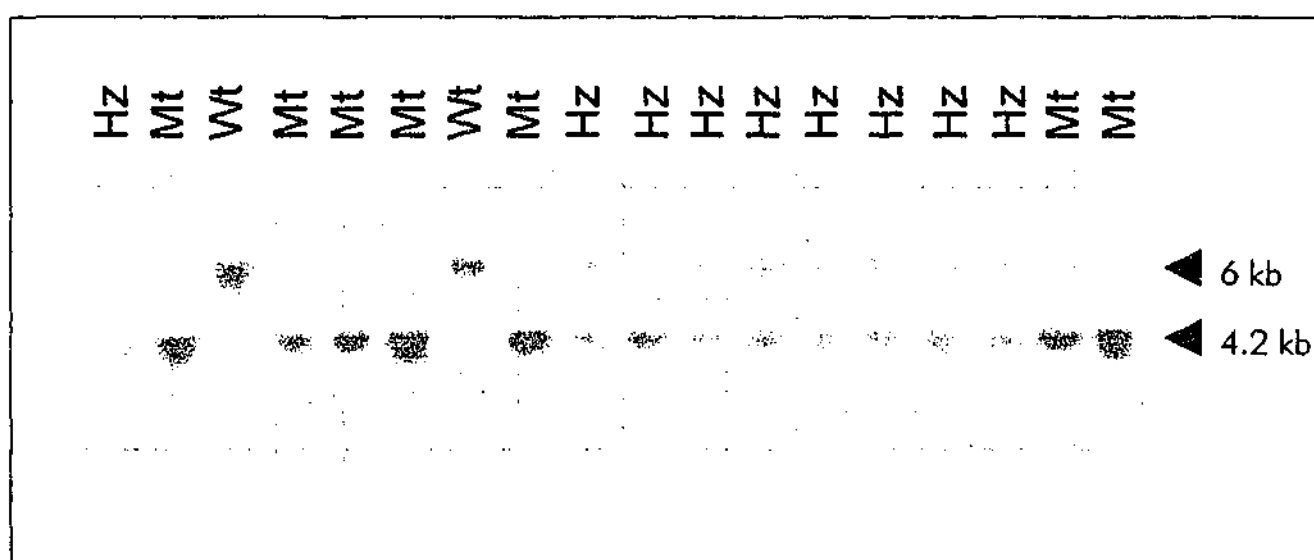
Figure 3.5 Genomic Southern blot of DNA from F1 animals generated by Hz / Hz mating pairs.

Genomic Southern blot of *Hind III* digested DNA probed with pE1. The filter was exposed to X-ray film for 7 days at -70°C with an intensifying screen. The Wt allele is represented by the 6 kb band and the mutated allele by the 4.2 kb band.

CHAPTER FOUR

PHENOTYPIC CHARACTERIZATION OF AN α_4

NICOTINIC ACETYLCHOLINE RECEPTOR

SUBUNT GENE KNOCKOUT MOUSE.

4.1 ABSTRACT

Neuronal nAChRs are present in high abundance in the nervous system. There are a large number of subunits expressed in the brain which combine to form multimeric functional receptors. An α_4 nAChR subunit knockout line was generated and this chapter focuses on defining the behavioural role of this receptor subunit. Homozygous mutant (Mt) mice are normal in size, fertility and home cage behaviour. Spontaneous unconditioned motor behaviour revealed an ethogram characterized by significant increases in several topographies of exploratory behaviour in Mt mice relative to wildtype (Wt) mice over the course of habituation to a novel environment. Furthermore, the behaviour of Mt mice in the elevated plus-maze assay was consistent with increased basal levels of anxiety. In response to nicotine, Wt mice exhibited early reductions in a number of behavioural topographies, under both unhabituated and habituated conditions; conversely, heightened levels of behavioural topographies in Mt mice were reduced by nicotine in the late phase of the unhabituated condition. Ligand autoradiography confirmed the lack of high affinity binding to radiolabeled nicotine, cytisine and epibatidine in the thalamus, cortex and caudate putamen although binding to a number of discrete nuclei remained. The study confirms the pivotal role played by the α_4 nAChR subunit in the modulation of a number of constituents of the normal mouse ethogram and in anxiety as assessed using the elevated plus-maze. Furthermore, the response of Mt mice to nicotine administration suggests that persistent nicotine binding sites in the habenulo-interpeduncular system are sufficient to modulate motor activity in actively exploring mice.

4.2 INTRODUCTION

Nicotine is one of the most widely consumed psychoactive drugs and exerts a number of pharmacological actions in the central and peripheral nervous system (Decker, et al., 1995). Neuronal nicotinic acetylcholine (ACh) receptors (nAChR) constitute a heterogenous family of pentameric oligomers with contributions from 11 subunits (Le Novere and Changeux, 1995). Five types of α subunits (α_2-α_6) and three types of β subunits (β_2-β_4) permit combinations of α-type and β-type subunits to form a number of functional receptors with subunits of two or more different types (Changeux, et al., 1998), whilst subunits α_7-α_9 can form α-bungarotoxin sensitive homo-pentameric receptors (Corringer, et al., 1995). The topography of nAChR subunits varies (Deneris, et al., 1989; Duvoisin, et al., 1989; Wada, et al., 1989; Wada, et al., 1990; Hill, et al., 1993; Elgoyhen, et al., 1994; Court and Perry, 1995; Le Novere, et al., 1996; Brioni, et al., 1997; Zoli, et al., 1998) with α_4 and β_2 transcripts being found in a large number of CNS nuclei whereas α_2, α_3, α_5, α_6, β_3 and β_4 mRNAs are restricted to a few cholinergic pathways, which also express α_4 and β_2.

Despite detailed characterization of nAChR subunits at the molecular level, not much is known about the *in vivo* functional role of individual subunits. Most nAChR ligands show similar patterns of high-affinity labelling that resembles the distribution of α_4/β_2 subunits. A number of nAChR agonists which bind to the α_4/β_2 receptor configuration *in vitro* are known to have an effect on anxiety (Gilbert, et al., 1989; Pomerleau, 1986; Brioni, et al., 1993), attention (Brioni, et al., 1997) and antinociception (Tripathi, et al., 1982; Damaj, et al., 1998) implicating the α_4/β_2 receptor in the mediation of a number of physiological processes. Analysis of an independently generated line of α_4 nAChR subunit knockout mice (Marubio, et al.,

1999) validated the significant role played by this receptor subunit in nociception. Loss of nicotinic binding sites and a decrease of nAChR protein expression has been shown in patients with Alzheimer's disease and patients with Parkinson's disease with cognitive dysfunction (Giacobini, 1991; Brioni, et al., 1997). Furthermore, several mutations in the α_4 nAChR subunit have been identified in Autosomal Dominant Nocturnal Frontal Lobe Epilepsy (Steinlein, et al., 1995; Steinlein, et al., 1997). The large number of subunits suggests a potential for considerable diversity in nAChR function(s). Defining the specific role played by individual subunits in determining spontaneous motor behaviour and responses to drug challenge will be aided by ongoing analysis of nAChR subunit gene knockout mice (Picciotto, et al., 1995; Orr-Urtreger, et al., 1997; Marubio, et al., 1999; Xu, et al., 1999).

Nicotine is known to reduce anxiety in both chronic smokers (Gilbert, et al.,1979; Pomerleau, 1986; Gilbert, et al., 1989) and non-smokers (Hutchinson and Emley, 1973). Anxiolytic-like effects of nicotine and a select number of neuronal nicotinic receptor agonists have also been documented in experimental animals (Costall, et al., 1989; Brioni, et al., 1993; Cao, et al., 1993). The differential behavioural profile of neuronal nicotinic agonists implies that nicotine's anxiolytic actions may be mediated by a specific subunit configuration of the nAChR. An α_4 nAChR knockout line was generated to test the hypothesis that mice lacking α_4 nAChR subunits would show behavioural features consistent with heightened basal levels of anxiety.

4.3 MATERIALS AND METHODS

Animals

All procedures involving the use of live animals conformed to the National Health and Medical Research Council (NH&MRC) code of practice.

Tissue preparation

Adult (Wt, n=9; Hz, n=9; and Mt, n=11) mice were killed by decapitation, the brains snap frozen in cold isopentane and stored at -70°C before use. Twenty μm frozen coronal sections were cut in a cryostat and mounted onto 3-aminopropyl triethoxysilane (Sigma St. Louis, MO) coated slides for *in situ* hybridization and gelatin coated slides for ligand binding studies.

***In situ* hybridization**

In situ hybridization was performed for α_3, α_4, α_6, α_7, β_2, β_3 and β_4 nAChR subunits. The sequences of the oligonucleotides used are as shown in Table 2.1 (chapter 2, section 2.1.7). Four oligonucleotides were designed to identify α_4 nAChR specific transcript. Probes ISACh3 and ISACh4 were designed to hybridize with mRNA encoded in transcribed gene sequence upstream of the deleted Bgl II / Sca I fragment (see chapter 3, Figure 3.3), ISACh 1 and ISACh2 were designed to hybridize with mRNA derived from this deleted sequence. This strategy allowed identification of cells that normally express the α_4 nAChR subunit in both Wt and Mt mice as well as verify the knockout paradigm. All oligonucleotide probes were 5'-end labelled using a standard kinase protocol (Wong, et al., 1997) with $[\gamma\text{-}^{33}P]$-ATP and T4 polynucleotide kinase. Specificity of probes used in this study was determined by using a 100-fold excess of unlabeled antisense oligonucleotides added to the *in situ* hybridization reactions to

competitively inhibit probe hybridization. Slides were exposed to Hyperfilm (Amersham) for between 2 and 4 weeks and then the images were scanned. The density of mRNA expression for α_4 (ISACh3/4), α_3, α_4, α_6, α_7, β_2, β_3 and β_4 nAChR subunits was quantified using a Microcomputer Imaging Device (MCID) with software (Image Research Inc. Brock University, St. Catherine's, Ont., Canada). All values are expressed as cpm/mm^2 for mRNA expression (mean $\pm$ SEM). The cpm/mm^2 values were calculated by exposing commercial generated [^{33}P] standards together with sections. The specific binding for densitometric purposes was calculated by subtracting background binding (determined by cold competition) from results using labeled antisense oligonucleotides alone.

Receptor autoradiography:

All nicotinic agonists were obtained from Sigma (St Louis, Mo).

[^{3}H]-nicotine binding

[^{3}H]-nicotine binding experiments were performed as described by Marks et al., 1992. The slides were pre-incubated in Krebs-Ringers HEPES (NaCl, 118 mM; KCl, 4.8 mM; CaCl$_2$, 2.5 mM; MgSO$_4$7H$_2$O, 1.3 mM; HEPES, 20 mM; pH to 7.5 with NaOH) for 30 min at 4°C. They were then transferred to Krebs-Ringers HEPES containing 5.1 nM L-[N-methyl-^{3}H]-nicotine (NEN Life Science Products. Inc., MA, specific activity 81.5 Ci/mmol) and incubated for 90 min at 4 °C. Following incubation the slides were washed as follows: 2 x 5 sec, Krebs-Ringers HEPES; 2 x 5 sec, 20 mM HEPES (pH 7.5) and 2 x 5 sec in distilled water. All washes were performed at 4°C. The slides were then air dried at room temperature and apposed to Hyperfilm (Amersham,

England) for 6 weeks in the presence of tritiated microscales (Amersham, England).

Binding in the presence of 1 µM unlabeled nicotine did not exceed film background.

[^{3}H]-epibatidine binding

[^{3}H]-epibatidine binding experiments were performed as described by Marks et al.,

1992. Slides were pre-incubated in Krebs-Ringers HEPES for 20 min at room

temperature and then transferred to Krebs-Ringers HEPES containing 400 pM ($\pm$)[5,6-

bicycloheptyl-^{3}H]-epibatidine (NEN, 33.8 Ci/mmol) for 60 min at room temperature.

The slides were then washed as follows: 2 x 10 sec in Krebs-Ringers HEPES; 2 x 10 sec

in 0.1 x Krebs-Ringers HEPES; 10 sec in 5 mM HEPES pH 7.5 and distilled water for 5

sec. All washes were performed at 0°C. The slides were then air dried at room

temperature and apposed to Hyperfilm for 3 weeks together with standard tritiated

microscales. Nonspecific binding was defined as the binding in the presence of

unlabeled epibatidine (10 µM). Cold competition assays were also performed with

unlabeled 300 µM nicotine and 150 nM cytisine.

[^{3}H]-cytisine binding

[^{3}H]-cytisine binding experiments were performed as described by Zoli et al., 1998.

The slides were incubated at 4°C for 60 min in 50 mM Tris-HCl, pH 7.4, containing 120

mM NaCl, 5 mM KCl, 2.5 mM $CaCl_2$, 1 mM $MgCl_2$ and 5 nM [3,5-^{3}H (N)]-cytisine

hydrochloride (NEN, 32Ci/mmol). The washes were as follows; 3 x 2.5 min in 50 mM

Tris-HCl, pH 7.4, followed by a brief rinse in distilled water, all performed at 4°C.

Nonspecific binding was defined as the binding in the presence of unlabeled nicotine

(10 µM). The film was exposed for 3 months.

[^{125}I]-α-bungarotoxin binding

[^{125}I]-α-bungarotoxin binding experiments were performed as described by Ashworth-Preece et al., 1998.   The slides were preincubated in 50 mM Tris-HCl, pH 7.4, containing 0.1% bovine serum albumin (BSA) for 30 min at room temperature. They were then incubated in 50 mM Tris-HCl, pH 7.4, containing [^{125}I]-α-Bungarotoxin (2000 Ci/mmol, a gift from Prof. Bevyn Jarrott, Department of Pharmacology, Monash University) at a concentration of 1.5 nM for 120 min at room temperature. The washes were as follows; 2 x 15 min in 50 mM Tris-HCl, pH 7.4, 0.1% BSA; 2 x 15 min in 50 mM Tris-HCl, pH 7.4, followed by a brief rinse in distilled water, all performed at 4°C. Nonspecific binding was defined as the binding in the presence of unlabeled acetylcholine (10 mM). The slides were exposed to XAR5 film (Eastman Kodak, Rochester, NY) together with laboratory prepared standards for 36 hs. "[^{3}H] microscales were used for [^{3}H] ligands and [^{14}C] standards were used for [^{125}I] bungarotoxin".

Binding densities were measured using the MCID M4 system under constant illumination. Standardisation was achieved by comparing binding densities with [^{3}H]-microscales and standards exposed with each film. [^{3}H] microscales were used for [^{3}H] ligands and [^{14}C] standards were used for [^{125}I] bungarotoxin. All values are expressed as fmol/mg tissue for receptor binding studies (mean ± SEM). The specific binding was calculated by subtracting non-specific binding determined when labeled ligand was co-incubated with respective unlabeled receptor agonist.

Topography of spontaneous motor behaviour

On experimental days mice were removed from their home cage and placed individually in clear glass observation cages (36x20x20 cm). Behavioural assessments were carried out in a manner similar to that used extensively for rats (Clifford and Waddington, 1998) and mice (Clifford, et al., 1999, Clifford, et al., 1998) using a rapid time-sampling behavioural checklist technique. For this procedure, each of ten randomly allocated mice was observed individually for 5 sec periods at 1 min intervals over 15 consecutive mins, using an extended, ethologically-based behavioural checklist. This allowed the presence or absence of the following individual behaviours (occurring alone or in any combination) to be determined in each 5 sec period: sniffing (Sn); locomotion (L; co-ordinated movement of all four limbs producing a change in location); total rearing (Rt; rearing of any form); rearing from a sitting position (Rs; front paws reaching upwards with hind limbs on floor in sitting position); rearing free (Rf; front paws reaching upwards away from any cage wall while standing on hind limbs); rearing towards a cage wall (Rw; front paws reaching upwards on a cage wall while standing on hind limbs); biting (B); sifting (S; sifting movements of the front paws through cage bedding material); grooming (Gr; of any form); intense grooming (Gri; grooming of the face with the forepaws followed by vigorous grooming of the hind flank or anogenital region with the snout); vacuous chewing (VCh; chewing movements not directed onto any physical material); chewing (Ch; chewing movements directed onto cage bedding and/or faecal pellets without consumption); eating (E; chewing with consumption); climbing (Cl; jumping onto cage top with climbing along grill in inverted or hanging position); stillness (St; motionless, with no behaviour evident). This cycle of assessment by behavioural checklist over a 15 min period (0-15 min) was repeated twice (20-35 min and 40-55 min); thereafter, 10 cycles of otherwise identical

assessments were repeated at 80-90, 120-130, 160-170, 200-210, 240-250, 280-290, 340-350 and 360-370 min.

Effect of nicotine on behaviour

Examination of the effect of nicotine was conducted under two conditions: (i) unhabituated, i.e. active exploration; and (ii) habituated, whereby mice were placed individually in the clear glass observation cages and left undisturbed for a period of 3 h. Following injection of drug or vehicle animals were assessed using the rapid time-sampling behavioural checklist technique. The time of injection was taken as the zero time point. For assessment of spontaneous behaviour and effects of nicotine on unhabituated behaviour, animals were used on one occasion only; for the assessment of effects of nicotine on habituated behaviour, animals were used on two occasions only separated by a drug-free interval of one week.

Rotarod

The rotarod apparatus (Ugo Basile, Milan, Italy) was used in accelerating mode, gradually increasing from 4 to 40 rpm over the course of 5 min. Mice were placed on the apparatus at a fixed speed of 4 rpm for 1 revolution; the apparatus was then set to accelerating mode and the stopwatch started. Latency to fall was recorded for each mouse in three trials per day, separated by an inter-trial interval of two hours. Each mouse was subjected to this schedule for three successive days. Mice that stayed on the rotarod for >360 sec were considered complete responders; their latencies were recorded as 360 sec. All experiments were carried out during the hs of 11:00–18:00 to avoid circadian effects.

Elevated plus-maze

Anxiolytic-like activity was evaluated using the elevated plus-maze, a pharmacologically validated model (Pellow, et al., 1985; Brioni, et al., 1993) according to procedures previously described in which nicotinic receptor agonists were demonstrated to have an anxiolytic-like effect (Brioni, et al., 1993). The elevated plus-maze was custom-made of black perspex consisting of two open arms (5 x 30cm) and two enclosed arms (5 x 30 x 14cm) extending from a central platform (5 x 5cm) mounted on a wooden base raised 57 cm above the floor; thus the maze formed a "plus" shape. Overhead light levels on the open and enclosed arms were similar. At the beginning of the experiment, mice were placed in the center of the maze facing an enclosed arm and the following variables were scored: 1) the time spent on the open and enclosed arms, reported as time spent on open (or enclosed) arms expressed as a percentage of total time (300 sec): 2) the number of entries into open and closed arms. An arm entry was defined as the entry of all four feet of the animal into one arm; an arm exit was defined by the exit of both forelimbs from one arm. Plus-maze behaviour was assessed by direct observation.

Data analysis

For determination of ethograms for spontaneous behaviour over the phase of initial exploratory activity, the total 'counts' for each individual behaviour was determined as the number of 5 sec observation windows in which a given behaviour was evident, summed over the initial 3 x 15 min (0-15, 20-35, 40-55 min) cycle periods and expressed as means ± SEM. Data for individual behaviours were analysed using analysis of variance (ANOVA) following square-root transformation, to allow examination of interaction effects in the absence of non-parametric techniques for

interaction terms. For determination of the habituation profiles of these ethograms, total 'counts' for each individual behaviour were summed as above over each of the following periods: 0-10, 20-30, 40-50, 80-90, 120-130, 160-170, 200-210, 240-250, 280-290, 340-350, 360-370; these were expressed also as means $\pm$ SEM and analysed using repeated-measures ANOVA following square-root transformation.

For determination of the effect of nicotine on both active exploration and under habituated conditions, the total counts for each individual behaviour were determined as the number of 5 sec observation 'windows' in which a given behaviour was evident, summed over the initial 3 x 15 min (0-15, 20-35, 40-55 min) cycle periods, and expressed as means $\pm$ SEM. Data for individual behaviours were analysed using ANOVA following square-root transformation; data were then analysed using either Student's t-test or Mann-Whitney U test to identify those particular drug doses at which responsivity differed by genotype, for a given topography of behaviour.

For determination of rotarod performance, latency to fall was calculated for each mouse on three occasions each day, for three successive days, and expressed as means $\pm$ SEM. Data were analysed using ANOVA following square-root transformation; data were then analysed using either Student's t-test or Mann-Whitney U test to identify those particular time points at which responsivity differed by genotype. For elevated plus maze performance, the percentage of time spent in and number of entries into open and closed arms was calculated for each mouse. Data were expressed and analysed as above to identify those particular parameters for which responsivity differed by genotype.

4.4 RESULTS

Mice homozygous for the α_4 nAChR mutation were born in the expected Mendelian proportion, were capable of reproduction, and were of normal body weight (data not shown). Haematoxylin and Eosin stained sections of the brain of Mt mice were examined histologically and no differences in the size or location of the brain nuclei or cortical lamination were apparent (data not shown). In addition, gross anatomical and histological screening failed to show any abnormalities in heart, liver, spleen, kidney, lung, muscle and thymus (data not shown).

In situ hybridization

In situ hybridization carried out on a number of animals (Wt, n=9; Hz, n=6; and Mt, n=9) identified a strong hybridization signal for ISACh3 and ISACh4 localized to the thalamus (Th), cortex (Cx) in Wt mice, (Figure 4.1A, C, E & G) Mt mice (Figure 4.1B, D, F & H) and Hz (data not shown). A moderate hybridization signal was also seen in the caudate putamen (CPu), hippocampus (Hp), dentate gyrus (DG) and substantia nigra (SN) (data not shown). ISACh1 and ISACh2 probes, which hybridize to the deleted sequence, showed no regional specific signal throughout the brain of Mt mice (Figure 4.1B & D) and a reduced signal in Hz mice (data not shown). The hybridization pattern seen in Wt mice using ISACh1 and ISACh2 probes was the same as for ISACh3 and ISACh4 (Figure 4.1E & G).

In situ hybribization was also performed for α_3, α_6, α_7, β_2, β_3 and β_4 nAChR subunits (Figure 4.2). An intense signal for α_3 mRNA was detected in the medial habenular (MHb) (Figure 4.2A & B), α_6 signal was detected in the SN (Figure 4.2C & D), α_7 was

seen in the Hp and DG (Figure 4.2E & F), β_2 showed a strong signal in the MHb, Th and moderate hybridization was seen in the Cx, Hp and DG (Figure 4.2G & H) whereas β_3 had limited distribution with signal only in the MHb and the SN (Figure 4.2I, J, K & L). β_4 expression was restricted to the MHb (Figure 4.2M & N). There were no statistically significant differences between Mt and Wt mice in the relative abundance of α_3, α_6, α_7, β_2, β_3 and β_4 nAChR subunits transcripts (Figure 4.3). Furthermore, the level of the α_4 nAChR subunit specific transcripts detected by probes ISACh3/4 were the same in Mt and Wt mice (Figure 4.3).

Figure 4.1 Expression of the α_4 neuronal nAChR subunit in Wt and Mt mouse brain.

In situ hybridization using antisense α_4 nAChR specific cDNA oligonucleotide probes. Panels A, C, E, G, I and K represent sections derived from Wt mice and panels B, D, F, H, J and L represent sections derived from Mt mice. Sections shown in panels A, B, C, D, E and F were probed with ISACh1 and ISACh2 whereas sections shown in panels G, H, I, J, K and L were probed with ISACh3 and ISACh4. In Wt mice, signal was detected for both ISACh1/ISACh2 and ISACh3/ISACh4, with signal detected at high levels in the thalamus (Th), medial habenula (MHb), substantia nigra (SN); moderate levels were detected in the cortex (Cx), hippocampus (Hp) and dentate gyrus (DG) and low levels in the caudate putamen (CPu). No signal was seen in the Mt mice with ISACh1/ISACh2, which detects the deleted sequence (B, D and F), but signal was detected using ISACh3/ISACh4, which recognizes transcript derived from non-deleted gene sequence (H, J and L). Sections shown in panels A, B, G and H were taken at Bregma levels - 0.84; C, D, I and J were taken at Bregma levels -1.82 and E, F, K and L were taken at Bregma levels - 3.80 (Franklin and Paxinos, 1997).

Wt   Mt

ISACh1/2   A   B

ISACh1/2   C   D

ISACh3/4   E   F

ISACh3/4   G   H

NSB (ISACh1/2)   NSB (ISACh3/4)

I   J
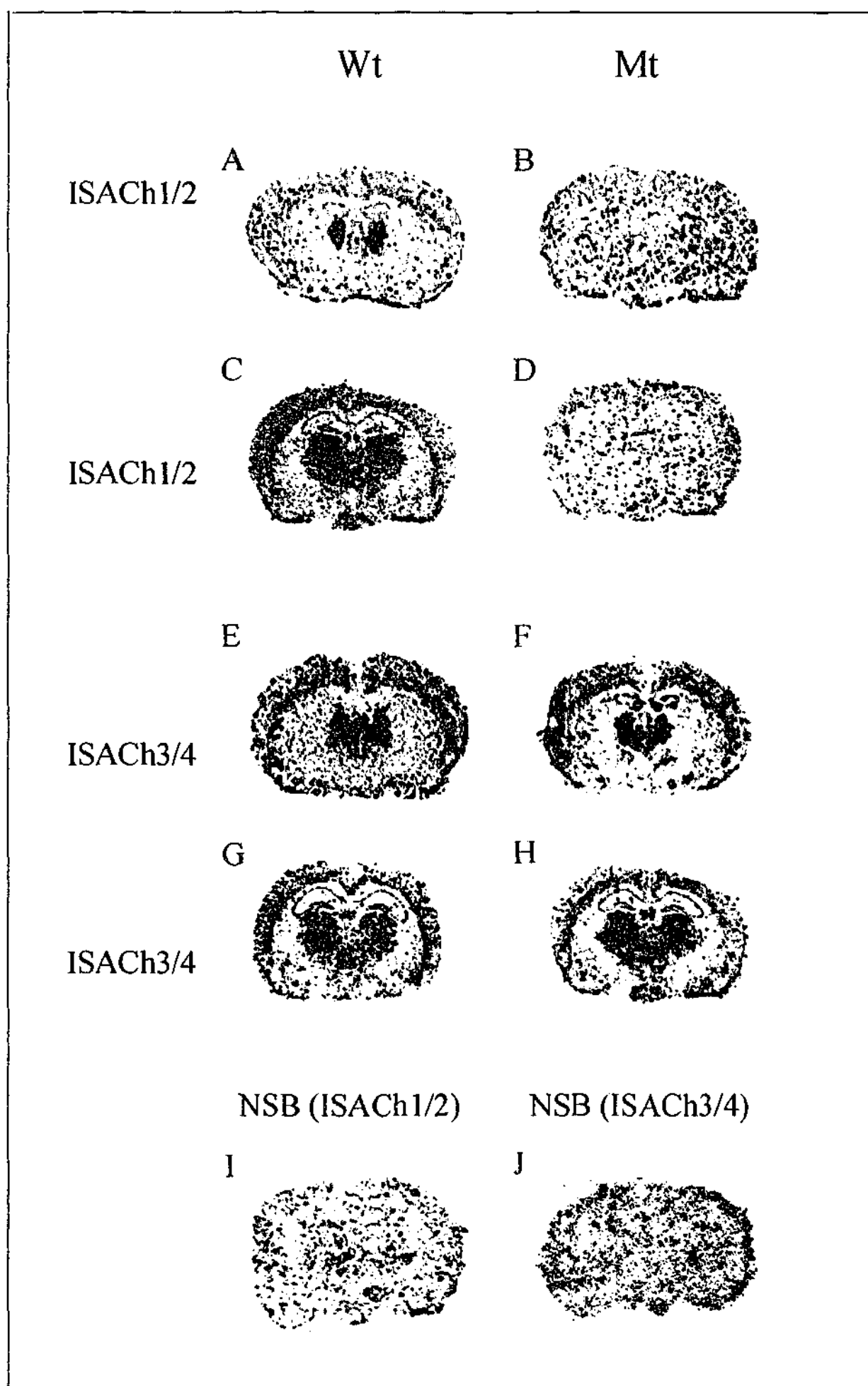
Figure 4.2 Expression of α_3, α_6, α_7, β_2, β_3 and β_4 nAChR subunits in Wt and Mt mouse brain using *in situ* hybridization.

An intense hybridization signal was detected in the medial habenula (MHb) in both Wt (A) and Mt (B) mice probed with α_3 specific probes. A strong hybridization signal was seen in the substantia nigra (SN) in Wt (C) and Mt (D) mice probed with α_6 specific probes. A strong hybridization signal was detected in the hippocampus (Hp) and dentate gyrus (DG) in both Wt (E) and Mt (F) mice probed with α_7 specific probes. A strong hybridization signal was seen in the MHb and Thalamus (Th) and moderate hybridization was seen in the cortex (Cx), Hp and DG in Wt (G) and Mt (H) mice probed with β_2 specific probes. A strong hybridization signal was seen in the MHb and the SN in Wt (I, K) and Mt (J, L) mice probed with β_3 specific probes and a strong hybridization signal was seen in the MHb in Wt (M) and Mt (N) mice probed with β_4 specific probes. There was no difference between Wt and Mt mice in the expression of any of the subunits examined.
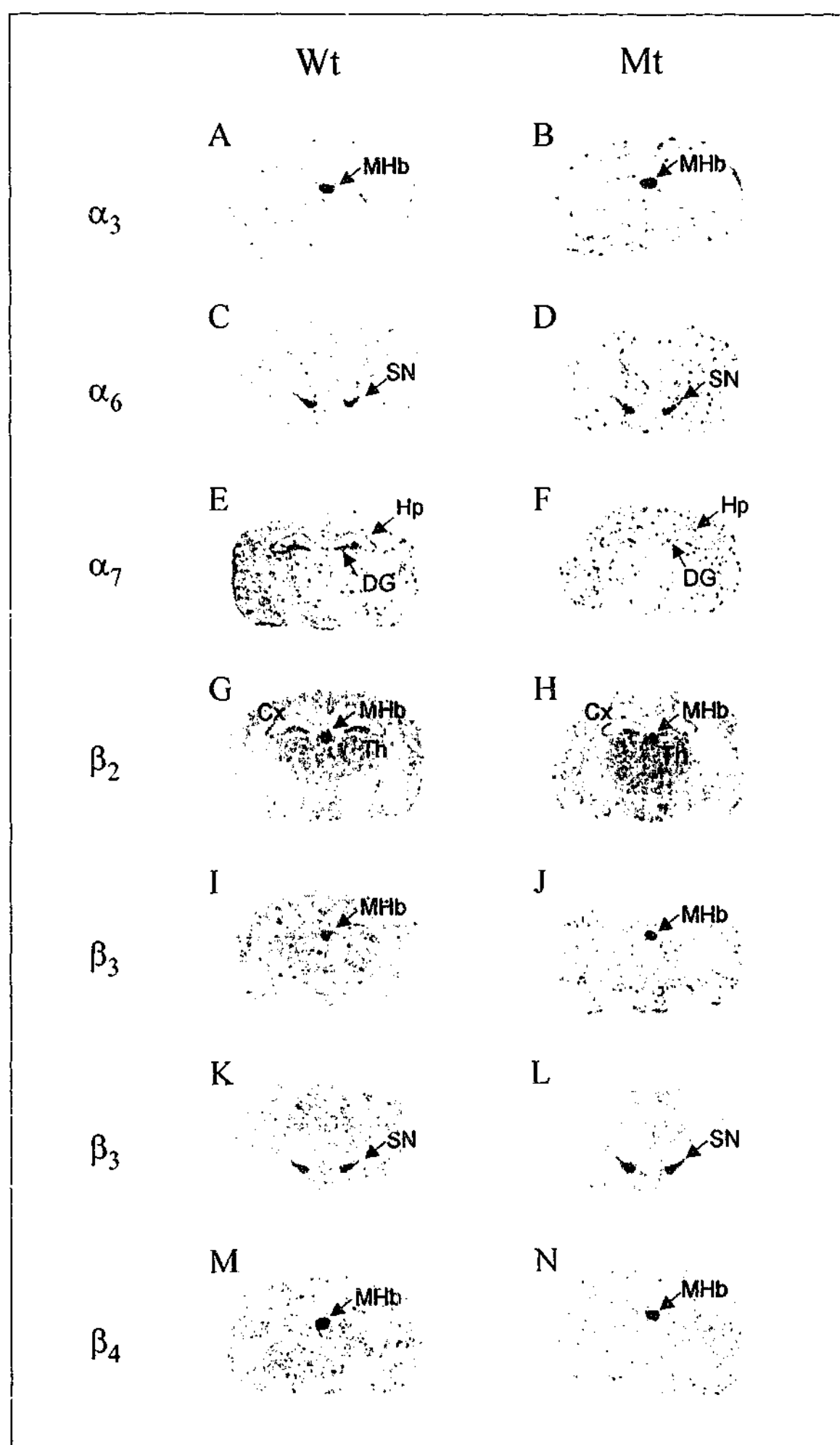
Figure 4.3 Quantitative autoradiography for ISACh 3/4, α_3, α_6, α_7, β_2, β_3 and β_4 neuronal nAChR subunits in Wt and Mt mice.

Quantitative analysis of ISACh 3/4 (A), α_3 (B), α_6 (C), α_7 (D), β_2 (E), β_3 (F) and β_4 (G) binding in Wt and Mt mice. The results are expressed as mean ± SEM (cpm/mm^2). Statistical analysis was performed using a student t-test. There were no statistically significant differences between Mt and Wt mice for any of the probes examined. Regions quantitated were, cortex (Cx); caudate putamen (CPu); thalamus (Th); medial habenula (MHb); substantia nigra (SN) and hippocampus (Hp).
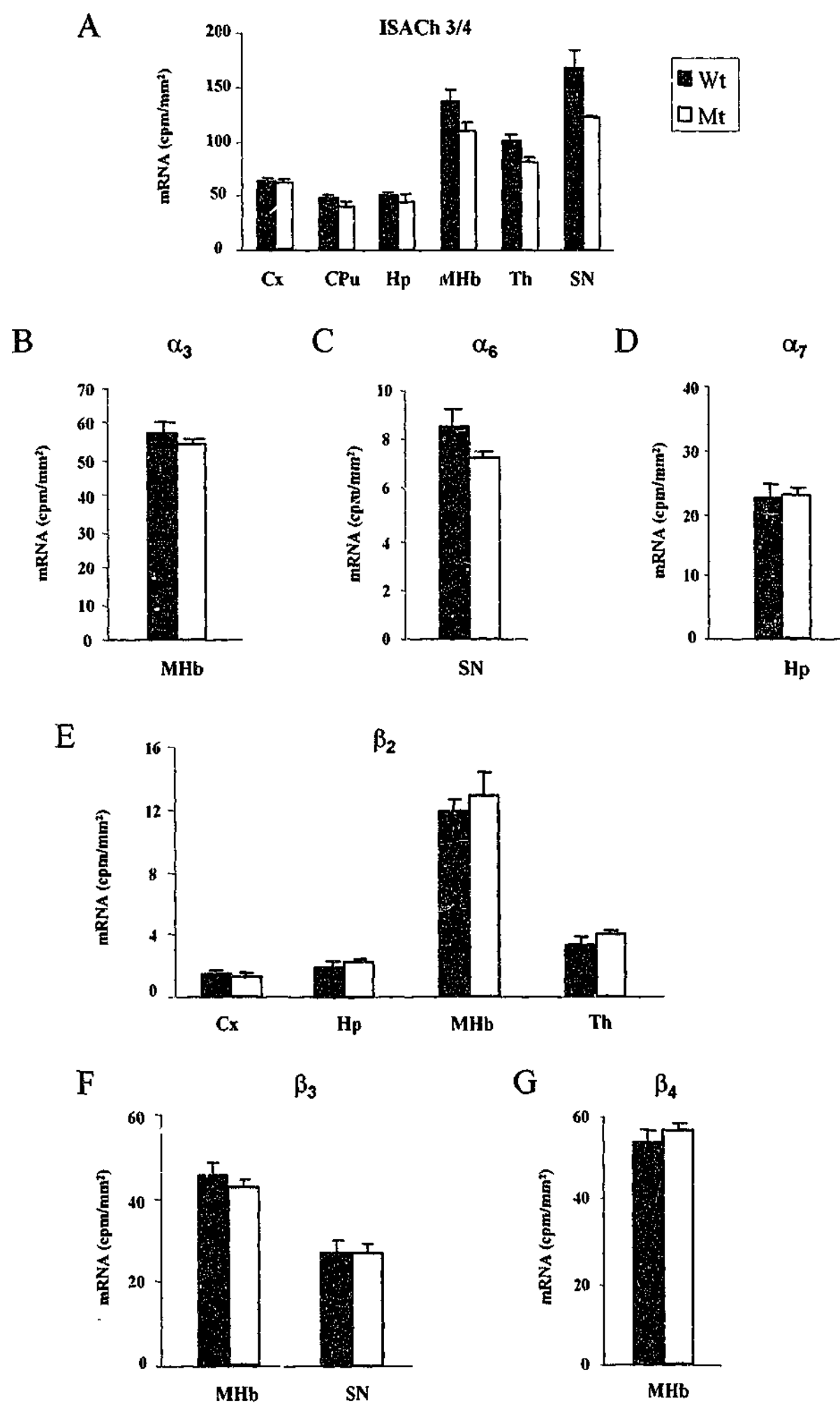
Receptor autoradiography

Autoradiographic ligand binding experiments were performed on a number of animals (Wt, n=9; Hz, n=11; and Mt, n=11). Binding experiments conducted in Wt mice using tritiated nicotine, cytisine and epibatidine showed a similar pattern of high affinity binding (Figure 4.4). [^{3}H]-nicotine labelling was detected at highest levels in the thalamic nuclei, MHb, interpeduncular nucleus (IPn), superior colliculus (SC) and presubiculum (PrS) and moderate levels were found in the Cx, CPu and fasciculus retroflexus (fr) (Figure 4.4A, E & I). [^{3}H]-cytisine (Figure 4.4M) binding showed a similar pattern to [^{3}H]-nicotine binding in Wt mice. [^{3}H]-epibatidine (Figure 4.4C, G & K) binding differed from [^{3}H]-nicotine binding in that [^{3}H]-epibatidine binding to the MHb and fr was more intense as shown by quantitative analysis (Figure 4.5). [^{3}H]-nicotine and [^{3}H]-epibatidine binding showed a qualitatively similar pattern in Mt mice with binding for both radioligands detected in the MHb, IPn, fr and SC (Figure 4.4). The main difference was that [^{3}H]-epibatidine binding was detected at high levels in MHb, IPn, fr and SC (Figure 4.4D, H & L). [^{3}H]-cytisine binding was only detected in the IPn of Mt mice (Figure 4.4N). [^{3}H]-epibatidine binding in Wt and Mt mice with cytisine or nicotine cold competition resulted in loss of SC signal but preservation of binding in the habenulo-interpeduncular pathway (i.e MHb, IPn and fr) (data not shown). [^{125}I]-α-bungarotoxin binding was found to be unchanged in Mt mice compared with Wt mice (Figure 4.4O & P).

Autoradiographic ligand binding experiments performed on an independently generated line of α_4 nAChR subunit knockout mice (Marubio, et al., 1999) also demonstrated high level binding to [^{3}H]-epibatidine in a number of nuclei and reduced [^{3}H]-nicotine binding in the MHb. Quantititative autoradiography however demonstrated that [^{3}H]-

epibatidine binding was reduced in Mt mice compared to Wt mice in the SC and IPn whereas there was no difference in the MHb (Figure 4.5). Furthermore, Marubio and colleagues (Marubio, et al., 1999) showed that [^{3}H]-nicotine binding was found at reduced levels only in the MHb whereas we detected [^{3}H]-nicotine binding in both the IPn and the SC in addition to the previously described binding sites in the MHb (Figure 4.5). Quantitative analysis confirmed that [^{3}H]-nicotine binding was moderately reduced in Mt mice compared to Wt mice in all three nuclei (Figure 4.5).

Topography of spontaneous behaviour

General observation

No gross neurological deficits were apparent in 40 Mt mice [20 female; weight 25.97 ± 0.53 g, 20 male; weight 31.79 ± 0.87 g; age 105 ± 4 days] when compared with 40 Wt controls [20 female; weight 24.59 ± 59, 20 male; weight 33.40 ± 0.64 g; age 109 ± 6 days]; in particular, no epileptic seizures were observed over prolonged observation.

Exploratory phase

Over an initial 1 hr phase of exploratory activity (Figure 4.6A), Mt mice were characterized by increased sniffing [+13%; $F_{(1,76)} = 6.76$, P=0.01] and decreased grooming [-15%; $F_{(1,76)} = 4.98$, P=0.03], for both genders; females groomed less than males for each genotype.

Figure 4.4. Ligand autoradiography of nicotinic receptor agonists in mouse brain.

Autoradiographic mapping using [^{3}H]-nicotine identifying the presence of high-affinity nicotinic receptors in Wt (A, E & I) and Mt (B, F & J) mouse brain sections at Bregma levels -2.06 (for A & B), -3.08 (for E & F) and -3.40 (for I & J). Panels A, E & I show binding in the thalamus (Th), cortex (Cx), medial habenula (MHb), fasciculus retroflexus (fr), superior colliculus (SC) and interpeduncular nucleus (IPn). Panel B, F and J show persistent binding in the Mt mice, arrows indicate the location of the MHb, fr, SC and IPn. Autoradiographic mapping using [^{3}H]-epibatidine in Wt (C, G and K) and Mt (D, H and L) mouse brain sections at Bregma levels -2.06 (for C & D), -3.08 (for G & H) and -3.40 (for K & L). Binding is present in Wt mice in the Th, Cx, MHb, fr, SC and IPn. Mt mice showed binding in the MHb, fr, SC and IPn. Autoradiographic mapping using [^{3}H]-cytisine in Wt (M) and Mt (N) mouse brain sections at Bregma levels -3.40, showing persistent binding in the IPn. Autoradiographic mapping using [I^{125}]-α-bungarotoxin in Wt (O) and Mt (P) mouse brain sections at Bregma levels -2.54 (Franklin and Paxinos, 1997). No difference was apparent between the genotypes.
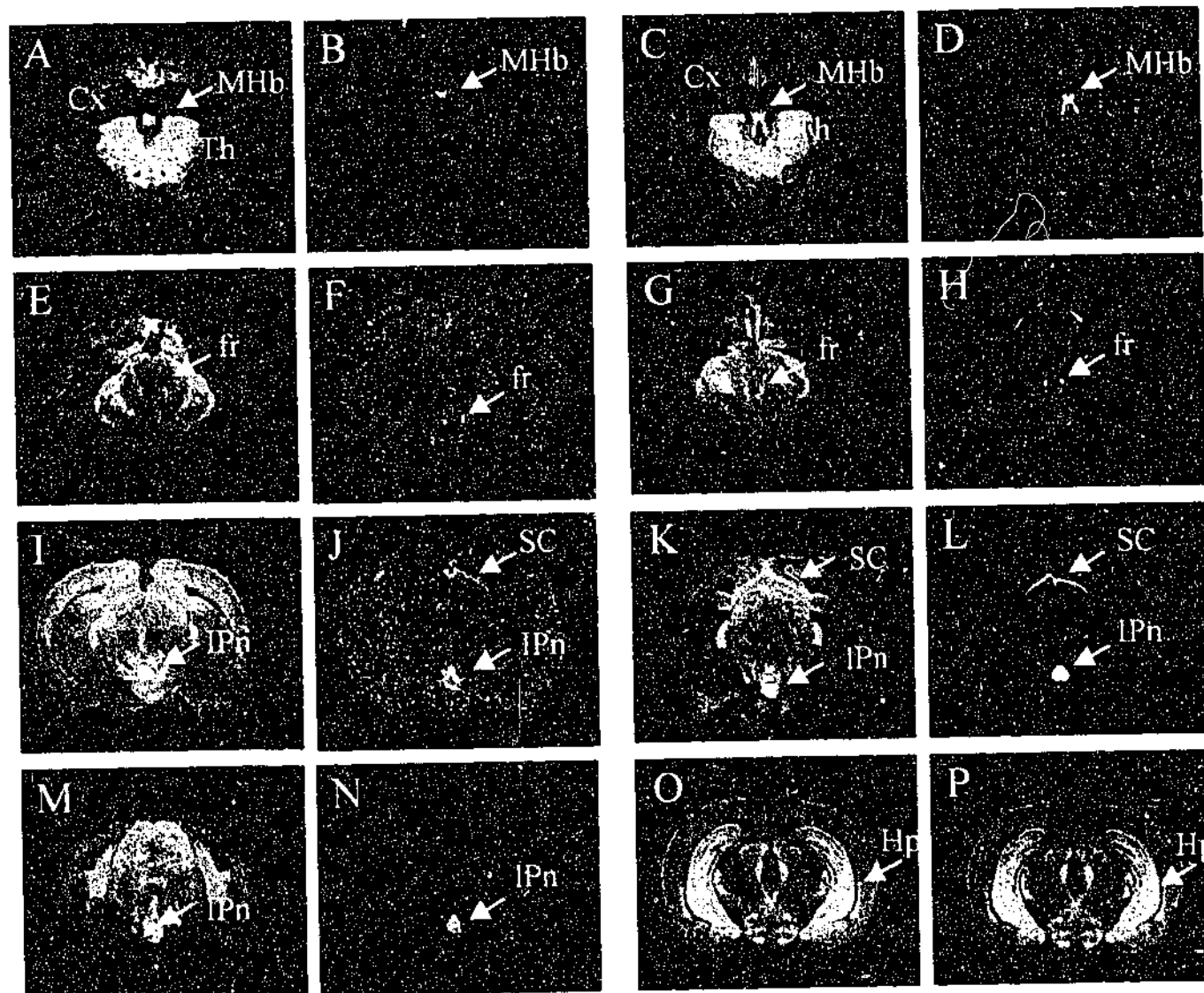
Figure 4.5 Quantitative autoradiography for nicotinic agonists in the mouse brain.
Quantitative analysis of [^{3}H]-nicotine (A), [^{3}H]-cytisine (B), [^{3}H]-epibatidine (C) and [^{125}I]-α-bungarotoxin (D) binding in Wt, Hz and Mt mice. The results are expressed as mean ± SEM (fmol/mg). Statistical analysis was performed using a one-way ANOVA. *$P<0.05$ versus Wt controls. Regions quantitated were, cortex (Cx); caudate putamen (CPu); thalamus (Th); medial habenula (MHb); superior colliculus (SC); interpeduncular nucleus (IPn); fasciculus retroflexus (fr); retroparafasciculus (RPF); hippocampus (Hp) and the presubiculum (PrS).

A. Nicotine

B. Cytisine

C. Epibatidine

D. α-Bungarotoxin

Legend: ■ Wt □ Hz □ Mt
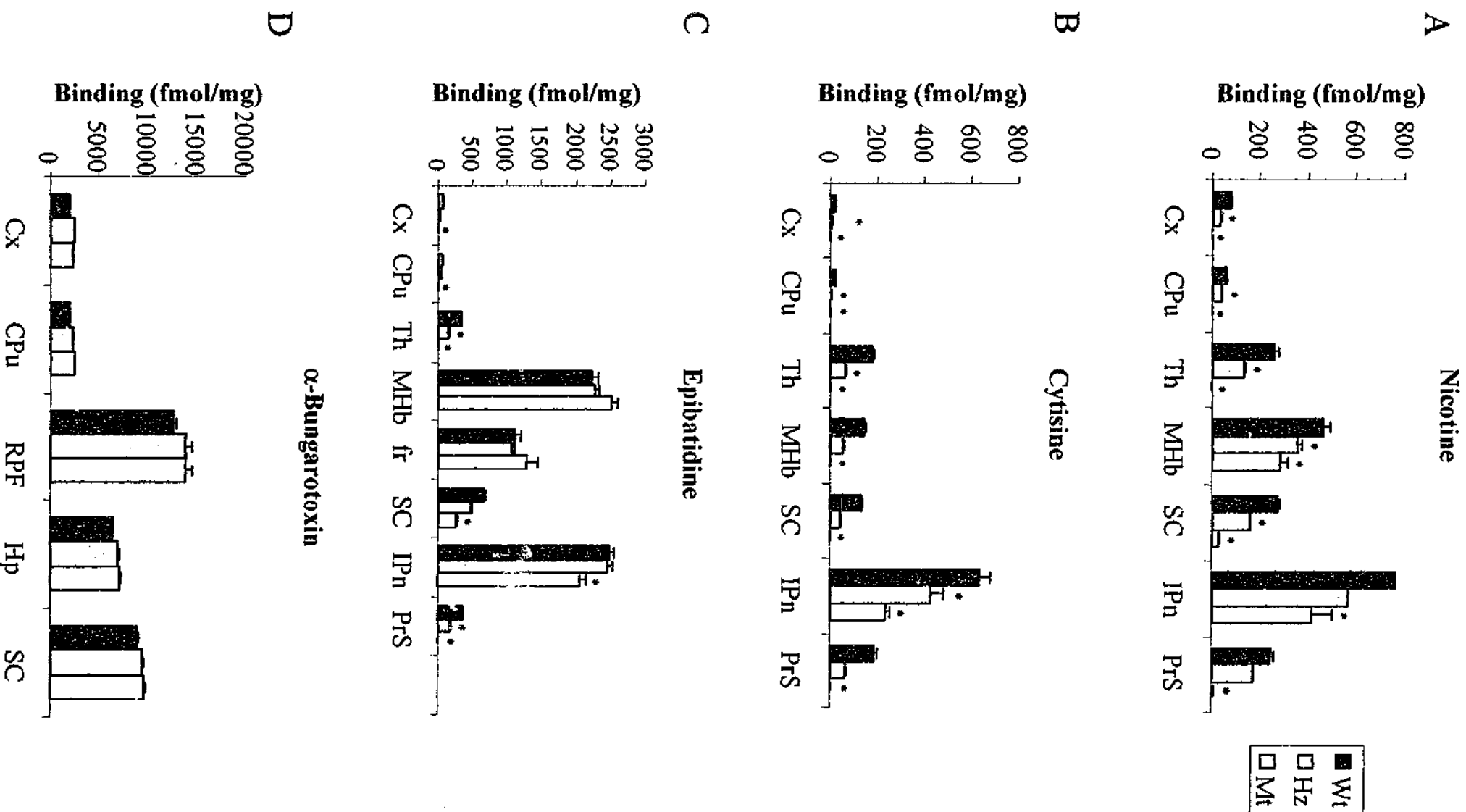
Habituation phase

Over the subsequent phase of habituation (Figure 4.6B), additional effects were evident. Each of sniffing, total rearing, rearing seated, rearing to wall, rearing free and chewing occurred to excess in Mt mice throughout this phase [$F_{(1,76)} = 17.56$, $P<0.001$; $F_{(1,76)} = 14.95$, $P<0.001$; $F_{(1,76)} = 13.96$, $P<0.001$; $F_{(1,76)} = 16.15$, $P<0.001$; $F_{(1,76)} = 4.94$, $P<0.05$; $F_{(1,76)} = 5.19$, $P<0.05$, respectively]; for those behaviours which declined significantly by time-bins (i.e habituation of sniffing, total rearing, rearing seated, rearing to wall), this did not differ by genotype or gender, while for those low frequency behaviours for which habituation was not apparent (i.e. rearing free and chewing), males habituated more rapidly than did females for each genotype. Locomotion also occurred to excess in Mt mice [$F_{(1,76)} = 11.11$, $P=0.001$], due to their reduced rate of habituation [time x genotype interaction: $F_{(10,760)} = 1.97$, $P=0.03$], for both genders. While overall levels of grooming were comparable, this behaviour varied over time-bins in a manner that differed between the genotypes [time x genotype interaction: $F_{(10,760)} = 3.38$, $P<0.001$] for both genders. Overall levels of stillness were decreased in Mt mice [$F_{(1,76)} = 24.83$, $P<0.001$] due to their reduced rate of habituation [time x genotype interaction: $F_{(10,760)} = 1.98$, $P=0.03$], for both genders.

In summary, over an initial exploratory phase, Mt mice showed increased sniffing with decreased grooming. Over the subsequent habituation phase, increased sniffing in Mt mice endured together with the emergence of increases in most other topographies of behaviour; in particular, increased locomotion in Mt mice was characterized by a reduced rate of habituation relative to Wt mice.

Figure 4.6 Topography of spontaneous behaviour.

(A) Behavioural counts for sniffing (Sn), Locomotion (L), sifting (S), total rearing (Rt), rearing from a seated position (Rs), rearing free (Rf), rearing to wall (Rw), grooming (Gr), biting (B), stillness (St), chewing (Ch), vacuous chewing (VCh), eating (E) and licking (Li) in Wt (n=40) versus Mt (n=40) mice. Data are mean counts ± SEM over a 1 hour phase of initial exploratory activity. $**P<0.01$, $*P<0.05$ versus Wt mice. (B) Behavioural counts for sniffing, eating, grooming, locomotion, rearing total, stillness, rearing seated, rearing free and rearing to wall in Wt (n=40) versus Mt (n=40) mice. Data are mean counts ± SEM per 10 min period at indicated intervals over habituation phase. Over the initial 1 hour exploratory phase, Mt mice showed a small increase in sniffing and a reduction in grooming. Over the habituation period, Mt mice retained a higher level of activity in locomotion, chewing and all measures of rearing.

Time (min)
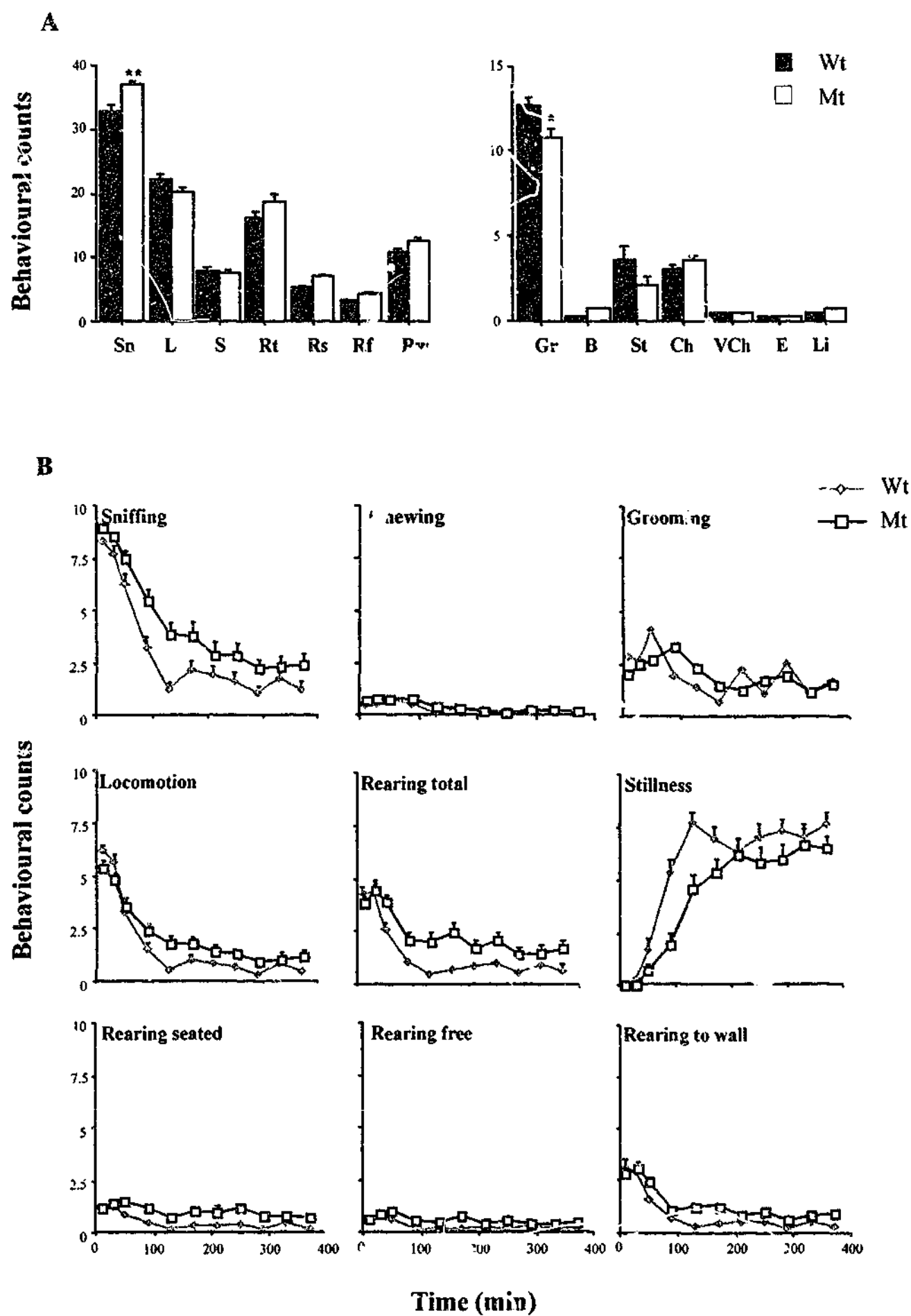
Rotarod performance

Among 37 Mt mice [15 female; weight 25.01 ± 0.58, 22 male; weight 31.32 ± 0.8 g; age 97 ± 3 days] and 44 Wt controls [20 female; weight 24.45 ± 0.76, 24 male; weight 33.27± 0.51 g; age 96 ± 5 days], performance improved with time [three trials on each of three successive test days: $F_{(8,632)} = 18.47$, $P < 0.001$] in a manner that did not differ by genotype or by gender (Figure 4.7). Thus, in this test of sensorimotor coordination, Mt mice evidenced no deficits.

Elevated plus-maze performance

When compared with 51 Wt controls [21 female; weight 24.2 ± 0.47, 30 male; weight 31.44 ± 1.0 g; age 96 ± 5 days], 70 Mt mice [36 female; weight 25.7. ± 0.47, 34 male; weight 32.81 ± 0.71 g; age 97 ± 3 days] spent less time in open arms [$F_{(1,115)} = 6.92$, $P < 0.01$] and made fewer open arm entries [$F_{(1,115)} = 6.9$, $P < 0.01$], in a manner that did not differ by gender (Figure 4.8); for each genotype, males entered fewer arms than females. Thus, in this test of 'anxiety-like' behaviour Mt mice evidenced heightened levels.
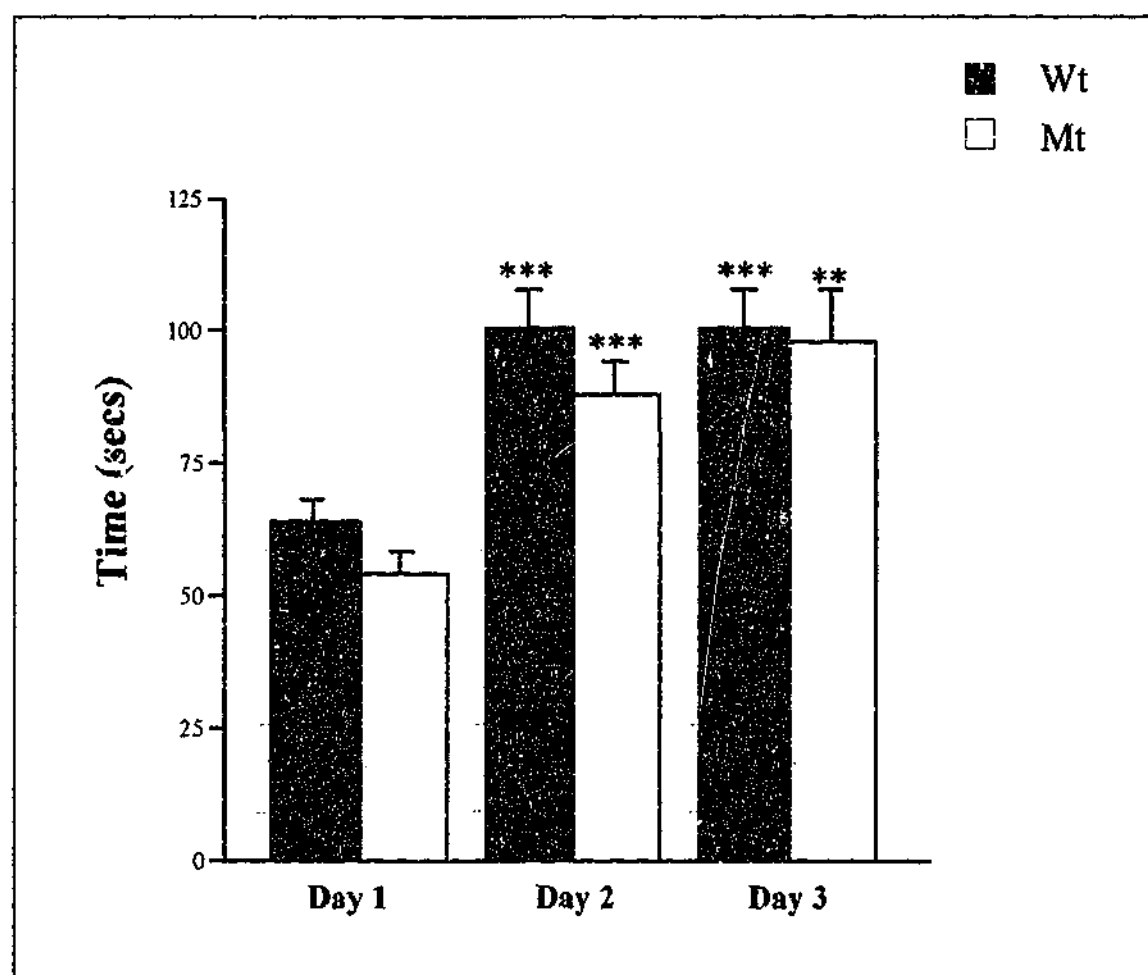
Figure 4.7 Rotarod performance

Performance on a repeated motor coordination task in Wt (n=37) versus Mt (n=44) mice. Mice were evaluated on the rotarod test three times a day for three consecutive days. Data are presented as the mean ± SEM of the daily averages. ***P<0.001, **P<0.01, versus same genotype on day 1. Both genotypes acquired the task to a similar extent with no effect of gender or any gender x genotype interaction. Performance improved over three successive days (F=18.47, df=8, P<0.001) and which did not differ by gender or genotype in the absence of any time x gender x genotype interaction.

■ Wt
☐ Mt

A

B
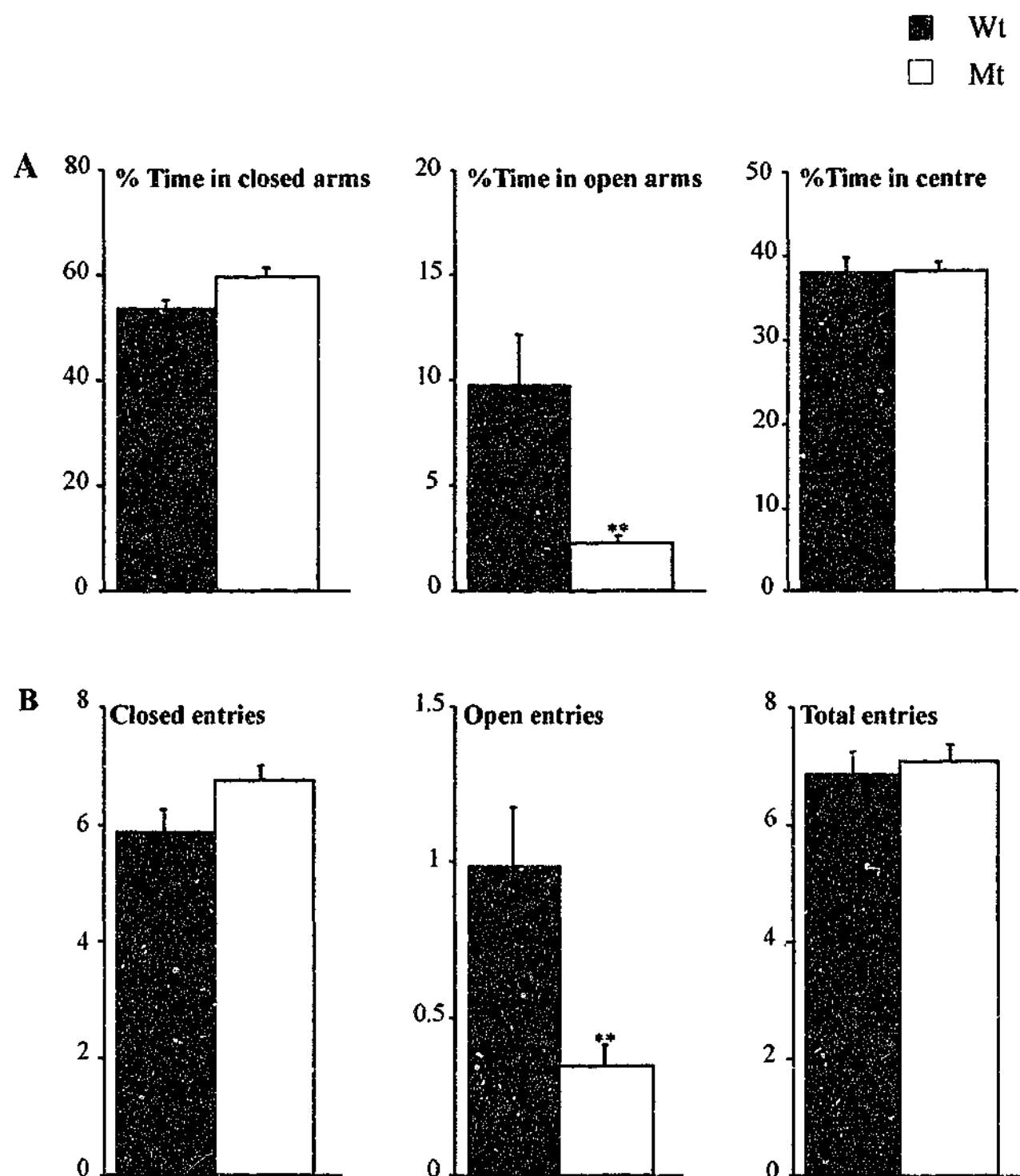
Figure 4.8 The elevated plus-maze assay

Data are presented as the mean $\pm$ SEM of (A) % time in closed arms, % time in open arms and % time in centre.   (B) Number of entries into closed arms, open arms and centre, Wt mice (n=51) and Mt mice (n=70) **P<0.01, *P<0.05 versus Wt mice. In Mt mice there was significantly less time spent in open arms and significantly fewer open arm entries compared to Wt mice.

Effects of nicotine – unhabituated condition

Results from this study differed from those of Marubio and colleagues (Marubio et al., 1999) who analysed an independently generated line of α_4 nAChR subunit knockout mice finding no significant differences from baseline in non-habituated locomotor activity in response to 1 or 2 mg/kg nicotine. On comparing 40 Mt mice [20 female; weight 25.62 ± 0.46, 20 male; weight 31.55 ± 0.82 g; age 97 ± 3 days] with 40 Wt controls [20 female; weight 25.16 ± 0.45, male; weight 32.47 ± 0.55 g; age 100 ± 2 days], declines in each of sniffing, locomotion and total rearing over the three time periods were influenced by dose of nicotine administered in a genotype-specific manner [genotype x dose x time interactions: $F_{(8,120)} = 2.23$, $P=0.03$; $F_{(8,120)} = 3.98$, $P<0.001$; $F_{(8,120)} = 2.16$, $P<0.05$, respectively] (Figure 4.9A, B & C). For sifting, a generally comparable though blunted profile was apparent (Figure 4.9D). For individual topographies of rearing, grooming and chewing, less consistent profiles of effect were apparent (data not shown).

In summary, under this unhabituated condition, Mt mice showed less decline in sniffing, locomotion, total rearing and sifting over these three time periods than was evident in Wt mice; decline in behaviour in Mt mice was restored by low-mid doses of nicotine, particularly over the late (40-55 min) period.

Figure 4.9 Response to nicotine administration in unhabituated mice.

Behavioural counts summed over 0-15, 20-35 and 40-55 minutes for sniffing (A), locomotion (B), rearing total (C) and sifting (D) responses to (-) – nicotine (0.1-2.7 mg/kg, s.c.) versus vehicle (V) in unhabituated Wt and Mt mice. Data are means $\pm$ SEM for n=8 per group; $**P<0.01$, $*P<0.05$ versus Wt mice. $^aP<0.05$, $^bP<0.01$, $^cP<0.001$ versus vehicle treated mice of same genotype. In the first 15 minutes of the exploratory phase following nicotine administration, Wt mice showed a dose-dependent reduction in the locomotor activity and total rearing whereas in the Mt mice, no effect on locomotion and total rearing was seen. In the last period of the exploratory phase, vehicle-treated Mt mice showed basal hyperactivity. The Mt mice also responded to nicotine in the late phase where nicotine induced a reduction in locomotion, sniffing, rearing and sifting to the levels of their Wt mice counterparts.
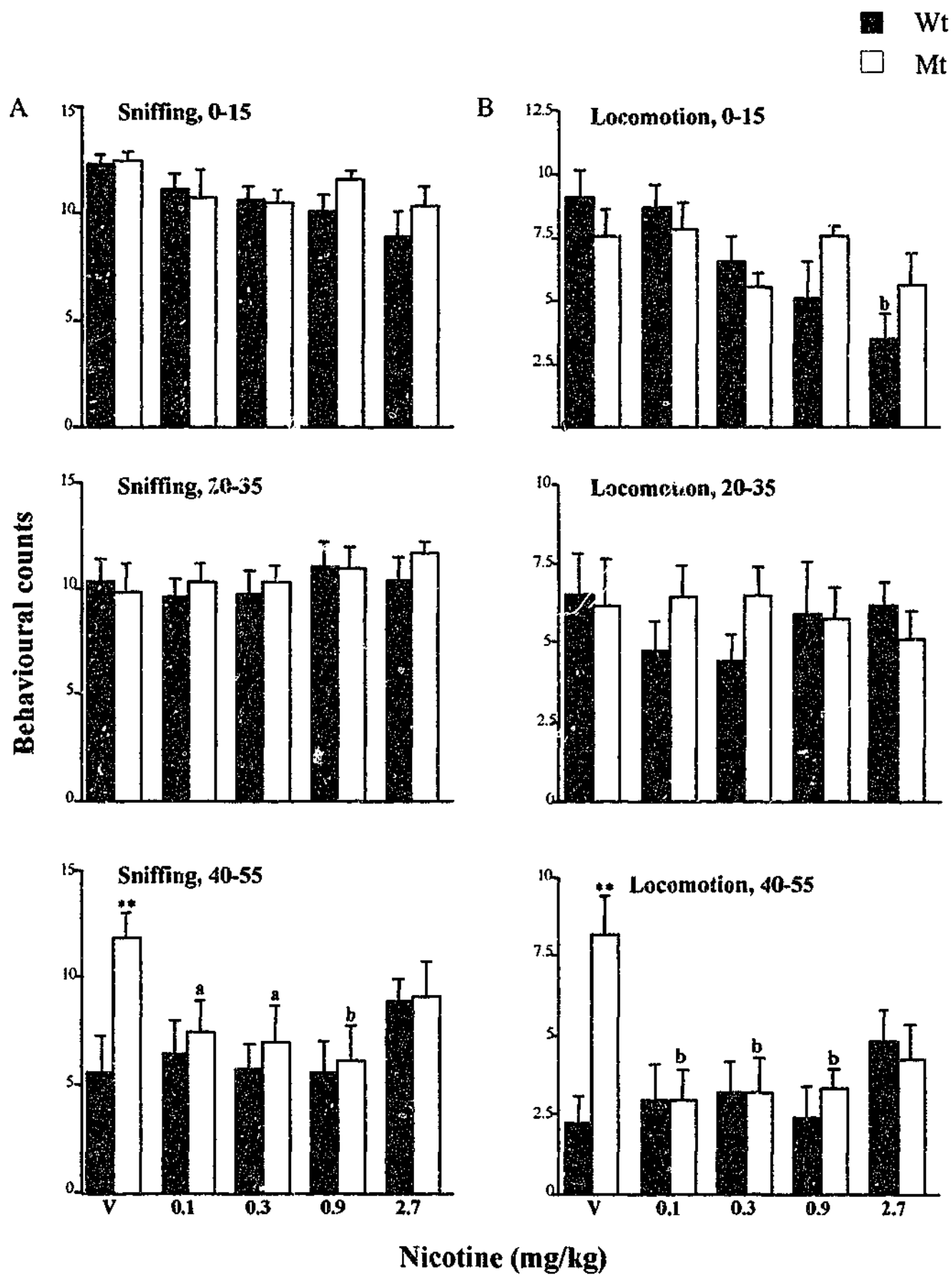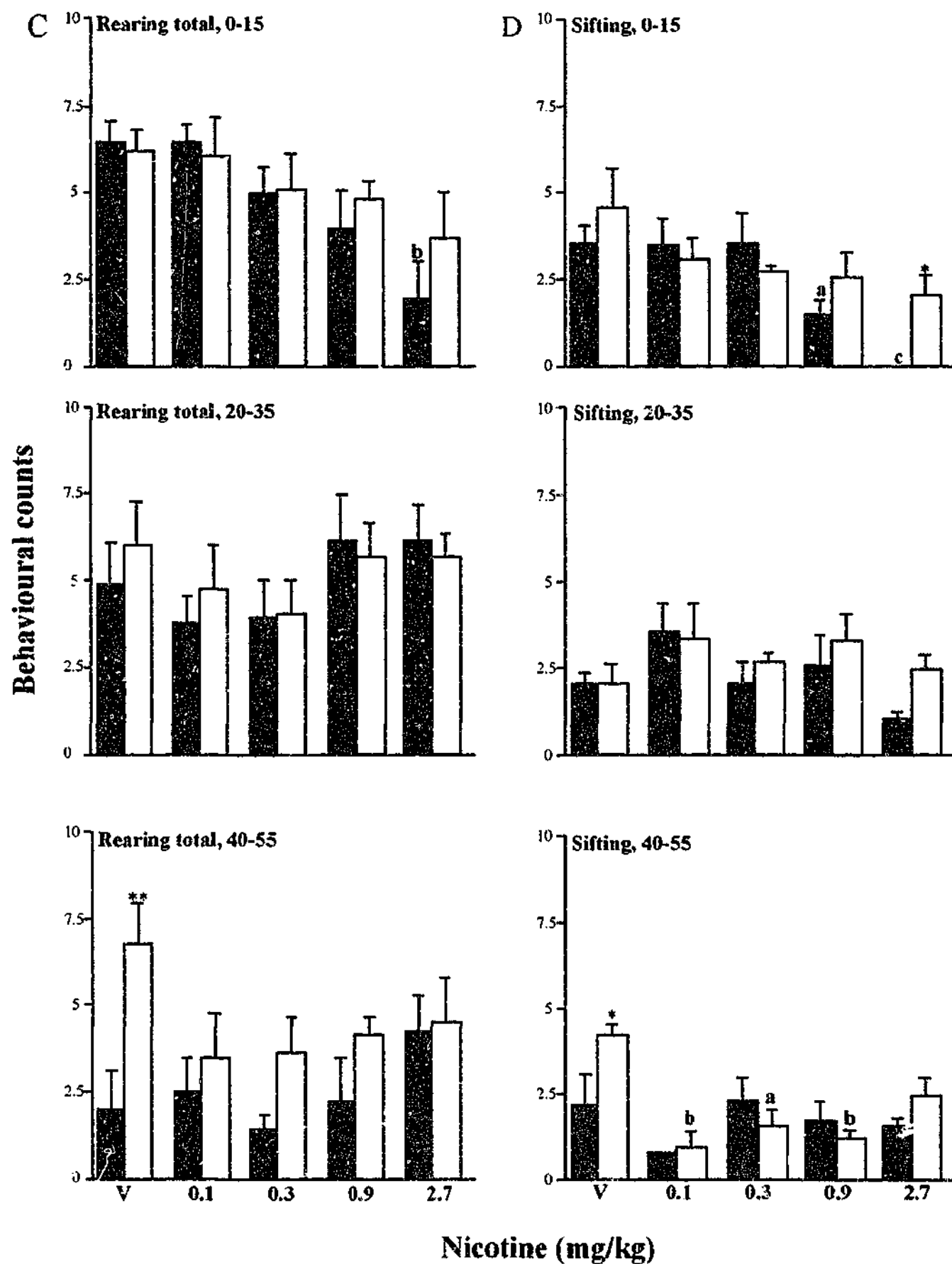
Effects of nicotine – habituated condition

On comparing 20 Mt mice [10 female; weight 25.2 ± 0.7, 10 male; weight 33.2 ± 0.2 g; age 95 ± 3 days] with 20 Wt controls [10 female; weight 26.28 ± 0.6, 10 male; weight 32.38 ± 0.38 g; age 95 ± 5 days], each of sniffing, locomotion and total rearing declined over the three time periods; for locomotion and total rearing, an action of nicotine to reduce these behaviours declined with time in a manner that was influenced by dose of nicotine administered [dose x time interactions: $F_{(8,120)} = 3.14$, $P=0.01$; $F_{(8,120)} = 4.64$, $P<0.001$, respectively] (Figure 4.10A, B & C). For sifting, a generally comparable though blunted profile was apparent (Figure 4.10D), and for individual topographies of rearing, grooming and chewing, similar profiles of effect were apparent (data not shown).

In summary, under this habituated condition, lower levels of behaviour continued to decline with time; nicotine acted mainly to further reduce behaviour, primarily over the early [20-35 min] period, in a manner that tended to be less prominent in Mt mice than in Wt mice. Thus, the above late-period action of nicotine to restore in Mt mice a Wt-like behavioural profile appeared specific to the unhabituated condition.

Figure 4.10 Response to nicotine administration in well-habituated mice.

Behavioural counts summed over 0-15, 20-35 and 40-55 minutes for sniffing (A), locomotion (B), rearing total (C) and sifting (D) responses to (-) – nicotine (0.1-2.7 mg/kg, s.c.) versus vehicle (V) in well-habituated Wt and Mt mice. Data are means ± SEM for n=8 per group; **P<0.01, *P<0.05 versus Wt mice. [a]P<0.05, [b]P<0.01, [c]P<0.001 versus vehicle treated mice of same genotype. Nicotine administration in Wt mice resulted in a reduction in locomotion, total rearing and sifting, in the first 15 minutes, however in comparison to Wt mice, nicotine had no measurable behavioural effect in well-habituated Mt mice.

C Rearing total, 0-15

D Sifting, 0-15

Rearing total, 20-35

Sifting, 20-35

Rearing total, 40-55

Sifting, 40-55

Behavioural counts

Nicotine (mg/kg)
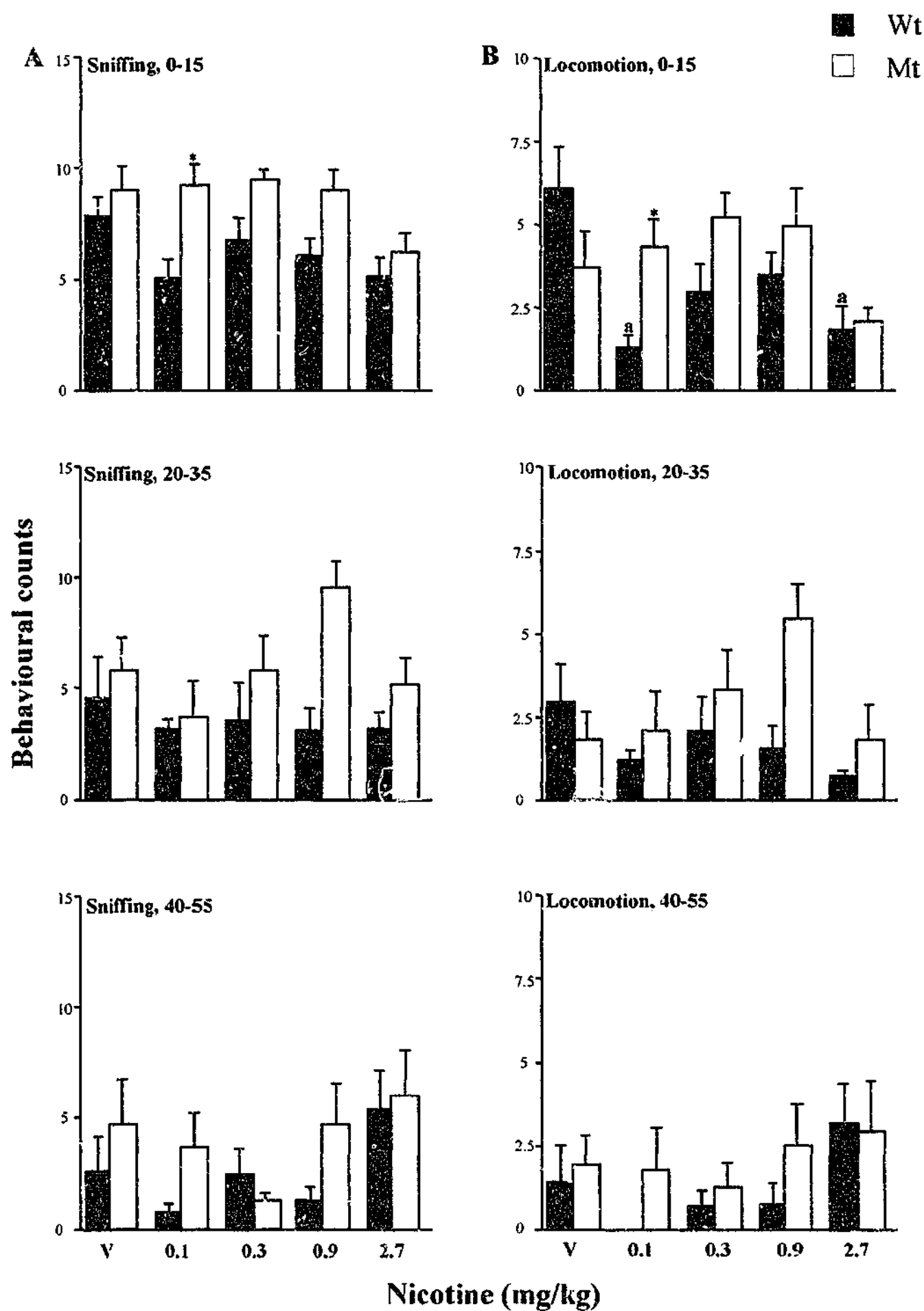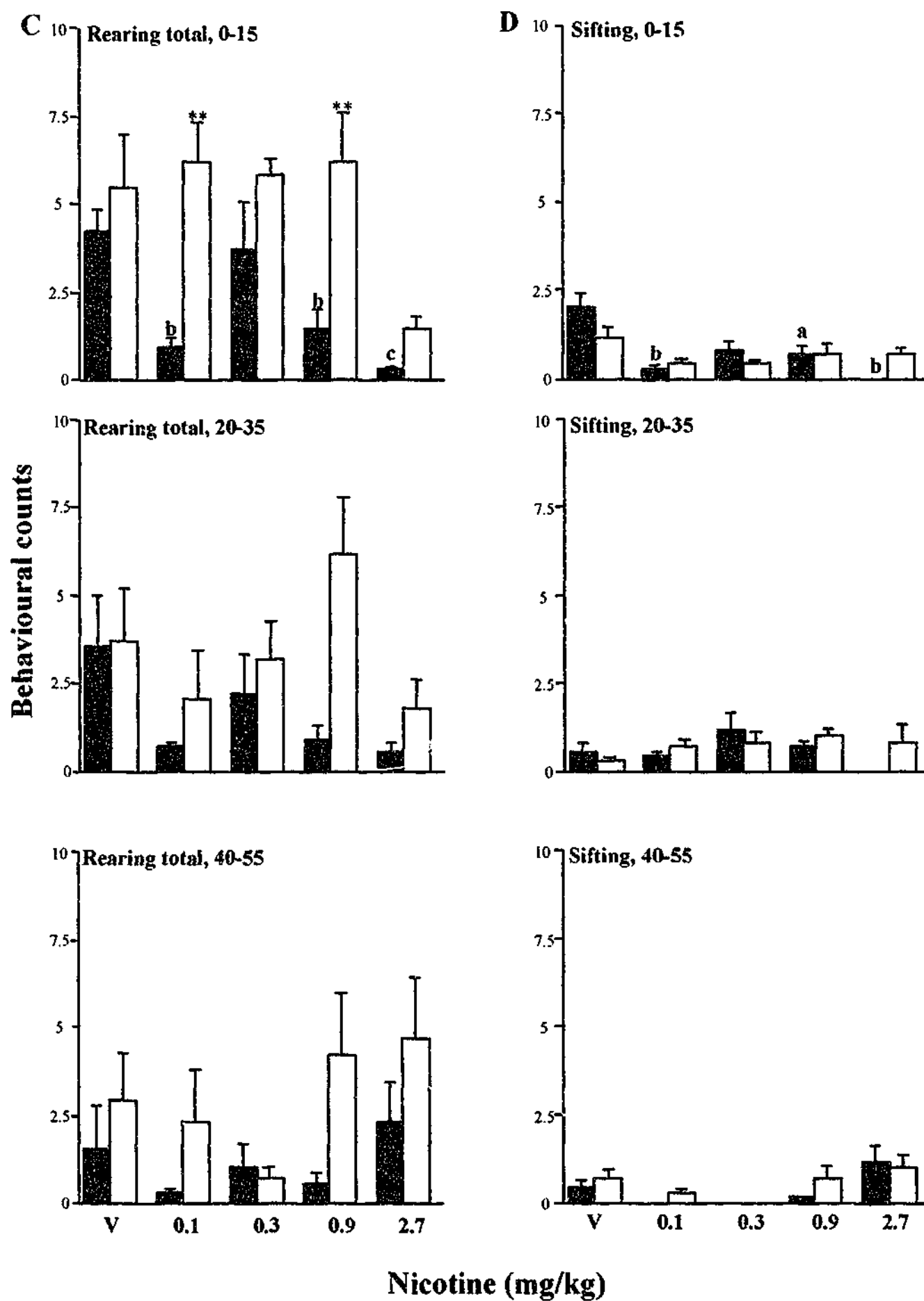
4.5   DISCUSSION

A line of α_4 nAChR subunit knockout mice has been successfully generated and a detailed behavioural characterization undertaken. Mt mice were normal with respect to body weight, fertility, home cage behaviour and did not exhibit spontaneous epileptic seizures. There were no differences in size or morphology of the brain and screening of a number of organs failed to show any gross structural or histological abnormalities. In addition, no significant quantitative differences were found between Mt and Wt mice in the expression level of α_4 nAChR subunit transcripts identified by hybridization with probes ISACh3/4. These oligonucleotide probes were designed to hybridize to mRNA transcribed from preserved DNA upstream of deleted gene sequence and thereby specifically identify α_4 nAChR subunit positive cells. The lack of apparent structural changes in the brain together with the results of *in situ* hybridization analysis suggests that the α_4 nAChR subunit is not required for the survival of α_4 nAChR subunit positive cell precursors or for the maintenance of mature α_4 nAChR subunit positive neurons in the adult brain.

The α_4/β_2 subunit receptor configuration, known to be expressed at high levels in the thalamus and the habenulo-interpeduncular system (Zoli, et al., 1998), is responsible for the vast majority of agonist binding. In this study the binding patterns of a number of nicotinic agonists in Wt and Mt mice have been described. These data combined with the results of previous studies (Zoli, et al., 1998) on mice lacking functional β_2 nAChRs allows further characterization of brain nAChRs. Mt mice maintain high level [^{3}H]-nicotine binding in the MHb, IPn and low level binding in the SC and fr whereas the β_2 knockout mice showed no binding with this ligand (Picciotto, et al., 1995). β_2 knockout mice had [^{3}H]-cytisine binding sites in the MHb, IPn and fr

(Zoli, et al., 1998) whereas Mt mice had binding in the IPn but not in the MHb or fr. β_2 knockout mice differ from Mt mice in that Mt mice showed additional [^{3}H]-epibatidine binding sites in the SC. [^{3}H]-nicotine autoradiography results from Mt mice, differed from ligand binding experiments performed on an independently generated line of α_4 nAChR knockout mice (Marubio, et al., 1999). In this earlier study, [^{3}H]-nicotine binding was found at low levels only in the MHb whereas additional low level binding sites were found in the IPn, SC and fr of Mt mice (Figure 4.4 and 4.5). [I^{125}]-α-bungarotoxin high affinity binding was similar in both α_4 and β_2 nAChR knockout mice whereas it was absent in α_7 knockout mice (Orr-Urtreger, et al., 1997) confirming the selectivity for this ligand. The differences in the binding patterns seen in α_4 and β_2 knockout mice is an important finding because it highlights the fact that the α_4 and β_2 knockout mice are different with respect to the topography of functional high affinity nicotinic receptors. This difference may underpin variation in spontaneous behaviour and drug responses.

There are known to be high levels of α_3, α_4 (Wada, et al., 1989) and low levels of α_6 mRNA (Le Novere, et al., 1996) in the rodent MHb whereas all β subunits surveyed are detected in this nucleus (Deneris, et al., 1989, Duvoisin, et al., 1989, Wada, et al., 1989). No significant differences were found in the expression profile of a large number of subunits within the MHb of Mt and Wt mice. Strong hybridization signals were detected for α_3, β_2, β_3 and β_4 confirming the results of previous studies (Le Novere, et al., 1996). The receptor configuration responsible for the MHb binding to [^{3}H]-nicotine seen in Mt mice therefore involves the β_2 subunit in combination with the α_3 subunit expressed at high levels and/or the α_6 subunit, expressed at low levels. Nicotine autoradiographic analysis in β_2 knockout mice suggests that the β_3 and β_4

expression detected in the MHb is insufficient to mediate [³H]-nicotine binding. The finding that β_2 knockout mice retain high affinity [³H]-cytisine binding in the MHb and that Mt mice lack MHb binding confirms that cytisine binding in the MHb requires the α_4 subunit but does not require the β_2 subunit. [³H]-epibatidine binding was detected in the MHb of both knockout lines suggesting that [³H]-epibatidine binding can occur in the absence of β_2 or α_4 subunits.

A detailed topographical analysis of spontaneous and nicotine-stimulated behaviour was undertaken. Performance on the rotarod, a test of sensorimotor co-ordination, revealed no significant differences between genotypes; both Mt and Wt mice acquired the task over comparable periods and to similar extents. Over the initial 1 h exploratory phase, Mt mice showed an increase in sniffing and a reduction in grooming. Over the subsequent phase of habituation, additional effects were revealed, as certain topographies of behaviour did not habituate to the same extent in Mt mice. For sniffing, both genotypes habituated to similar extents, whereas for locomotion and topographies of rearing and chewing, Mt mice retained a higher level of activity throughout the habituation phase. Thus, as noted previously for D_{1A} dopamine receptor knockout (Clifford, et al., 1998), confining assessments to a limited period or using composite indices of 'activity' can obscure important effects of a given knockout that are manifested only later in the course of habituation and/or involve specific behavioural topographies. The present data indicate a topographically-specific interaction between α_4 nAChR knockout and the neuronal processes of habituation in the regulation of behaviour.

Alterations in 'motor activity' following nicotine administration have been described previously. Though these studies have most commonly used techniques which fail to resolve individual topographies of behaviour (Morrison and Stephenson,

1972; Clarke, 1987, Clarke and Kumar, 1983), state-dependency of effect, e.g. treatment in a familiar versus a novel environment, has been reported (Picciotto, et al., 2000). Using the present ethologically-based approach, over the first 15 mins of the exploratory phase, nicotine induced in Wt mice a dose-dependent reduction in locomotion, total rearing, sifting and less so sniffing, while there was no such drug effect in Mt mice; rather, as above, Mt mice showed relative preservation of these behaviours over the exploratory phase, with late decline in behaviour restored in Mt mice to Wt levels by low-mid doses of nicotine. Under the habituated condition, however, during which lower levels of behaviour continued to decline with time, nicotine was still able to further reduce locomotion, total rearing, sifting and less so sniffing; this occurred primarily over the early period, in a manner that tended to be less prominent in Mt mice than in Wt mice. Thus, the above late-period action of nicotine to restore in Mt mice a Wt-like behavioural profile appeared specific to the unhabituated condition. The lack of modulation of locomotion and sniffing behaviour in Mt mice with high doses of nicotine (Figure 4.9) may reflect pharmacological desensitization of remaining nicotinic receptors (Vibat, et al., 1995; Couturier, et al., 1990; Fenster, et al., 1997). These data indicate a topographically-specific interaction between α_4 nAChR knockout and the neuronal processes of habituation in determining not only the regulation of spontaneous behaviour but also the effects of nicotine on behaviour.

One hypothesis is that the α_4 nAChR subunit is required for activation of inhibitory neural circuits, hence its absence would result in an elevated baseline of specific behavioural topographies. Pharmacological doses of nicotine may nonetheless act through non-α_4 nAChR containing nicotine binding sites, perhaps those present in the habenulo-interpeduncular pathway, to reduce inhibitory tone. However, this might only be evident when such inhibitory neural tone is at a low level, as would be expected

in actively exploring mice; the delayed effect of nicotine administration in reducing locomotion, sniffing, rearing and sifting in this exploratory condition may reflect some temporal inefficiency of this parallel pathway in responding to change. Furthermore, the effect of an agent which acts primarily to activate inhibitory pathways may be less apparent in well-habituated mice, where inhibitory pathways (both nAChR dependent and independent) might be already prominently activated. There are a number of studies describing nicotine-induced release of the inhibitory neurotransmitter GABA either from isolated synaptosomes or in slice preparations (Lena, et al., 1993; Kayadjanian, et al., 1994; McMahon, et al., 1994). Of particular relevance to our findings is the observation of Lena and colleagues (Lena, et al., 1993) showing that nicotine increases the frequency of postsynaptic GABAergic currents in rat interpeduncular nucleus neurons. There is evidence for the presence of α_3, α_6, α_7, β_3 and β_4 transcripts in the Mt mouse brain, however, as there are no subunit selective nAChR antagonists which can be administered to the whole animal, the identification of the molecular species of α and/or β subunits involved in mediating this behavioural effect of nicotine in Mt mice may ultimately require the generation of subunit double knockout mutants. Evidence from the literature (Lena, et al., 1993; Kayadjanian, et al., 1994; McMahon, et al., 1994) in addition to the observation of enhanced sensitivity of Mt mice to GABA antagonists (see chapter 5) is consistent with the concept that downregulated GABA neurotransmission is likely to underlie the exploratory phase hyperactivity.

Nicotinic receptor agonists which bind the α_4/β_2 receptor configuration are known to have an effect on anxiety (Gilbert, et al., 1989; Pomerleau, 1986; Brioni, et al., 1993). Nicotine in particular appears to have anxiolytic-like effects in a number of behavioural paradigms, including the elevated plus-maze assay (Costall, et al., 1989;

Brioni, et al., 1993). These results suggest that the α_4 subunit may indeed be intimately involved in mediating anxiolytic-like effects. The nicotinic receptor agonists ABT-418 and lobeline share nicotine's anxiolytic-like actions whereas cytisine (Brioni, et al., 1993), anabasine and epibatidine are devoid of anxiolytic-like properties (Decker, et al., 1995). The differential behavioural profile of neuronal nicotinic agonists implies that the anxiolytic-like actions may be mediated by a specific subunit configuration of the nAChR. If this were indeed the case, it would expected that agonists which have similar effects on anxiety have comparable ligand binding profiles with respect to both qualitative (i.e topography of binding) and quantitative (i.e agonist specific intensity of binding) parameters. The differential preservation of binding in Mt mice may explain the lack of anxiolytic-like effects seen with cytisine as it implies selectivity for a specific receptor subpopulation but would not readily explain the lack of anxiolytic-like effect of epibatidine as the binding pattern of epibatidine is qualitatively similar to nicotine in Mt mice. Quantitative autoradiographic analysis demonstrates comparable epibatidine binding in Wt and Mt mice in the MHb and fr (although a minor reduction of epibatidine binding of 16% in the IPn of Mt mice compared to Wt mice). In contrast, nicotine binding shows a substantial reduction of 40% in the MHb and 45% in the IPn in Mt mice compared to Wt mice. The situation is further complicated by the potential for differential segregation of nAChR subunits on individual neurons.

The finding of increased exploratory activity evident on assessment of spontaneous behaviour was surprising given the anxiety-like profile demonstrated by elevated plus-maze analysis, as anxiety in rodents is thought to result in motor freezing. However, elevated anxiety may not invariably be associated with locomotor hypoactivity. Withdrawal of benzodiazepine is associated with anxiety-like behaviour and locomotor hyperactivity (Nowakowska, et al., 1997). In addition, a very large

number of clinical studies report on the coexistence of anxiety and motor restlessness following cessation of cigarette smoking (Hughes, et al., 1991; Hughes, 1992; Hilleman, et al., 1992; McKenna and Cox, 1992; Hughes and Hatsukami, 1986; Hughes, et al., 1994; Jorenby, et al., 1996; Schneider, et al., 1996, Shiffman, et al., 2000). A putative state-dependency model, in which the behavioural topography of anxiety-like responses depends on the environmental context, may be useful in understanding the data. In this model, the sustained level of behaviour in mutants over habituation in a 'naturalistic' setting would appear to compliment the finding of reduced open arm entries in the 'stressful' setting of the plus-maze.

In conclusion, our data suggests that in a 'stressful' setting Mt mice have a heightened basal level of anxiety-like behaviour; furthermore, in a 'naturalistic' setting, topographies of exploratory behaviour are increased and that these behaviours may nonetheless be modulated by nicotine administration. This study will act as a substrate for future pharmacological studies with a spectrum of nicotinic agonists to delineate specifically the contribution of the α_4 nAChR subunit to anxiolysis and other aspects of behavioural regulations.

CHAPTER FIVE

ENHANCED PROCONVULSANT-INDUCED

SEIZURES IN α_4 NICOTINIC ACETYLCHOLINE

RECEPTOR SUBUNIT KNOCKOUT MICE.

5.1 ABSTRACT

The genetic basis of a number of epilepsy syndromes has been identified but the precise mechanism whereby mutations produce seizures is unknown. Three mutations of the α_4 subunit of the nAChR have been identified in Autosomal Dominant Nocturnal Frontal Lobe Epilepsy (ADNFLE). In vitro studies of two of these mutations suggest an alteration of receptor function resulting in decreased ion channel current flow. In this study the response of α_4 nAChR subunit knockout mice to the γ-aminobutyric acid (GABA) non-competitive receptor antagonist pentylenetetrazol (PTZ) and the glutamate receptor agonist kainic acid (KA) was investigated. Although Mt mice have no spontaneous seizures they had a greater number of PTZ-induced major motor seizures and seizure related deaths. They also had a shorter onset latency to PTZ-induced hypokinetic and partial motor seizures. Furthermore, KA decreased normal behaviour in Mt mice in addition to producing a greater number of hypokinetic and minor motor seizures. The results confirm that α_4 nAChR subunit hypofunction in vivo is associated with reduced seizure thresholds.

5.2   INTRODUCTION

A large number of structurally related nAChR subunits are expressed in the developing and mature CNS. The α_4/β_2 receptor configuration is expressed at high levels and is thought to be important in anxiety (Brioni et al., 1993; Pomerleau, 1986; Ross et al., 2000), cognition, neurodegeneration (Brioni et al., 1997) and antinociception (Damaj et al., 1998; Marubio et al., 1999). ADNFLE is a recently recognized form of epilepsy in which brief partial seizures occur during light sleep and often are misdiagnosed as nightmares. Three mutations in the α_4 subunit of the nAChR have been described in families with ADNFLE (Steinlein et al., 1995; Steinlein et al., 1997; Hirose et al., 1999). Two mutations involve amino acid substitutions [Ser248Phe (Steinlein et al., 1995) and Ser252Leu (Hirose et al., 1999)] and one involves a leucine insertion [259insLeu (Steinlein et al., 1997)]. All three mutations are located in the second transmembrane domain which lines the ion channel pore of the receptor (Akabas et al., 1994; Steinlein et al., 1995).

The site and nature of the mutations identified in ADNFLE suggests that they may have major adverse functional effects on receptor activity. For the Ser248Phe and 259insLeu mutations this is supported by *in vitro* examination of *Xenopus oocytes* expressing the mutated α_4 nAChR subunits; functional studies of the Ser252Leu mutation are yet to be reported. Studies of the Ser248Phe mutation have suggested an alteration of receptor function resulting in decreased current flow through the ion channel following receptor activation (Weiland et al., 1996; Kuryatov et al., 1997). This may occur through four mechanisms that reduce the net flow of ions through the receptor: reduced or absent calcium permeability; reduced channel conductance; decreased channel open time and increased desensitization (Weiland et al., 1996; Kuryatov et al., 1997; Figl et al., 1998).

Reduced calcium permeability and enhanced desensitization were also seen with 259insLeu mutation (Bertrand et al., 1998). These studies argue that the net effect of the α_4 nAChR subunit mutations associated with ADNFLE is to reduce nAChR activity.

Mice with a targeted deletion of the α_4 nAChR subunit (chapters 3 and 4) were used to address the hypothesis that lack of α_4 nAChR subunits is associated with a lowered seizure threshold. Seizure activity was assessed by response to the proconvulsants PTZ and KA. The GABA receptor non-competitive antagonist PTZ produces convulsions by acting at the picrotoxin-sensitive site of the benzodiazepine-GABA receptor complex (Ramanjaneyalu and Ticku, 1984). PTZ has been used in epilepsy models to identify clinically useful anticonvulsant drugs, particularly for treatment of absence seizures (Macdonald and McLean, 1986; Marescaux et al., 1984). In contrast, KA is an extensively studied proconvulsant (Ben-Ari et al., 1981; Collins et al., 1980; Nadler, 1981) which produces seizures by activating glutamate receptors (Wisden and Seeburg, 1993; Mulle et al., 1998) and modulating synaptic GABA and glutamate release (Ben-Ari and Cossart, 2000).

5.3 MATERIALS AND METHODS

All procedures involving the use of live animals conformed to the Australian National Health and Medical Research Council (NH&MRC) code of practice. Gene knockout and control mice used in the experiments were generated as described in chapters 3. Adult mice used in the seizure and ligand autoradiography experiments were between the ages of 11 weeks and 15 weeks. Possible differences in the number and latency of seizures between groups of mice were tested using both Student's two-sample t-test and the Mann-Whitney test; in all cases both tests led to similar statistical conclusions.

Seizure studies

Fourteen (8 female, 6 male) PTZ treated Mt mice, (mean body weight 25.7 ± 3.0g) were examined relative to 15 (8 female, 7 male) PTZ treated wild type (Wt) control mice (mean body weight 23.2 ± 0.5 g). In addition, 5 (3 female, 2 male) vehicle treated Mt mice (mean body weight 25.6 ± 1.1 g) were examined relative to 5 (3 female, 2 male) vehicle treated Wt controls (mean body weight 24.2 ± 0.5 g). Testing was conducted using a single injection of PTZ of 80 mg/kg administered subcutaneously (s/c) (Sigma, St Louis, MO). On experimental days, mice were removed from their home cage and placed individually in clear glass observation cages (36 x 20 x 20 cm) for 1 h before PTZ injection. Immediately after the injection individual mice were observed continuously for 5 sec intervals in one min cycles over a 1 h period. PTZ induced seizures were classified as described in Ferraro et al., (1999). The most commonly observed PTZ induced seizure began with an arrest of normal exploratory behaviour followed by a decrease in motor activity with the animal coming to a complete rest in a crouched or prone position. This hypokinetic seizure type was described as a phase 1 seizure. Phase 2 or partial clonus seizures were characterized by brief twitching

movements involving face, head and/or forelimb or forelimbs. Phase 3 or generalized clonic seizure type, occurred when focal twitching was rapidly followed by loss of postural control and repetitive or clonic movements involving all limbs and tail. Jumping and repetitive rearing behaviour was classified as phase 3 activity. A phase 4 or tonic-clonic seizure type was characterized by tonic hind limb extension. Phase 4 seizures commonly resulted in death. PTZ induced seizures were a continuum from phase 1 to phase 4.

KA (Sigma) was administered s/c at a dose of 30 mg/kg following a one h habituation period. A total of 14 male mice of each genotype were examined. All mice were aged between 12 and 13 weeks and were of similar weights (Wt 27.0 ± 0.9 g, Mt 29.3 ± 0.7 g). Four mice were tested at any one time and all experiments conducted between 1230-1700 hrs. Drug effects were scored independently by two observers (Dr John Wong and Jim Massalas) over a 90 min period. Individual mice were observed continuously, and the worst event recorded, in non overlapping 15 sec periods by each observer in each 60 sec time period and the total score for each mouse/min calculated by adding the two scores. This approach therefore allowed visual assessment and documentation of KA-induced effects for 50% of the time. Phase 0 events represented normal exploratory mouse behaviour. Phase 1 to phase 5 were as described in Yang et al., (1997). In brief, phase 1 involved an arrest of motion, fixed gaze and abnormal forelimb or hindlimb posturing. Phase 2 involved myoclonic jerks of head and upper body with associated back arching. Phase 3 involved unilateral clonic activity. Phase 4 involved bilateral synchronous forelimb clonic activity and phase 5, loss of postural tone and generalized tonic-clonic seizure activity.

GABA$_A$ receptor binding

The GABA$_A$ receptor antagonist, [^{3}H]-SR95531 (NET-946, New England Nuclear, Boston, MA) was used to characterize the distribution of ionotropic GABA receptors in Wt and Mt mouse brains. Frozen slide-mounted tissues (20 μm) derived from drug naïve mice were thawed at room temperature before pre-incubation in 50 mM Tris/citrate buffer (pH 7.4) containing 100 mM MgCl$_2$. The sections were cooled in ice-cold buffer for five mins before incubation in 6.5 nM [^{3}H]-SR95531 in the same buffer for 30 mins. The sections were washed three times in ice-cold buffer for 5 secs and rinsed in distilled water twice for 10 secs before drying. Non-specific binding was determined in the presence of 10 mM GABA (Research Biochemicals International, MA). Autoradiographic detection was carried out by exposing the slide-mounted sections, together with [^{3}H]-microscales (RPA 510, Amersham International, UK) to Hyperfilm (RPN12, Amersham) for 12 days. The films were developed using Kodak D-19 Photo Developer. Binding densities were measured using a Microcomputer Imaging Device (MCID) with software (Imaging Research Inc. Brock University, St. Catherine's, Ont., Canada). For all studies, a minimum of 3 coronal sections from each animal were used for calculation of individual means. Striatal sections were taken between the region corresponding to levels 0.14 mm and 1.10 mm, rostral to the bregma line (Franklin and Paxinos, 1997). Standardization was achieved by comparing binding densities with standards exposed with each film. All values are expressed as mean ± SEM (fmol/mg). Student t-tests were used for statistical analysis of autoradiographic regional quantitative binding densities.

5.4 RESULTS

Behaviour of Mt mice was normal during routine handling, feeding and cage changes. Mt mice did not die unexpectedly making it unlikely that nocturnal major motor seizures were unobserved. Vehicle treated Mt and Wt mice did not exhibit clinical seizure activity.

PTZ-induced seizures

Mice not noted to have an event were excluded from all latency calculations. All Mt and Wt mice were observed to have hypokinetic seizures (phase 1) within the first three mins. Although all Mt mice had phase 1 seizures within the first minute, Wt mice had an average latency of 1.7 mins (P=0.002, Mann-Whitney). The latency to partial clonus (phase 2) for Wt mice was 13.6 ± 2.6 mins (mean ± SEM) compared to 5.0 ± 0.3 mins for Mt mice (P=0.015, Mann-Whitney), with both genotypes displaying brief partial or focal seizures, typically lasting 1 to 2 sec. There was no significant difference between genotypes with respect to onset latency of phase 3 and phase 4 events (P=0.928 and P=0.91 respectively calculated using Mann-Whitney test) (Figure 5.1). In both genotypes phase 3 seizures were characterized by repetitive rearing and jumping behaviour and/or a sudden loss of upright posture followed by whole body clonic activity involving all four limbs and tail. Mt mice had a significantly increased number of phase 3 (P=0.001, Mann-Whitney) and phase 4 seizures (P= 0.002, Mann-Whitney) compared to Wt control mice. Phase 4 seizures were often associated with death and in Mt mice the overall mortality was 57% compared to a PTZ associated mortality of 7% in Wt controls, confirming that the two genotypes are significantly different with respect to PTZ associated mortality (Fisher's exact test P=0.0047). A small number of mice sustaining phase 4 seizures (1 of 2 Wt mice and 3 of 11 Mt mice) were able to

recover spontaneously although Fisher's exact test failed to demonstrate any significant difference between genotypes (P=0.54). Although the number of PTZ related deaths were small, this observation suggests that the increased death rate in Mt mice reflected the fact that Mt mice were more likely to have phase 4 events rather than the fact that they were more likely to die if they were to have a phase 4 event. There were significantly less phase 1 seizures in Mt mice than observed in Wt mice (average ± SEM/mouse/h of 50 ± 2.8 for Wt mice compared to 21 ± 4.3 for Mt mice, P< 0.0001, Mann-Whitney). The reduced number of hypokinetic seizures in Mt mice may have reflected the increased rate of Mt mice progressing to clonic seizures (Figure 5.1). There appeared to be a phenotype shift in Mt mice with a significant increase in the number of major motor seizures (Figure 5.1). Ninety three percent of PTZ treated Mt mice succumbed to generalized clonic and 79% to tonic/clonic seizures, as compared to 28% and 14% respectively in PTZ treated Wt mice. If the data is examined in terms of the worst seizure event, then 21% of Mt mice progressed to a phase 3 seizure and 79% had a phase 4 seizure. In comparison, 20% of Wt mice only had a phase 1 event, 47% progressed to a phase 2 event, 20% a phase 3 event and only 13% a phase 4 seizure type (P<0.0001, Fisher's exact test) (Table 5.1).
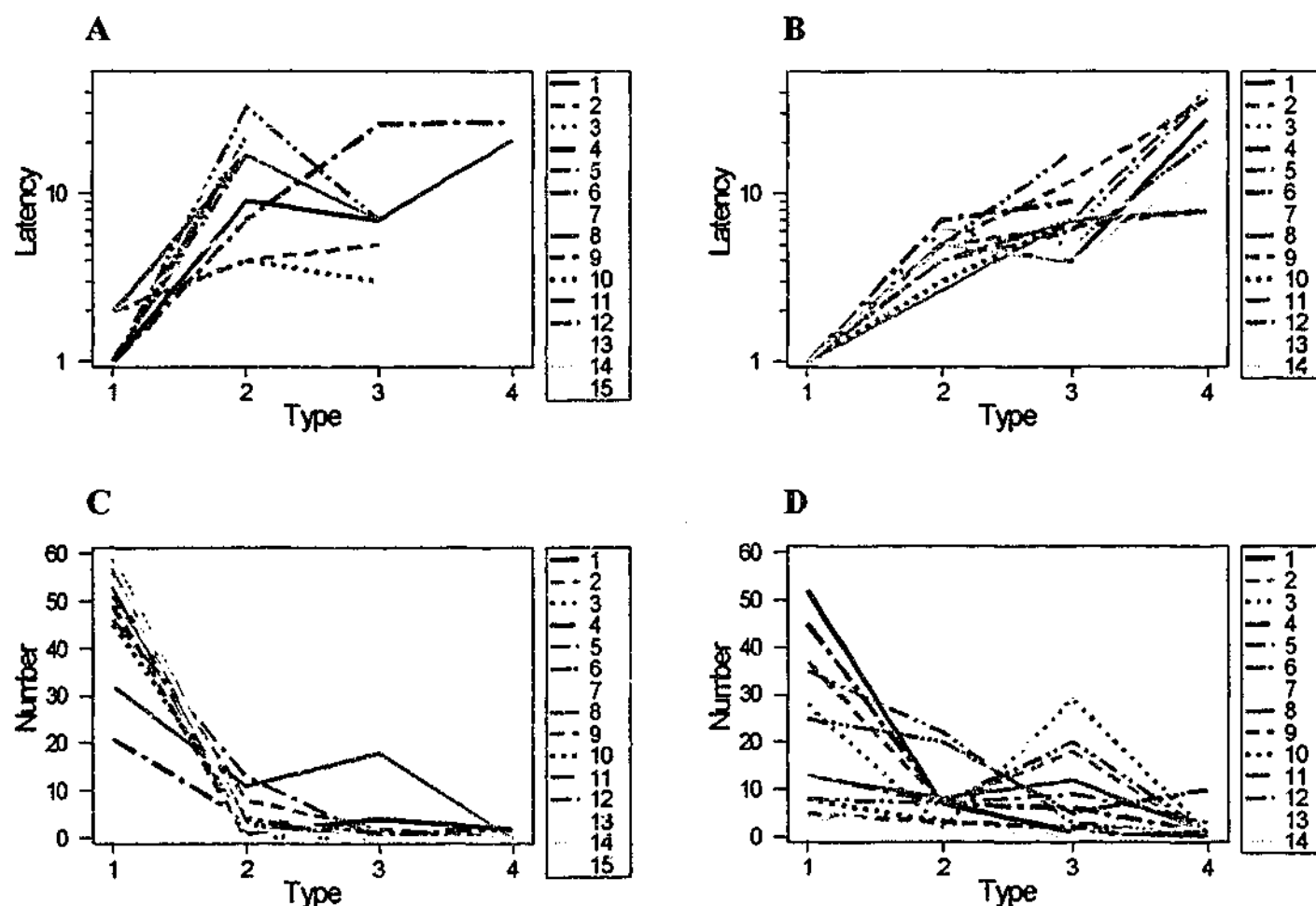
Figure 5.1 PTZ-induced seizures in Wt and Mt mice

Wt and Mt mice were given a single injection of PTZ (80 mg/kg s/c) and observed for 5 second periods every minute for one hour. Time in minutes to onset (latency) of observed seizure type is shown for individual mice. The latency for Wt mice are shown in panel (A) and Mt mice in panel (B). The number of observed seizures according to type in individual mice during the 60 min observation period is shown in panel (C) for Wt mice and panel (D) for Mt mice. Within individual panels, each mouse is represented by a different color.

Table 5.1

	Phase 1	Phase 2	Phase 3	Phase 4
Wt	(3/15) 20%	(7/15) 47%	(3/15) 20%	(2/15) 13%
Mt	(0/14) 0%	(0/14) 0%	(3/14) 21%	(11/14) 79%

Table 5.1. The worst observed seizure type expressed as a percentage of all Wt and Mt mice.

The absolute sample size from which percentages are calculated are indicated in parentheses.

KA-induced seizures

KA administration resulted in a six fold decrease in normal exploratory behaviour in Mt mice as compared to Wt mice (average number of events ± SEM/mouse/90 min:Wt; 64.5 ± 10, compared to 11.0 ± 4.0 in Mt mice, P= 0.003, t-test) (Table 5.2). In addition, Mt mice had greater number of hypokinetic (phase 1) (P=0.002, t-test) and phase 2 events (P=0.001, t-test) (Table 5.2). There was no significant difference between genotypes with respect to the number of phase 3, 4, or 5 events nor was there any difference in the latency to onset of KA-induced seizures for any seizure type (data not shown).

Table 5.2

	Phase 0	Phase 1	Phase 2	Phase 3	Phase 4	Phase 5
Wt	64.5 ± 10.7	96.1 ± 9.0	8.4 ± 1.4	2.9 ± 1.3	2.8 ± 1.3	5.3± 0.9
Mt	11.1 ± 4.1[a]	137.0 ± 8.0[b]	18.5 ± 2.3[c]	4.0 ± 2.1	8.5 ± 4.5	0.9 ± 0.3

Table 5.2 The behavioural response of Wt and Mt mice to KA injection.

Mt mice had a significant reduction in normal behaviour (P=0.003) and an increase in phase 1 (P=0.002) and phase 2 events (P=0.001). [a]P = 0.003, [b]P=0.002 and [c]P=0.001 (t-test). There were no detectable differences between genotypes at phase 3, 4, or 5.

GABA$_A$ receptor binding

Brain regions analyzed were: cortex (Cx), caudate/putamen (CPu), nucleus accumbens (NAc), olfactory tubercle (T), lateral globus pallidus (LPG), interpeduncular nucleus (IPn), lateral septum (LS), periaqueductal grey (PAG), pontine nucleus (Pn), anterior paraventricular thalamus (Pva), substantia nigra pars reticulata (SNr) and superior colliculus (SC). There were no significant differences between Wt and Mt mice in all regions assessed (Figure 5.2).
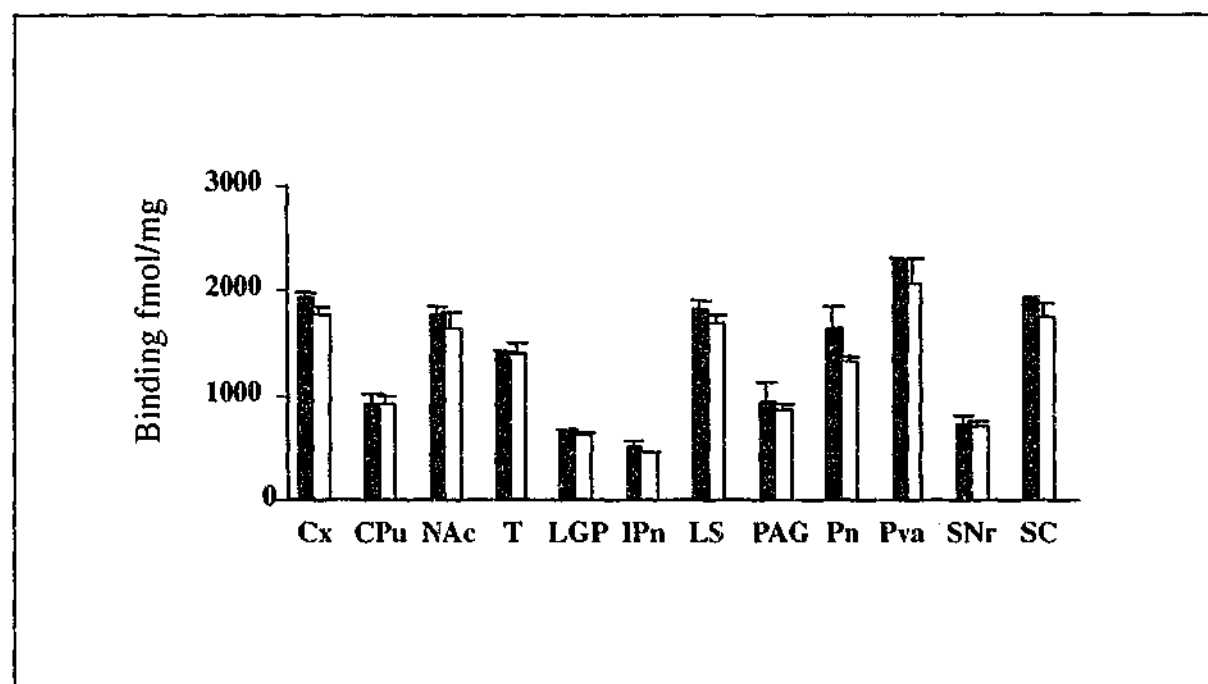
Figure 5.2 Quantitative GABA$_A$ receptor binding in Wt and Mt brains.

Brain regions analyzed were: cortex (Cx), caudate/putamen (CPu), nucleus accumbens (NAc), olfactory tubercle (T), lateral globus pallidus (LGP), interpeduncular nucleus (IPn), lateral septum (LS), periaqueductal grey (PAG), pontine nucleus (Pn), anterior paraventricular thalamus (Pva), substantia nigra pars reticulata (SNr) and superior colliculus (SC). There were no significant differences in quantitative ligand binding between Wt and Mt brains for any of the brain regions examined (Student's t-tests).

5.5 DISCUSSION

The seizure responses of α_4 nAChR subunit knockout mice to PTZ and KA have been investigated. The effects of PTZ and KA on Mt mice are unlikely to be due to compensatory changes in non-α_4 nAChR subunits as there was no change in α_3, α_6, α_7, β_2, β_3 and β_4 Mt brain mRNA levels (see chapter 4). Mice with targeted deletion of the α_4 nAChR subunit showed an overall increase in PTZ-induced seizures. Mt mice have a shorter latency to onset of PTZ-induced phase 1 and phase 2 seizure events and a significant increase in incidence of major motor seizures. As they have a greater number of phase 4 events, they are more likely to die following PTZ administration.

The observation that many proconvulsant agents reduce CNS GABA activity and a number of anti-convulsant drugs enhance the activity of GABAergic neurotransmission (White, 1999; Olsen, 1981) provides support for the idea that downregulated CNS GABAergic neurotransmission is important in seizure generation and propagation. Recent evidence suggests that the principle function of the nAChRs may be to modulate presynaptic release of other neurotransmitters including dopamine, acetylcholine, noradrenaline, GABA and glutamate (Role and Berg, 1996). There are a number of studies describing nicotine-induced release of the inhibitory neurotransmitter GABA either from isolated synaptosomes or in slice preparations (Lena et al., 1993; Kayadjanian et al., 1994; McMahon et al., 1994). It seems likely that receptor dysfunction due to the presence of channel pore mutations or targeted deletion of the α_4 nAChR subunit leads to disruption of presynaptic transmitter release mechanisms. As PTZ produces seizures by blockade of brain GABA receptors, it is postulated that the marked sensitivity of Mt mice to PTZ may reflect reduced steady state levels of

GABAergic inhibitory tone. Neurotransmitter receptor and transporter knockout mice are known to undergo a number of secondary compensatory changes in associated neurotransmitter systems (Drago et al., 1998). Normal GABA receptor binding in drug naïve Mt mice suggests that enhanced sensitivity to GABA receptor blockade is not related simply to compensatory downregulation in the level of GABA receptors.

Unlike PTZ-induced seizures, the seizure response to the dose of KA used in this study was not dramatic although a clear difference between genotypes was apparent. Compared to Wt mice, Mt mice showed a significant reduction in normal behavioural counts and an increase in the number of hypokinetic and minor motor seizures although no difference was seen in latency to seizure onset. The reduction in normal exploratory behaviour may have reflected subclinical seizure activity or recovery following seizures. The response to KA confirms that Mt mice show an increased seizure response to drugs other than those acting primarily through the GABAergic system. Recent data suggests that KA produces seizures by activating GluR6 receptors located in CA3 hippocampal neurons (Mulle et al., 1998) where presynaptic α_7 nAChRs are thought to be important in the regulation of glutamatergic synaptic transmission (Radcliffe and Dani, 1998). Seizures may then spread to the neocortex from their origin in the hippocampus (Lothman and Collins, 1981; Lothman et al., 1981), although early and potentially independent involvement of the neocortex in KA-induced motor convulsive events has been proposed (Willoughby et al., 1997; Medvedev et al., 2000). The idea that KA may have a direct action in the neocortex is supported by glutamate receptor expression studies (Wisden & Seeburg, 1993). Nicotinic receptors have been shown to modulate excitatory amino acid (EAA) neurotransmission at a number of sites in the CNS. Presynaptic nicotinic receptors are present on thalamocortical projections

where they are thought to regulate glutamate release from presynaptic terminals (Gioanni et al., 1999) as well as augment [^{3}H]-D-aspartate efflux in primary cultures of cortical neurons (Beani et al., 2000). The response of Mt mice to KA is the opposite from what would be predicted if the principal role of α_4 nAChR subunit containing nicotinic receptors were facilitation of neocortical EAA release. There are a number of possible explanations. First, post-synaptic receptors containing the α_4 nAChR subunit have been identified in a subpopulation of cortical interneurons (Porter et al., 1999) and altered cortical excitability resulting from loss of the receptor in this cell population may underlie the KA response. Second, there may be major developmentally determined compensatory changes in glutamate receptor kinetics or downstream signaling mechanisms. The third and most plausible explanation, particularly given our observations with PTZ, may relate to failure of the Mt brain to upregulate GABA release following glutamatergic challenge. In other words, what may be important is the balance between pertubations to GABAergic and EAA neurotransmission, a concept which has been put forth by Ben-A $^{..}$. id Cossant (Ben-Ari and Cossart, 2000).

In conclusion, the observation of lowered seizure threshold in Mt mice is consistent with the idea that this induced mutation is associated with a generalized activation of neuronal activity. The heightened anxiety-like behaviour and elevation of unconditioned motor activity observed in Mt mice (chapter 4) is also consistent with this hypothesis. *In vitro* studies of α_4 nAChR subunit mutations identified in human ADNFLE have previously suggested that nicotinic receptor hypofunction was responsible for the epilepsy phenotype. The current study shows that the null mutation is associated with abnormal excitability and a lowered seizure threshold and suggests

that the likely *in vivo* consequence of the ADNFLE mutations is a global reduction in

the function of the nAChR.

CHAPTER SIX

GENERATION OF A MOUSE MODEL FOR ADNFLE

6.1 INTRODUCTION

The association between the α_4 nAChR knockout mutation and enhanced proconvulsant induced seizure activity is now clear. As part of my thesis, I also generated a knockin construct containing the mutation identified in patients with ADNFLE. Analysis of this mutant model will answer in a more specific way, the relationship between the serine to phenylalanine mutation and enhanced spontaneous seizure activity.

6.2 RESULTS

Knockin construct design

In humans the mutation characterized in the Australian ADNFLE family is a C to T nucleotide missense mutation, which results in the replacement of the neutral amino acid serine with the aromatic amino acid phenylalanine. As for the knockout construct (chapter 3), the knockin construct was made using the pPNT neomycin-thymidine kinase-1 gene containing plasmid (Tybulewicz et al., 1991) as the base. Homologous flanks were chosen based on their lack of repetitive sequences. The cloning strategy used to generate the knockin construct is outlined in Figure 6.1.

Strategy for cloning the 5' fragment

The 5' Lox P site was subcloned into the pPNT targeting vector by inserting the oligonucleotide pair encoding the sequence Not I Hind III Xho I Lox P Sal I into the Not I / Xho I site of pPNT plasmid generating pPNT.M (5' Lox P) (Figure 6.1). The 5' flank (2.7 kb Bgl II / Sma I fragment) was isolated from the lambda genomic clone (pBS.genomic.clone) and subcloned into the Bam HI / Eco RV site of pBluescript SK +/- (pBS), generating pBS.M (5'flank). This fragment was then excised with Not I and

Xho I and ligated into the Not I / Xho I site of pPNT.M (5' Lox P) generating pPNT.M
(5' Lox P 5' flank).

Strategy for cloning the 3' fragment

The 3' Lox P site was first subcloned into pBS by inserting the oligonucleotide pair
encoding the sequence Bam HI Lox P Sca I Sma I into the Bam HI / Sma I site of pBS,
generating pBS.M (3' Lox P). The 3' flank (3.0 kb Sma I / Sma I fragment) was isolated
from the lambda genomic clone (pBS.genomic.clone) and subcloned into the pBS.M (3'
Lox P), generating pBS.M (3' Lox P 3' flank).

In ADNFLE patients the C is replaced with a T resulting in the mutated codon TTC,
which encodes for the amino acid phenylalanine. The normal human codon is TCC and
the mouse codon TCG, which encode for the amino acid serine.   Because of the
redundancy in the genetic code, mutagenesis was required at two bases (C to T and a G
to C) in order to create the amino acid change, serine to phenylalanine. For site-directed
mutagenesis, 2 primers were designed which contained the mutation in the middle of the
primer.

Mu1 (Sense)	- 5' CACGCTGTGCATCT▮▮GTGCTGCTTTCTCT C 3'
Mu2 (Antisense)	- 5' GAGAGAAAGCAGCAC▮▮AGATGCACAGCGTG 3'.

In a PCR reaction, the pBS (3' Lox P 3' flank) plasmid was amplified using the two
primers. The methylated nonmutated parental DNA template was digested using the
Dpn I enzyme and remaining plasmids (containing the mutation) were transformed into
supercompetent XL-1 blue cells (section 2.5.14) and purified by mini prep (section

2.5.16). The incorporation of the mutation into the pBS.M (3' Lox P 3' flank) was confirmed by sequencing using the primer E1 (Sequencing Facility in the Department of Microbiology, Monash University) (Figure 6.2). The mutated 3' flank was then excised from pBS.M (3' Lox P 3' flank) using Bam HI and Eco RI and subcloned into pPNT.M (5' Lox P) (Figure 6.1).

In summary, the 5' flank was a 2.7 kb Sma I / Bgl II genomic fragment and the 3' flank was a 3.0 kb Sma I / Sma I genomic fragment containing the ADNFLE mutation encoding the serine to phenylalanine substitution. The final targeting vector was called pEP.M (Figure 6.1) and all restriction sites were confirmed by restriction mapping (data not shown).

Figure 6.1 Cloning Strategy for generating the knockin construct.

Strategy for subcloning 5' Lox P into pPNT

1. Ligate oligonucleotide (Not I Hind III Xho I Lox P Sal I) into pPNT digested with Not I and Xho I

Strategy for subcloning 5' flank into pPNT.M (5' Lox P)

1. Ligate 5' flank (2.7 kb Bgl II/Sma I fragment) into pBS digested with Bam HI and Eco RV

2. Excise 5' flank using Not I and Xho I

3. Ligate 5' flank into pPNT.M (5' Lox P) digested with Not I and Xho I
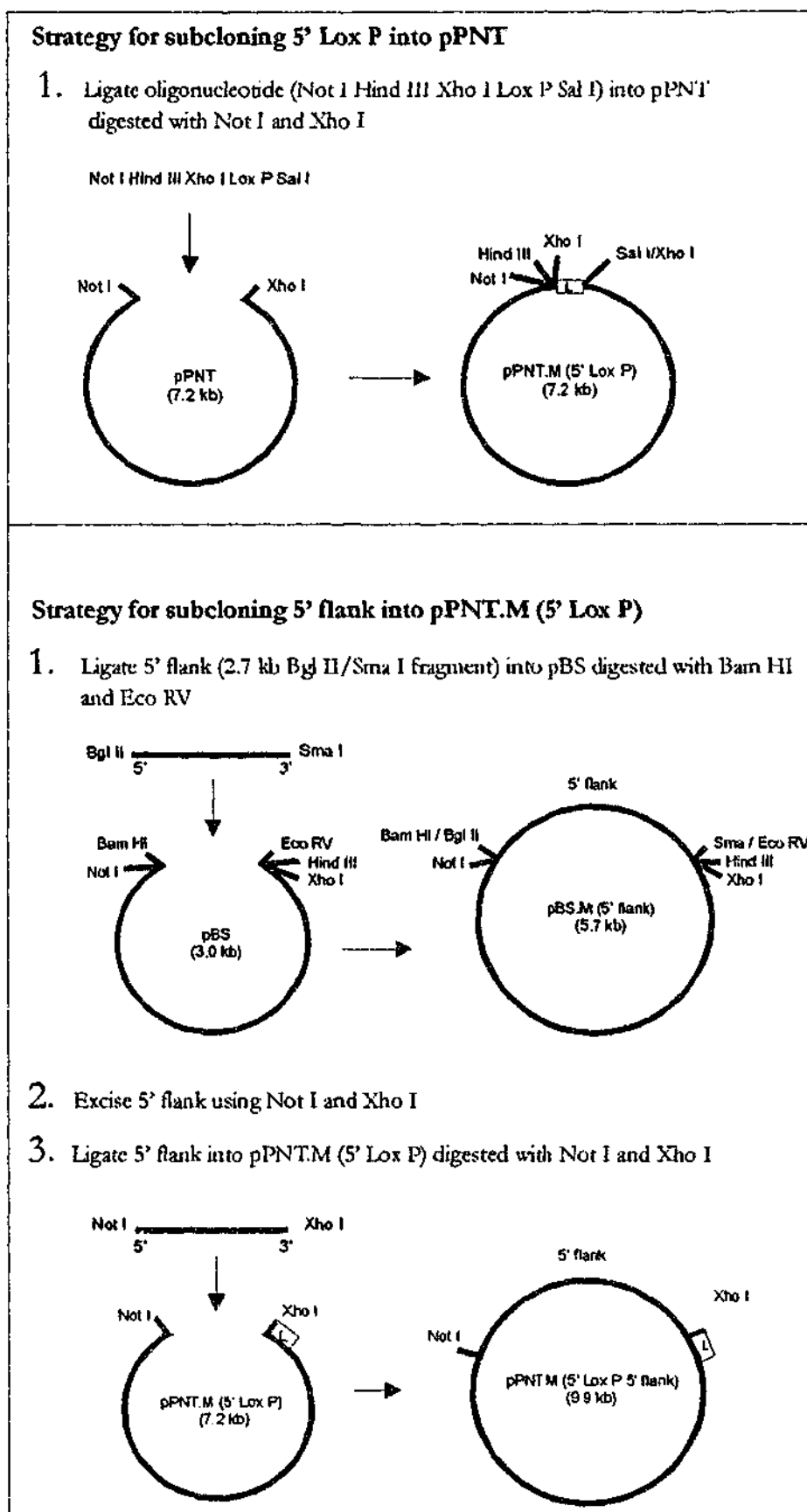
Strategy for subcloning 3' Lox P into pBS

1. Ligate oligonucleotide (Bam HI Lox P Sca I Sma I) into pBS digested with Bam HI and Sma I
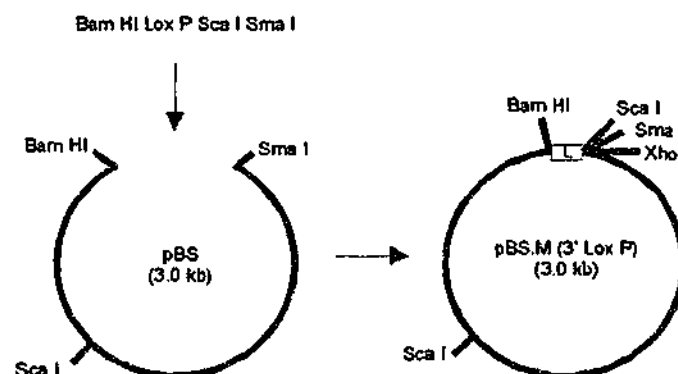
Strategy for subcloning 3' flank into pPNT.M (5' Lox P 5' flank)

1. Ligate 3' flank (3.0 kb Sma I / Sma I fragment) into pBS.M (3' Lox P) digested with Sma I
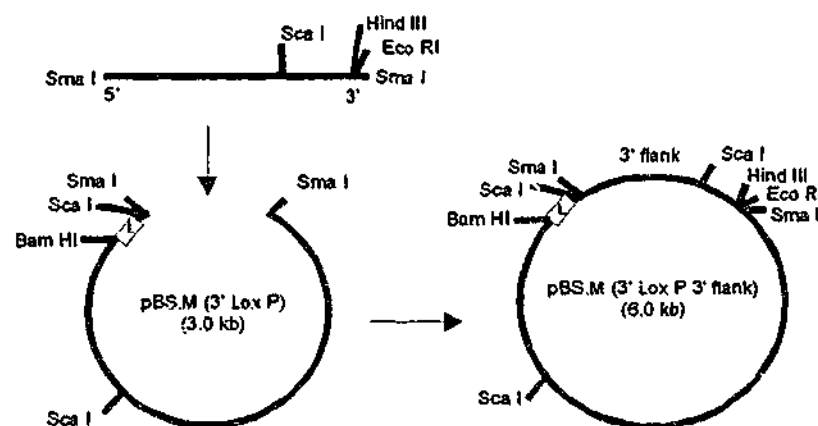
2. Site-directed mutatgenesis C to T, G to C

3. Excise 3' flank using Bam HI and Eco RI following mutagenesis as described in the text

4. Ligate 3' flank into pPNT.M (5' Lox P 5' flank) digested with Bam HI and Eco RI

Final knockin targeting construct, pEP.M.
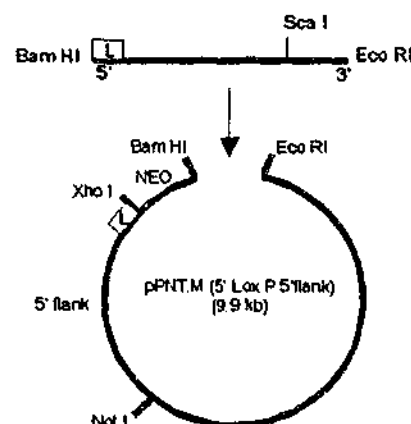
Figure 6.1 Cloning strategy for generating knockin targeting construct pEP.M.

The 5' flank is a 2.7 kb *Sma* 1 / *Bgl* II fragment and the 3' flank is a 3.0 kb *Sma* 1 / *Sma* 1 fragment.   pUC represents the plasmid backbone,   NEO represents the neomycin phosphotransferase resistance gene and HSV-TK represents the thymidine kinase gene from the herpes simplex virus.

Serine

A   G A A G G T C A C G C T G T G C A T C T C G G T G C T G C T T T C T C T C

Phenylalanine

B   G A A G G T C A C G C T G T G C A T C T T C G T G C T G C T T T C T C T C
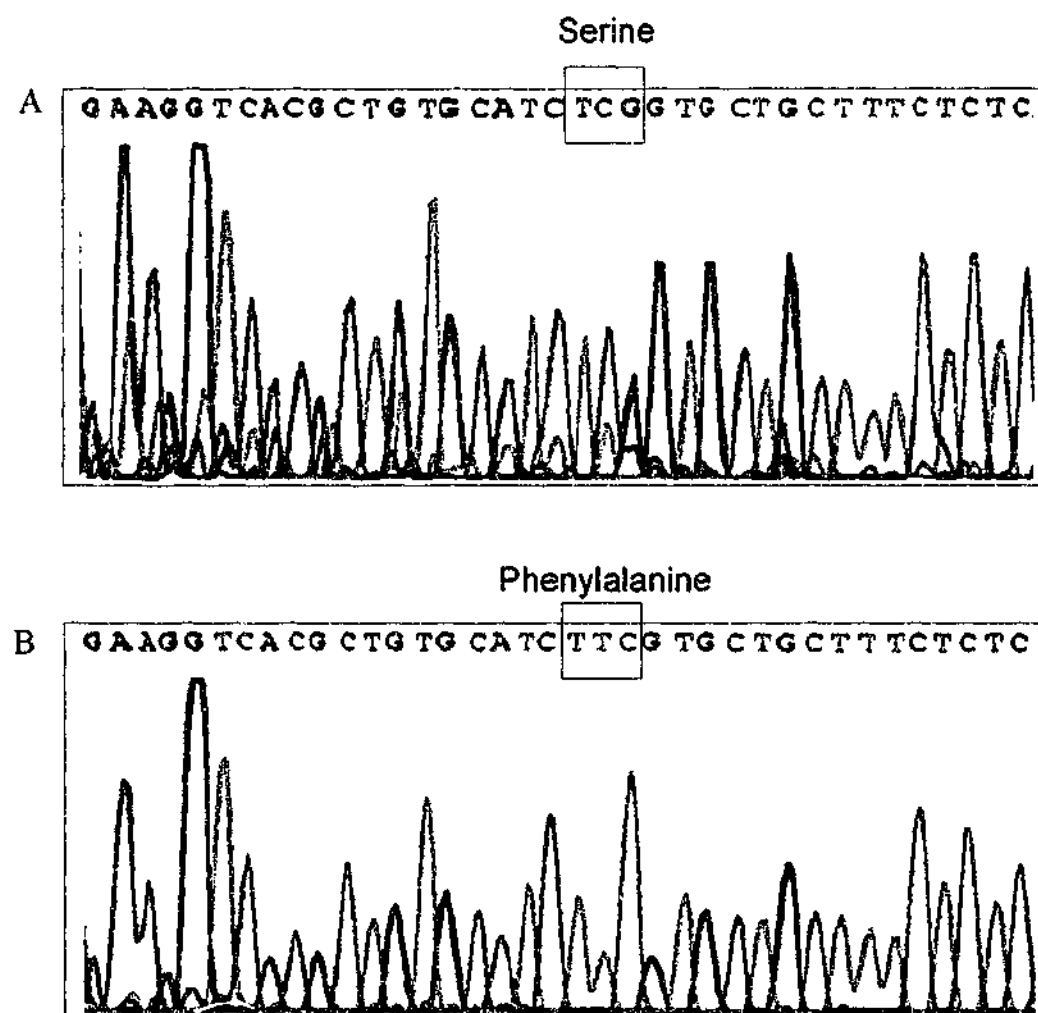
Figure 6.2 Electropherogram for sequencing results of pBS.M (3' Lox P 3' flank) to confirm mutation.
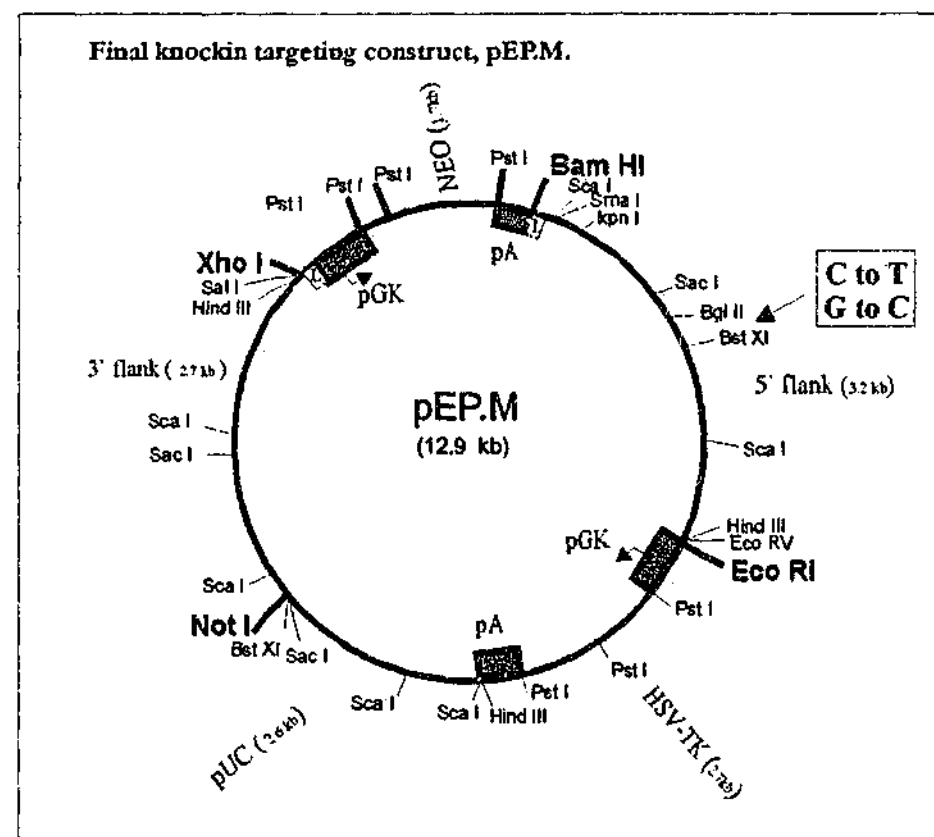
Sequencing was performed by the sequencing facility in the Department of Microbiology, Monash University. pBS.M (3' Lox P 3' flank) plasmid DNA and the E1 primer were provided and the sequencing was performed using ABI Prism BigDye Terminator reactions. (A) represents normal sequence from exon 5 of the α_4 nAChR subunit. The TCG codon encodes for the amino acid serine. (B) represents the mutated sequence of exon 5 after site-directed mutatgenesis. The CG has been replaced with a TC, resulting in a change from serine to phenylalanine.

Confirming integrity of Lox P sites

In the presence of the enzyme Cre recombinase, the DNA flanked by Lox P sites is spliced out. The pEP.M plasmid was transformed (section 2.5.14) into Cre producing bacteria and then purified by mini prep (section 2.5.16). The plasmid was then digested with Hind III and run on an agarose gel. In the control plasmid (non transformed), 3 bands were present, 5.0 kb, 2.7 kb and 2.6 kb. In the transformed plasmid, the Cre recombinase had spliced out the DNA flanked by the Lox P sites (the NEO gene, 1.7 kb) resulting in a reduction of the 5.0 kb fragment to a 3.2 kb fragment (data not shown).

The routine strategy of simultaneous positive selection with G418 and negative selection with gancyclovir was used to target both the J1 and R1 ES cell lines. A homologous recombination validation strategy which included 5' and 3' flanking genomic probes was designed (Figure 6.3).

Targeting experiments using J1 ES cell line

The targeting construct was linearized with the restriction enzyme Not I and purified by ethanol precipitation. J1 ES cells (passage 12) from an actively growing 2 day culture were electroporated with 50 µg of of linearized targeting construct, pEP.M. The electroporated cells were plated onto fifty-five 6 cm dishes at a concentration of 2.5×10^5 cells per 6 cm dish. After 9 days, 240 colonies were picked and transferred into 8 x 24 well plates on Mitomycin C treated EFN feeders (section 2.6.5). Of these colonies, 102 grew to give undifferentiated ES cell colonies which were harvested 2 to 4 days later for freezing (section 2.6.8) and DNA isolation (section 2.6.9). A Southern blot of a Bam HI digested ES cell genomic DNA was probed with pE1 and used to verify 5'

recombination. Four positive clones (CM35, CM 42, CM44, CM111) had undergone homologous recombination as indicated by the presence of 2 bands. The normal was 12 kb and the recombinant allele 9 kb. CM59, a non-targeted clone, is a negative control in Figure 6.3D. To verify 3' recombination, a Southern blot of a Bam HI digested ES cell genomic DNA was probed with pE2. All 4 clones had undergone accurate homologous recombination at the 3' end as indicated by the presence of 2 bands. The normal allele was 12 kb and the recombinant allele 5 kb (Figure 6.3F). To confirm single insertion of the vector into the genome of targeted clones, a Southern blot of Bam HI digested ES cell genomic DNA was probed with a NEO probe. An expected single band at 9 kb was identified in all 4 clones (Figure 6.3F).

Figure 6.3 Construction of knockin targeting vector (pEP.M) and Southern blot analysis of targeted J1 ES clones.

Panel A represents the genomic map of the α_4 nAChR gene, panel B represents the targeting vector pEP.M (please note, the Lox P NEO Lox P sequence was inserted into the native Sma I site), panel C represents the expected allelic disruption after homologous recombination and panel D represents the final chromosomal organization following Cre mediated excision of the Lox P bracketed DNA. The restriction sites shown are abbreviated as follows: N, *Not* I; H, *Hind* III; Bg, *Bgl* II; Sc, *Sca* I; X, *Xho* I; E, *Eco* RI; B, *Bam* HI. NEO represents the neomycin phosphotransferase resistance gene and TK the thymidine kinase gene. The origin of the probes used for homologous recombination screening are also shown. Probe pE1 is a *Hind* III - *Bgl* II fragment used to confirm 5' recombination and probe pE1 is a *Hind* III - *Bam* HI fragment used to confirm 3' recombination. Panel E, shows the Southern blot of *Bam HI* digested ES cell genomic DNA probed with pE2 (Wt allele is 12 kb, and the recombinant allele 9 kb), showing correctly targeted clones (CM35, CM42, CM44, CM111). CM59 is a randomly selected non-targeted clone. Panel F shows the Southern blot of *Bam HI* digested ES cell genomic DNA probed with pE2 (Wt allele is 12 kb and the recombinant allele 5 kb), showing correctly targeted clones CM35, CM42, CM44, CM111. Panel G shows a Southern blot of a *Bam HI* digest probed with a NEO specific probe. Clones CM35, CM42, CM44 and CM111 have a single band at the expected size of 9 kb confirming a single insertion event in all the clones examined. The schema outlined in this figure depicts removal of the Eco RI site 5' of the TK cassette. This has

Bam HI
probed with pE1

Bam HI
probed with pE1

Bam HI
probed with NEO
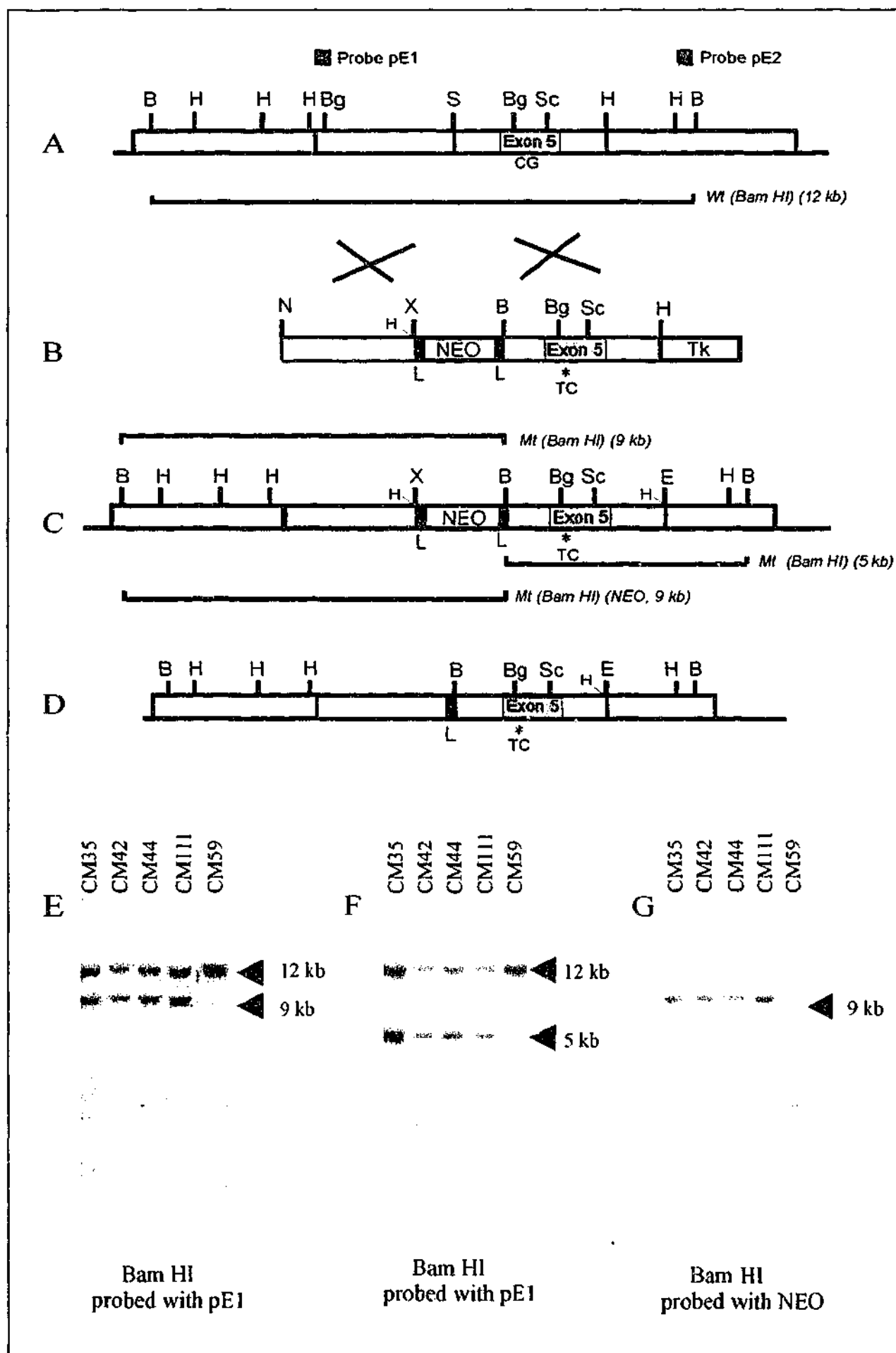
Targeting experiments using R1 cell line

The R1 cell line has also been successfully used to create germline transmitting chimeras (Nagy et al., 1993). R1 ES cells are also grown on EFN feeders in the presence of LIF. Under these conditions R1 cells show a morphology typical of undifferentiated ES cells. A Southern blot of a Bam HI digested ES cell genomic DNA was probed with pE1 and used to verify 5' recombination. Two clones (R148 and R162) had undergone homologous recombination as indicated by the presence of 2 bands. The normal allele was 10 kb and the recombinant allele 5.0 kb (Figure 6.4A). To verify 3' recombination, a Southern blot of Bam HI digested ES cell genomic DNA was probed with pE2. Both of the clones had undergone accurate homologous recombination at the 3' end as indicated by the presence of 2 bands. The normal allele was 12 kb and the recombinant allele 5 kb (Figure 6.4B). To confirm single insertion of the vector into the genome of targeted clones, a Southern blot of Bam HI digested ES cell genomic DNA was probed with a NEO probe. An expected single band at 9 kb was identified in all 4 clones (Figure 6.4C).
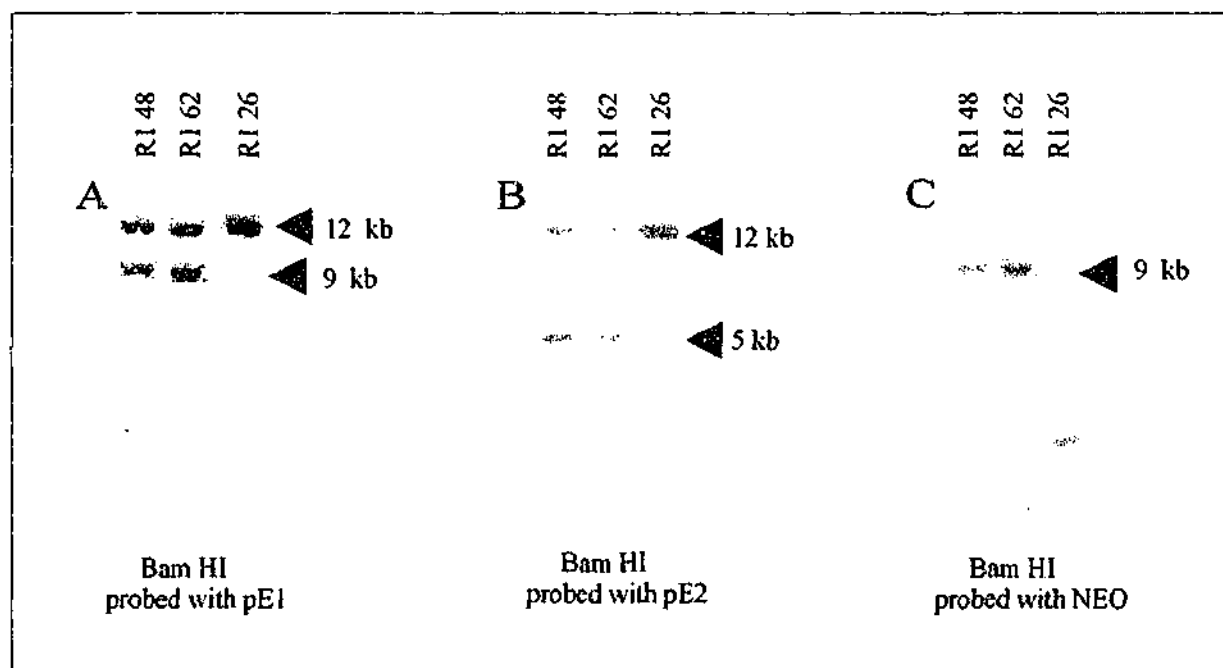
Figure 6.4 Southern blot analysis of pEP.M R1 targeted ES clones

Panel A shows the Southern blot of *Bam HI* digested ES cell genomic DNA probed with

pE1 (Wt allele is 12 kb and the recombinant allele is 9 kb), showing correctly targeted

clones R1 48 and R1 62. R1 26 is a randomly selected non-targeted clone. Panel B

shows the Southern blot of *Bam HI* digested ES cell genomic DNA probed with pE2

(Wt allele is 12 kb and the recombinant allele is 5 kb), showing correctly targeted clones

R1 48 and R1 62. Panel C shows a Southern blot of a *Bam HI* digest probed with a

NEO specific probe. Both clones have a single band at the expected size of 9 kb

confirming a single insertion event in all the clones examined.

Confirmation of the mutation in positive ES cell clones

A strategy for confirming the presence of the mutation in positive ES cell clones involved amplifying ES cell genomic DNA and subcloning amplicons into a pGem 7 vector to verify the presence of the mutation using specifically designed primers in a PCR assay. Firstly, mutation primers were designed based on generated mouse sequence to contain subtle base changes at the 3′ end. The M1 primer (shown below) was chosen because of its ability to distinguish normal sequence from mutated sequence. In PCR assay, pEP.M plasmid DNA (containing the mutated sequence) and plasmid containing normal sequence were amplified using the forward mutation primer M1 and the reverse primer E4. E4 was designed based on conserved regions between the human (accession #135901) and rat (accession #131620) published cDNA sequences (for sequence refer to chapter 2.1, section 2.1.5). A 200 bp fragment was amplified from mutated sequence (i.e targeting vector), whereas no bands were visible after amplification of the normal sequence (i.e genomic clone) (data not shown).

Mutated sequence (M1)	A C G C T G T C A A T C T T C
Normal sequence	A C G C T G T C A A T C T C G

To generate PCR genomic fragments to subclone into the pGem 7 vector, correctly targeted ES cell clones were amplified using E1 and E3 primers. E1 and E3 primers were designed based on conserved regions between the human (accession #135901) and rat (accession #131620) published cDNA sequences (for sequence refer to chapter 2.1, section 2.1.5). Positive ES cell clones (CM35 and CM42 from J1 targeted ES cells and R1 48 and R1 62 from R1 targeted ES cells) and a negative control (a negative clone from the knockout targeting experiment, pEP.N91), were amplified by PCR. The 1 kb

PCR fragments were then purified from an agarose gel (section 2.5.10) and subcloned into the pGem T vector and single colonies were purified by mini prep (section 2.5.16). In a statistically representative sample, there should be equal proportions of plasmids with and without the mutation, as both the normal and mutated alleles would be amplified in each targeted clone. For the J1 targeted ES cell clones, 8 plasmids were randomly chosen from CM35, CM42 and 8 plasmids were chosen from the negative control, pEP.N91. The plasmids were then amplified by PCR using the M1 and E4 primers. For clone CM35, 4 of the plasmids contained the mutation, as indicated by the presence of the 200 bp band and 4 plasmids were negative for the mutation (no band). For clone CM42, there were 2 positive plasmids and 6 negative plasmids (Figure 6.5A) and for clone pEP.KO 91, there were no positive plasmids (Figure 6.5B). For the R1 targeted ES cell clones, 13 plasmids were randomly chosen from R1 48 and R1 62 and amplified using the M1 and E4 primers. For clone R1 48, there were 4 negative plasmids and 9 positive plasmids and for clone R1 62, there were 7 negative plasmids and 6 positive plasmids (Figure 6.6). To confirm the presence of the mutation, one of the positive plasmids from CM35 and 1 from CM42 were sequenced. Both plasmids contained the expected sequence (data not shown).
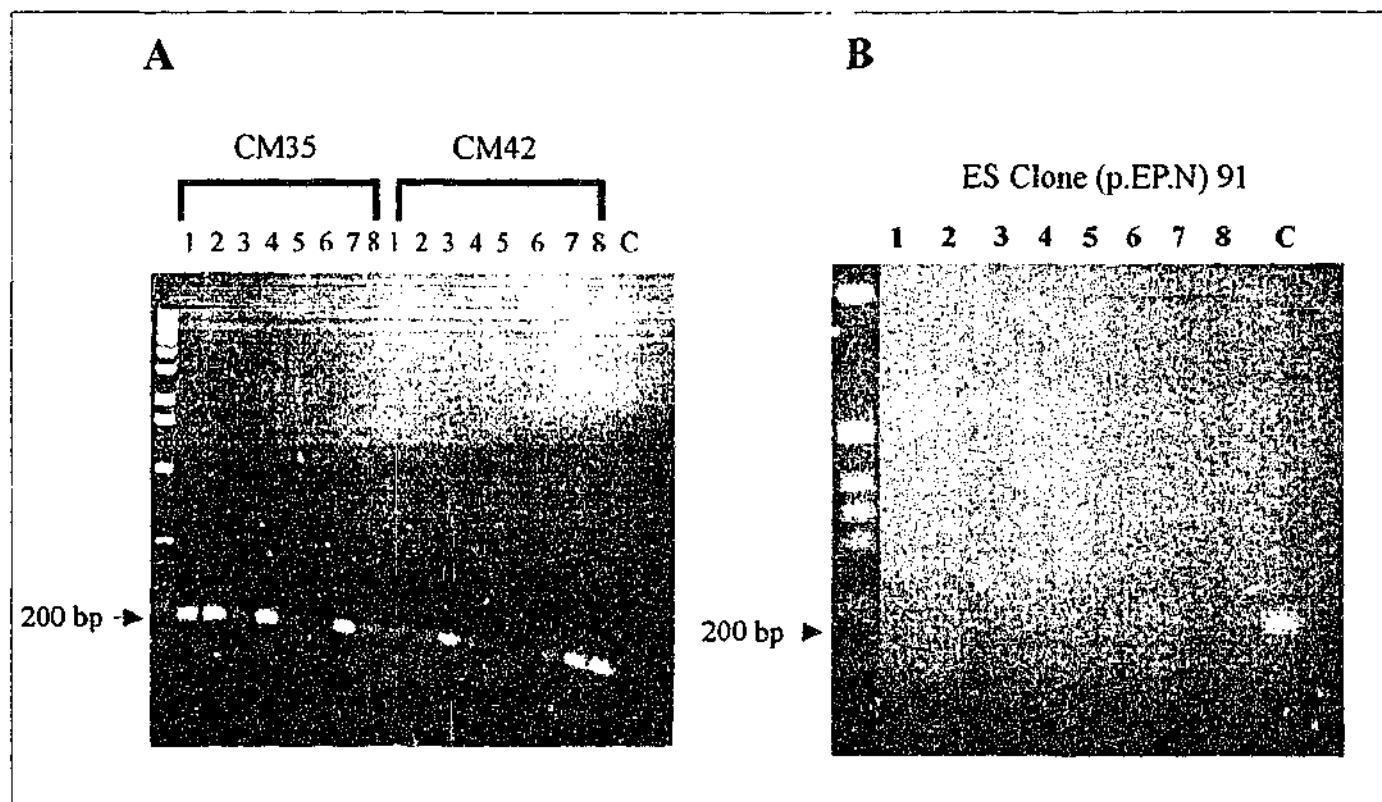
Figure 6.5 Confirmation of mutation in J1 targeted ES cell clones.

Genomic DNA from J1 targeted ES cell clones CM35 and CM42, and pEP.N 91 (negative control) were amplified and sublconed into the pGem 7 vector. Eight randomly selected plasmids were then amplified by PCR using the forward primer, M1 (mutation primer) and the reverse primer, E4. Only plasmids containing the mutation were amplified. For CM35, plasmid clones 1, 2, 4 and 7 were positive for the mutation (presence of 200 bp fragment), and plasmid clones 3,5,6 and 8 were negative for the mutation (no band). For CM42, plasmid clones 3 and 8 were positive and plasmid clones 1, 2, 4, 5, 6 and 7 were negative. C represents a positive control (amplification of the targeting vector DNA, pEP.M).
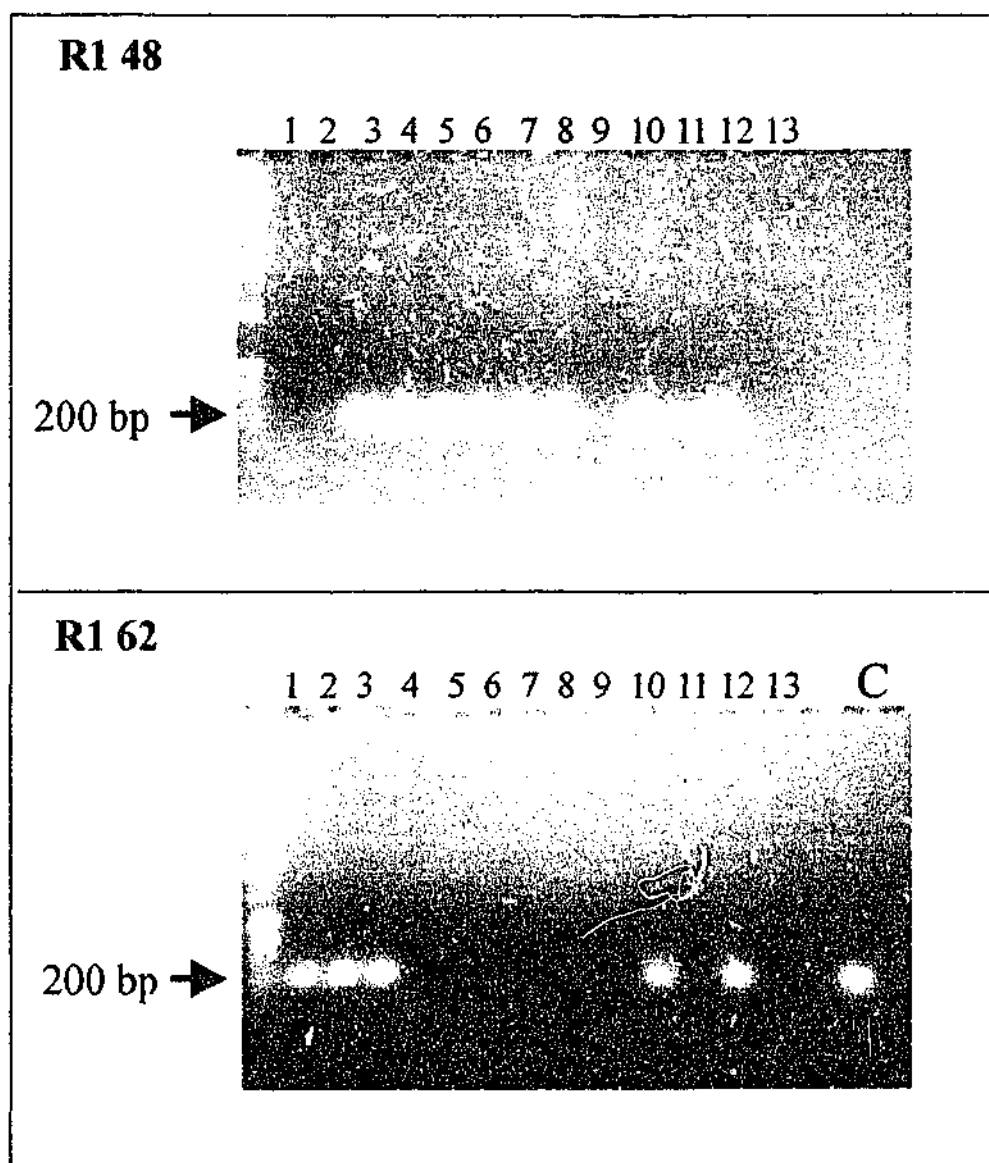
Figure 6.6 Confirmation of mutation in R1 targeted ES cell clones.

For R1 ES cell clones, R1 48 and R1 62, 13 plasmids were randomly selected and amplified by PCR using the M1 and E4 primers. For R1 48, plasmid clones 3, 4, 5, 6, 7, 8, 10, 11, 12 were positive for the mutation (presence of 200 bp fragment), and plasmid clones 1, 2, 9 and 13 were negative for the mutation (no band). For R1 62, plasmid clones 1, 2, 3, 10 and 12 were positive for the mutation and plasmid clones, 4, 5, 6, 7 8, 9 and 11 were negative for the mutation. C represents a positive control (amplification of the construct).

Injection

The blastocyst injections for the J1 targeted ES clones were undertaken in collaboration with Professor Ismail Kola at the Institute of Reproduction and Development, Monash University. Of the 4 recombinant clones, CM44 was chosen for injection as the cells were rapidly growing and appeared to have an undifferentiated morphology. The cells were injected into Balb/C blastocysts and 4 chimeras were generated of which 3 were female and 1 male. All were mated with CF1 mice, however none of them were capable of transmitting the mutated allele to their progeny, indicating that the introduced ES cells containing the mutated allele were not contributing to the germ cells in these chimeras. The blastocyst injections for the R1 targeted ES cell clones were undertaken in collaboration with Dr Peter G. Noakes in the Department of Physiology & Pharmacology at the University of Queensland. For the R1 ES cell line, clone R1 42 was chosen for injection. Currently, 9 chimeras have been generated all of which are male. Seven of the 9 chimeras are greater than 80% coat chimeric and will be mated with CF1 mice to test for germline transmission.

CHAPTER SEVEN

SUMMARY

Nicotinic AChRs are receiving increased attention due to their involvement in a number of physiological processes, however their complex pharmacology and the lack of receptor subtype specific ligands have been major obstacles in defining the precise role of these receptors *in vivo*. A review of the literature revealed that these receptors may provide insight into a number of disease states. In particular, a number of nicotinic agonists have been shown to have potential as therapeutic agents, such as analgesics and anxiolytics. Recently, three mutations in the α_4 nAChR subunit have been identified in the human epilepsy syndrome, ADNFLE. The primary aim of this project was to create an α_4 nAChR knockout line to further understand the role of this receptor subunit in behaviour and seizure induction. A detailed neurochemical and behavioural analysis was performed focusing on defining the behavioural role of this receptor subunit. Also the seizure threshold of Mt mice to the proconvulsants, PTZ and KA was determined. In addition, significant progress has been made in the design and generation of a mouse model for the human epilepsy syndrome, ADNFLE.

In this study, an α_4 nAChR subunit knockout line was generated using standard gene targeting techniques, and a detailed neurochemical and behavioural characterization was undertaken. This involved using *in situ* hybridization to validate the knockout paradigm and to determine the expression patterns of a number of other nAChR subunits. In addition, receptor autoradiography was carried out using a number of nicotinic agonists providing additional topographical characterization of these receptors. The behavioural analysis involved determining the normal spontaneous and nicotine-stimulated behaviour under habituated and unhabituated conditions. Sensorimotor coordination and anxiety-like behaviour were evaluated. Furthermore, a study was conducted to evaluate the effect of the deletion on seizure susceptibility to the proconvulsants, PTZ

and KA. Finally, a construct of the knockin mutation seen in ADNFLE patients was generated and successfully introduced into two ES cell lines.

7.1 MAIN FINDINGS

Neurochemical analysis of α_4 nAChR subunit knockout mice

The knockout paradigm was validated by *in situ* hybridization analysis using α_4 nAChR specific probes. Mt mice were found to be of normal size, fertile, displayed normal home cage behaviour and did not exhibit any spontaneous seizures. There were no differences in size or morphology of the brain and screening failed to show any gross structural or histological abnormalities in a number of organs.

A detailed neurochemical analysis was performed using *in situ* hybridization and ligand autoradiography. There were no statistical differences in the expression of a number of other nAChR subunits in Wt and Mt mice, indicating that there was no transcriptional upregulation of other nAChR in compensation for deletion of the α_4 subunit.

Ligand autoradiography confirmed the lack of high-affinity binding to radiolabeled nicotine, cytisine and epibatidine in the thalamus, cortex and caudate putamen, although binding to a number of discrete nuclei remained. These binding studies revealed a differential binding pattern of nicotinic agonists in Mt mice. There were no differences in $[I^{125}]$-α-Bgt high affinity binding between Mt and Wt mice, confirming that the disruption of the α_4 subunit did not result in changes in baseline expression of the α_7 subunit.

Behavioural analysis of α_4 nAChR subunit knockout mice

There were no significant differences in sensorimotor co-ordination between Mt and Wt mice. Over the of habituation phase, spontaneous unconditioned motor behaviour revealed an ethogram characterized by significant increases in sniffing, locomotion and all forms of rearing in Mt mice compared to Wt mice. In addition, the behaviour of Mt mice in the elevated plus-maze assay was consistent with increased basal levels of anxiety-like behaviour. In response to nicotine, Wt mice exhibited early reductions in a number of behavioural topographies, under both unhabituated and habituated conditions. Whereas, heightened levels of behavioural topographies in Mt mice were reduced by nicotine in the late phase of the unhabituated condition. The fact that Mt mice still respond to nicotine administration suggest that the persistent nicotine binding sites in the habenulo-interpeduncular system are sufficient to modulate motor activity in actively exploring mice. This study confirms the pivotal role of the α_4 nAChR subunit in the modulation of a number of constituents of the normal mouse ethogram and in anxiety-like behaviour.

Enhanced proconvulsant-induced seizures in α_4 nAChR subunit knockout mice.

The seizure responses to the subcutaneous administration of the proconvulsants, PTZ and KA were investigated in α_4 nAChR subunit knockout mice, revealing an overall decrease in seizure threshold in Mt mice. Although Mt mice have no spontaneous seizures, they had a greater number of PTZ-induced major motor seizures and seizure related deaths. They also had a shorter onset latency to PTZ-induced hypokinetic and partial motor seizures. The results from the KA study were not as dramatic as those seen with PTZ, although a clear difference was observed. In response to KA, Mt mice

showed a significant reduction in normal behaviour and an increase in the number of hypokinetic and minor motor seizures. The observation of lowered seizure threshold assessed using PTZ and KA is consistent with the idea that this genetic mutation is associated with a generalized activation of neuronal activity. The heightened anxiety-like behaviour and elevation of unconditioned motor activity observed in Mt mice is also consistent with this hypothesis. These results suggest that the likely *in vivo* consequence of the ADNFLE mutation is a global reduction in activity of the nAChR.

Generation of a mouse model for ADNFLE

The targeted R1 ES clones are currently being injected by Dr Peter G. Noakes in the Department of Physiology & Pharmacology at the University of Queensland and 9 high grade male chimeras have been generated. The ultimate analysis of knockin mice will enable the question of the relationship of the serine to phenylalanine to epilepsy to be directly addressed.

7.2 AREAS FOR FUTURE WORK

The α_4 nAChR subunit knockout mice are a substrate for future studies to delineate specifically the contribution of the α_4 subunit to a number of physiological processes, in particular, its contribution to anxiolysis. The most significant result from this study is the marked reduction in the sensitivity of Mt mice to PTZ. Future experiments will use different proconvulsants to further analyze the effect of this mutation on seizure susceptibility aiming to define the precise neurotransmission systems involved. In addition, Mt mice could be backcrossed to the Balb/C background, a strain very sensitive to a number of convulsive agents and to the C57BL/6 background, a strain thought to have a raised seizure threshold (Crawley, 1996; Gerlai, 1996). These

backcrossing studies and a number of other studies are presently underway. The Mt mice have been used to look at the effects of this mutation on nicotine, epibatidine and morphine mediated analgesia. Collaborative work has also been undertaken with Dr John Wong on the effects of amphetamine and cocaine with preliminary results suggesting that the α_4 nAChR subunit is a major *in vivo* regulator of dopaminergic neurotransmission. Furthermore, a collaborative project undertaken with Dr Richard Loiacono and Rebecca Ryan from the Department of Pharmaceutical Biology and Pharmacology, Victorian College of Pharmacy, Monash University, confirmed the pivotal role the α_4 nAChR subunit plays in a model of amphetamine-induced nigrostriatal degeneration. The generation of a mouse model for ADNFLE is an experiment which is currently ongoing. This model will be used to investigate the molecular and neurophysiological mechanisms of this form of inherited epilepsy and most importantly may be used to trial potential anticonvulsant drugs.

REFERENCES

Accili D, Fishburn CS, Drago J, Steiner H, Lachowicz JE, Park BH, Gauda EB, Lee EJ, Cool MH, Sibley DR, Gerfen CR, Westphal H, Fuchs S (1996). A targeted mutation of the D3 dopamine receptor gene is associated with hyperactivity in mice. Proc Natl Acad Sci U S A 93:1945-9.

Aceto MD, Awaya H, Martin BR, May EL (1983). Antinociceptive action of nicotine and its methiodide derivatives in mice and rats. Br J Pharmacol 79: 869-76.

Aceto MD, Bagley RS, Dewey WL, Fu TC, Martin BR (1986). The spinal cord as a major site for the antinociceptive action of nicotine in the rat. Neuropharmacology 25:1031-6.

Adamec RE (1990). Does kindling model anything clinically relevant? Biol Psychiatry 27:249-79.

Akabas MH, Kaufmann C, Archdeacon P, Karlin A (1994). Identification of acetylcholine receptor channel-lining residues in the entire M2 segment of the alpha subunit. Neuron 13: 919-27.

Anand R, Conroy WG, Schoepfer R, Whiting P, Lindstrom J (1991). Neuronal nicotinic acetylcholine receptors expressed in Xenopus oocytes have a pentameric quaternary structure. J Biol Chem 266:11192-8.

Andermann E (1982). *Multifactorial inheritance of generalized and focal epilepsy*. New York: Raven Press.

Armijo JA, de las Cuevas I, Adin J (2000). Ion channels and epilepsy. Rev Neurol 30 Suppl 1:S25-41.

Arqueros L, Naquira D, Zunino E (1978). Nicotine-induced release of catecholamines from rat hippocampus and striatum. Biochem Pharmacol 27:2667-74.

Arroyo-Jim nez MM, Bourgeois JP, Marubio LM, Le Sourd AM, Ottersen OP, Rinvik

    E, Fairen A, Changeux JP (1999). Ultrastructural localization of the alpha4-

    subunit of the neuronal acetylcholine nicotinic receptor in the rat substantia

    nigra. J Neurosci 19:6475-87.

Ashworth-Preece M, Jarrott B, Lawrence AJ (1998). Nicotinic acetylcholine receptors

    in the rat and primate nucleus tractus solitarius and on rat and human inferior

    vagal (nodose) ganglia: evidence from in vivo microdialysis and [125I]alpha-

    bungarotoxin autoradiography. Neuroscience 83:1113.1122.

Auerbach W, Dunmore JH, Fairchild-Huntress V, Fang Q, Auerbach AB, Huszar D,

    Joyner AL (2000). Establishment and chimera analysis of 129/SvEv- and

    C57BL/6-derived mouse embryonic stem cell lines [In Process Citation].

    Biotechniques 29:1024-8, 1030, 1032.

Azami J, Llewelyn MB, Roberts MH (1982). The contribution of nucleus reticularis

    paragigantocellularis and nucleus raphe magnus to the analgesia produced by

    systemically administered morphine, investigated with the microinjection

    technique. Pain 12:229-46.

Badio B, Daly JW (1994). Epibatidine, a potent analgetic and nicotinic agonist. Mol

    Pharmacol 45:563-9.

Balfour DJ (1982). The effects of nicotine on brain neurotransmitter systems.

    Pharmacol Ther 16:269-82.

Bannon AW, Decker MW, Holladay MW, Curzon P, Donnelly-Roberts D, Puttfarcken

    PS, Bitner RS, Diaz A, Dickenson AH, Porsolt RD, Williams M, Arneric SP

    (1998). Broad-spectrum, non-opioid analgesic activity by selective modulation

    of neuronal nicotinic acetylcholine receptors. Science 279:77-81.

Battig K, Driscoll P, Schlatter J, Uster HJ (1976). Effects of nicotine on the exploratory locomotion patterns of female Roman high- and low-avoidance rats. Pharmacol Biochem Behav 4:435-9.

Beani L, Antonelli T, Tomasini MC, Marani L, Bianchi C (2000). The nicotinic modulation of [^{3}H]D-aspartate outflow in primary cultures of rat neocortical neurons: effect of acute and long term nicotine treatment. Neuropharmacology, 39:2646-2653.

Ben-Ari Y (1985). Limbic seizure and brain damage produced by kainic acid: mechanisms and relevance to human temporal lobe epilepsy. Neuroscience 14:375-403.

Ben-Ari Y, Cossart R (2000). Kainate, a double agent that generates seizures: two decades of progress. Trends Neurosci, 23:580-7.

Ben-Ari Y, Tremblay E, Riche D, Ghilini G, Naquet R (1981). Electrographic, clinical and pathological alterations following systemic administration of kainic acid, bicuculline or pentetrazole: metabolic mapping using the deoxyglucose method with special reference to the pathology of epilepsy. Neuroscience, 6:1361-91.

Berkovic SF, McIntosh A, Howell RA, Mitchell A, Sheffield LJ, Hopper JL (1996). Familial temporal lobe epilepsy: a common disorder identified in twins. Ann Neurol 40:227-35.

Berkovic SF, Scheffer IE (1997). Genetics of human partial epilepsy. Curr Opin Neurol 10:110-4.

Bertrand S, Weiland S, Berkovic SF, Steinlein OK, Bertrand D (1998). Properties of neuronal nicotinic acetylcholine receptor mutants from humans suffering from autosomal dominant nocturnal frontal lobe epilepsy. Br J Pharmacol 125:751-60.

Betz H (1990). Ligand-gated ion channels in the brain: the amino acid receptor superfamily. Neuron 5:383-92.

Betz H, Graham D, Rehm H (1982). Identification of polypeptides associated with a putative neuronal nicotinic acetylcholine receptor. J Biol Chem 257:11390-4.

Bitner RS, Nikkel AL, Curzon P, Arneric SP, Bannon AW, Decker MW (1998). Role of the nucleus raphe magnus in antinociception produced by ABT- 594: immediate early gene responses possibly linked to neuronal nicotinic acetylcholine receptors on serotonergic neurons. J Neurosci 18:5426-32.

Boulter J, Connolly J, Deneris E, Goldman D, Heinemann S, Patrick J (1987). Functional expression of two neuronal nicotinic acetylcholine receptors from cDNA clones identifies a gene family. Proc Natl Acad Sci USA 84:7763-7.

Boulter J, Evans K, Goldman D, Martin G, Treco D, Heinemann S, Patrick J (1986). Isolation of a cDNA clone coding for a possible neural nicotinic acetylcholine receptor alpha-subunit. Nature 319:368-74.

Bowen DM, Smith CB, White P, Davison AN (1976). Neurotransmitter-related enzymes and indices of hypoxia in senile dementia and other abiotrophies. Brain 99:459-96.

Bradford HF (1995). Glutamate, GABA and epilepsy. Prog Neurobiol 47:477-511.

Brioni JD, Arneric SP (1993). Nicotinic receptor agonists facilitate retention of avoidance training: participation of dopaminergic mechanisms. Behav Neural Biol 59:57-62.

Brioni JD, Decker MW, Sullivan JP, Arneric SP (1997). The pharmacology of (-)-nicotine and novel cholinergic channel modulators. Adv Pharmacol 37:153-214.

Brioni JD, O'Neill AB, Kim DJ, Decker MW (1993). Nicotinic receptor agonists exhibit anxiolytic-like effects on the elevated plus-maze test. Eur J Pharmacol 238:1-8.

Britto LR, Keyser KT, Lindstrom JM, Karten HJ (1992). Immunohistochemical localization of nicotinic acetylcholine receptor subunits in the mesencephalon and diencephalon of the chick (Gallus gallus). J Comp Neurol 317:325-40.

Caggiula AR, Epstein LH, Perkins KA, Saylor S (1995). Different methods of assessing nicotine-induced antinociception may engage different neural mechanisms. Psychopharmacology (Berl) 122:301-6.

Cao W, Burkholder T, Wilkins L, Collins AC (1993). A genetic comparison of behavioural actions of ethanol and nicotine in the mirrored chamber. Pharmacol Biochem Behav 45:803-9.

Capecchi MR (1989a). Altering the genome by homologous recombination. Science 244:1288-92.

Capecchi MR (1989b). The new mouse genetics: altering the genome by gene targeting. Trends Genet 5:70-6.

Chambon P (1998). Spatio-temporally-controlled somatic mutations in the mouse. Pathol Biol (Paris) 46:671-3.

Changeux JP, Galzi JL, Devillers-Thiery A, Bertrand D (1992). The functional architecture of the acetylcholine nicotinic receptor explored by affinity 'abelling and site-directed mutagenesis. Q Rev Biophys 25:395-432.

Chavez-Noriega LE, Crona JH, Washburn MS, Urrutia A, Elliott KJ, Johnson EC (1997). Pharmacological characterization of recombinant human neuronal nicotinic acetylcholine receptors h alpha 2 beta 2, h alpha 2 beta 4, h alpha 3 beta 2, h alpha 3 beta 4, h alpha 4 beta 2, h alpha 4 beta 4 and h alpha 7 expressed in Xenopus oocytes. J Pharmacol Exp Ther 280:346-56.

Cherny NI (1996). Opioid analgesics: comparative features and prescribing guidelines. Drugs 51:713-37.

Christensen MK, Smith DF (1990). Antinociceptive effects of the stereoisomers of

nicotine given intrathecally in spinal rats. J Neural Transm Gen Sect 80:189-94.

Clarke PB (1990). Mesolimbic dopamine activation--the key to nicotine reinforcement?

Ciba Found Symp 152:153-62.

Clarke PB, Kumar R (1983). The effects of nicotine on locomotor activity in non-

tolerant and tolerant rats. Br J Pharmacol 78:329-37.

Clarke PB, Pert A (1985). Autoradiographic evidence for nicotine receptors on

nigrostriatal and mesolimbic dopaminergic neurons. Brain Res 348:355-8.

Clarke PB, Schwartz RD, Paul SM, Pert CB, Pert A (1985). Nicotinic binding in rat

brain: autoradiographic comparison of [3H]acetylcholine, [3H]nicotine, and

[125I]-alpha-bungarotoxin. J Neurosci 5:1307-15.

Clifford JJ, Tighe O, Croke DT, Kinsella A, Sibley DR, Drago J and Waddington JL

(1999) Conservation of behavioural topography to dopamine D1-like receptor

agonists in mutant mice lacking the D1A receptor implicates a D1-like receptor

not coupled to adenylyl cyclase [In Process Citation]. Neuroscience 93:1483-

1489.

Clifford JJ, Tighe O, Croke DT, Sibley DR, Drago J and Waddington JL (1998)

Topographical evaluation of the phenotype of spontaneous behaviour in mice with

targeted gene deletion of the D1A dopamine receptor: paradoxical elevation of

grooming syntax. Neuropharmacology 37: 595-1602.

Clifford JJ and Waddington JL (1998) Heterogeneity of behavioural profile between

three new putative selective D3 dopamine receptor antagonists using an ethologically

based approach. Psychopharmacology (Berl) 136:284-290.

Collins RC, McLean M, Olney J (1980). Cerebral metabolic response to systemic kainic

acid: ^{14}C-deoxyglucose studies. Life Sci, 27:855-62.

Colquhoun LM, Patrick JW (1997). Alpha3, beta2, and beta4 form heterotrimeric

    neuronal nicotinic acetylcholine receptors in Xenopus oocytes. J Neurochem

    69:2355-62.

Conroy WG, Vernallis AB, Berg DK (1992). The alpha 5 gene product assembles with

    multiple acetylcholine receptor subunits to form distinctive receptor subtypes in

    brain. Neuron 9:679-91.

Conti-Tronconi BM, Dunn SM, Barnard EA, Dolly JO, Lai FA, Ray N, Raftery MA

    (1985). Brain and muscle nicotinic acetylcholine receptors are different but

    homologous proteins. Proc Natl Acad Sci USA 82:5208-12.

Cooper E, Couturier S, Ballivet M (1991). Pentameric structure and subunit

    stoichiometry of a neuronal nicotinic acetylcholine receptor. Nature 350:235-8.

Corda MG, Giorgi O, Longoni B, Orlandi M,Biggio G (1990). Decrease in the function

    of the gamma-aminobutyric acid-coupled chloride channel produced by the

    repeated administration of pentylenetetrazol to rats. J Neurochem 55:1216-21.

Corringer PJ, Galzi JL, Eisele JL, Bertrand S, Changeux JP,Bertrand D (1995).

    Identification of a new component of the agonist binding site of the nicotinic

    alpha 7 homooligomeric receptor. J Biol Chem 270:11749-52.

Costall B, Kelly ME, Naylor RJ,Onaivi ES (1989). The actions of nicotine and cocaine

    in a mouse model of anxiety. Pharmacol Biochem Behav 33:197-203.

Couturier S, Bertrand D, Matter JM, Hernandez MC, Bertrand S, Millar N, Valera S,

    Barkas T,Ballivet M (1990a). A neuronal nicotinic acetylcholine receptor

    subunit (alpha 7) is developmentally regulated and forms a homo-oligomeric

    channel blocked by alpha-BTX. Neuron 5:847-56.

Couturier S, Erkman L, Valera S, Rungger D, Bertrand S, Boulter J, Ballivet

    M,Bertrand D (1990b). Alpha 5, alpha 3, and non-alpha 3. Three clustered avian

genes encoding neuronal nicotinic acetylcholine receptor-related subunits. J Biol Chem 265:17560-7.

Crabbe JC, Janowsky JS, Young ER,Rigter H (1980). Handling induced convulsions in twenty inbred strains of mice. Subst Alcohol Actions Misuse 1:159-63.

Crawley J,Goodwin FK (1980). Preliminary report of a simple animal behaviour model for the anxiolytic effects of benzodiazepines. Pharmacol Biochem Behav 13:167-70.

Crawley JN (1996). Unusual behavioural phenotypes of inbred mouse strains. Trends Neurosci 19:181-2; discussion 188-9.

Cross SA (1994). Pathophysiology of pain [see comments]. Mayo Clin Proc 69:375-83.

Croucher MJ, Bradford HF, Sunter DC, Watkins JC (1988). Inhibition of the development of electrical kindling of the prepyriform cortex by daily focal injections of excitatory amino acid antagonists. Eur J Pharmacol 152:29-38.

Crusio WE (1996). The neurobehavioural genetics of aggression. Behav Genet 26:459-61.

Damaj MI, Fei-Yin M, Dukat M, Glassco W, Glennon RA, Martin BR (1998). Antinociceptive responses to nicotinic acetylcholine receptor ligands after systemic and intrathecal administration in mice. J Pharmacol Exp Ther 284:1058-65.

Damaj MI, Glennon RA, Martin BR (1994). Involvement of the serotonergic system in the hypoactive and antinociceptive effects of nicotine in mice. Brain Res Bull 33:199-203.

Damsma G, Day J, Fibiger HC (1989). Lack of tolerance to nicotine-induced dopamine release in the nucleus accumbens. Eur J Pharmacol 168:363-8.

Davenport KE, Houdi AA, Van Loon GR (1990). Nicotine protects against mu-opioid

    receptor antagonism by beta- funaltrexamine: evidence for nicotine-induced

    release of endogenous opioids in brain. Neurosci Lett 113:40-6.

Davies P, Maloney AJ (1976). Selective loss of central cholinergic neurons in

    Alzheimer's disease [letter]. Lancet 2:1403.

Davis KL, Mohs RC, Tinklenberg JR, Pfefferbaum A, Hollister LE, Kopell BS (1978).

    Physostigmine: improvement of long-term memory processes in normal humans.

    Science 201:272-4.

de Belleroche JS, Bradford HF (1980). Presynaptic control of the synthesis and release

    of dopamine from striatal synaptosomes: a comparison between the effects of 5-

    hydroxytryptamine, acetylcholine, and glutamate. J Neurochem 35:1227-34.

Decker MW, Bannon AW, Buckley MJ, Kim DJ, Holladay MW, Ryther KB, Lin NH,

    Wasicak JT, Williams M, Arneric SP (1998). Antinociceptive effects of the

    novel neuronal nicotinic acetylcholine receptor agonist, ABT-594, in mice. Eur J

    Pharmacol 346:23-33.

Decker MW, Brioni JD, Bannon AW, Arneric SP (1995). Diversity of neuronal

    nicotinic acetylcholine receptors: lessons from behaviour and implications for

    CNS therapeutics. Life Sci 56:545-70.

Decker MW, Brioni JD, Sullivan JP, Buckley MJ, Radek RJ, Raszkiewicz JL, Kang

    CH, Kim DJ, Giardina WJ, Wasicak JT (1994). (S)-3-methyl-5-(1-methyl-2-

    pyrrolidinyl) isoxazole (ABT 418): a novel cholinergic ligand with cognition-

    enhancing and anxiolytic activities: II. In vivo characterization. J Pharmacol Exp

    Ther 270:319-28.

Decker MW, Majchrzak MJ (1992). Effects of systemic and intracerebroventricular

administration of mecamylamine, a nicotinic cholinergic antagonist, on spatial

memory in rats. Psychopharmacology 107:530-4.

Deneris ES, Boulter J, Swanson LW, Patrick J, Heinemann S (1989). Beta 3: a new

member of nicotinic acetylcholine receptor gene family is expressed in brain. J

Biol Chem 264:6268-72.

Deneris ES, Connolly J, Rogers SW, Duvoisin R (1991). Pharmacological and

functional diversity of neuronal nicotinic acetylcholine receptors. Trends

Pharmacol Sci 12:34-40.

Deutch AY, Holliday J, Roth RH, Chun LL, Hawrot E (1987). Immunohistochemical

localization of a neuronal nicotinic acetylcholine receptor in mammalian brain.

Proc Natl Acad Sci U S A 84:8697-701.

Devillers-Thiery A, Galzi JL, Bertrand S, Changeux JP, Bertrand D (1992). Stratified

organization of the nicotinic acetylcholine receptor channel. Neuroreport

3:1001-4.

Devillers-Thiery A, Galzi JL, Eisele JL, Bertrand S, Bertrand D, Changeux JP (1993).

Functional architecture of the nicotinic acetylcholine receptor: a prototype of

ligand-gated ion channels. J Membr Biol 136:97-112.

Dineley-Miller K, Patrick J (1992). Gene transcripts for the nicotinic acetylcholine

receptor subunit, beta4, are distributed in multiple areas of the rat central

nervous system. Brain Res Mol Brain Res 16:339-44.

Dominguez del Toro E, Juiz JM, Peng X, Lindstrom J, Criado M (1994).

Immunocytochemical localization of the alpha 7 subunit of the nicotinic

acetylcholine receptor in the rat central nervous system. J Comp Neurol

349:325-42.

Drago J, Gerfen CR, Lachowicz JE, Steiner H, Hollon TR, Love PE, Ooi GT, Grinberg A, Lee EJ, Huang SP (1994). Altered striatal function in a mutant mouse lacking D1A dopamine receptors. Proc Natl Acad Sci U S A 91:12564-8.

Drago J, Padungchaichot P, Accili D, Fuchs S (1998). Dopamine receptors and dopamine transporter in brain function and addictive behaviours: insights from targeted mouse mutants. Dev Neurosci, 20:188-203.

Drago J, Padungchaichot P, Wong JY, Lawrence AJ, McManus JF, Sumarsono SH, Natoli AL, Lakso M, Wreford N, Westphal H, Kola I, Finkelstein DI (1998). Targeted expression of a toxin gene to D1 dopamine receptor neurons by cre-mediated site-specific recombination. J Neurosci 18:9845-57.

Duvoisin RM, Deneris ES, Patrick J, Heinemann S (1989). The functional diversity of the neuronal nicotinic acetylcholine receptors is increased by a novel subunit: beta -4. Neuron 3:487-96.

Elgoyhen AB, Johnson DS, Boulter J, Vetter DE, Heinemann S (1994). Alpha 9: an acetylcholine receptor with novel pharmacological properties expressed in rat cochlear hair cells. Cell 79:705-15.

Favreau P, Le Gall F, Benoit E, Molgo J (1999). A review on conotoxins targeting ion channels and acetylcholine receptors of the vertebrate neuromuscular junction. Acta Physiol Pharmacol Ther Latinoam 49:257-67.

Fenster CP, Rains MF, Noerager B, Quick MW and Lester RA (1997) Influence of subunit composition on desensitization of neuronal acetylcholine receptors at low concentrations of nicotine. J Neurosci 17:5747-5759.

Ferraro TN, Golden GT, Smith GG, St Jean P, Schork NJ, Mulholland N, Ballas C, Schill J, Buono RJ, Berrettini WH (1999). Mapping loci for pentylenetetrazol-induced seizure susceptibility in mice. J Neurosci 19:6733-9.

File SE, Hyde JR, MacLeod NK (1979). 5,7-dihydroxytryptamine lesions of dorsal and

> median raphe nuclei and performance in the social interaction test of anxiety and
>
> in a home- cage aggression test. J Affect Disord 1:115-22.

Fischer JF,Cho AK (1979). Chemical release of dopamine from striatal homogenates:

> evidence for an exchange diffusion model. J Pharmacol Exp Ther 208:203-9.

Fisher RS (1989). Animal models of the epilepsies. Brain Res Brain Res Rev 14:245-

> 78.

Flavin HJ, Wieraszko A, Seyfried TN (1991). Enhanced aspartate release from

> hippocampal slices of epileptic (El) mice. J Neurochem 56:1007-11.

Flores CM, DeCamp RM, Kilo S, Rogers SW, Hargreaves KM (1996). Neuronal

> nicotinic receptor expression in sensory neurons of the rat trigeminal ganglion:
>
> demonstration of alpha3beta4, a novel subtype in the mammalian nervous
>
> system. J Neurosci 16:7892-901.

Flores CM, Rogers SW, Pabreza LA, Wolfe BB, Kellar KJ (1992). A subtype of

> nicotinic cholinergic receptor in rat brain is composed of alpha 4 and beta 2
>
> subunits and is up-regulated by chronic nicotine treatment. Mol Pharmacol
>
> 41:31-7.

Forsayeth JR, Kobrin E (1997). Formation of oligomers containing the beta3 and beta4

> subunits of the rat nicotinic receptor. J Neurosci 17:1531-8.

Frankel WN, Valenzuela A, Lutz CM, Johnson EW, Dietrich WF, Coffin JM (1995).

> New seizure frequency QTL and the complex genetics of epilepsy in EL mice.
>
> Mamm Genome 6:830-8.

Franklin KBJ and Paxinos G (1997) The Mouse Brain in Stereotaxic Coordinates.

Freeman GB, Sherman KA, Gibson GE (1987). Locomotor activity as a predictor of times and dosages for studies of nicotine's neurochemical actions. Pharmacol Biochem Behav 26:305-12.

Freund RK, Marley RJ, Wehner JM (1987). Differential sensitivity to bicuculline in three inbred mouse strains. Brain Res Bull 18:657-62.

Fucile S, Barabino B, Palma E, Grassi F, Limatola C, Mileo AM, Alema S, Ballivet M, Eusebi F (1997). Alpha 5 subunit forms functional alpha 3 beta 4 alpha 5 nAChRs in transfected human cells. Neuroreport 8:2433-6.

Fucile S, Matter JM, Erkman L, Ragozzino D, Barabino B, Grassi F, Alema S, Ballivet M, Eusebi F (1998). The neuronal alpha6 subunit forms functional heteromeric acetylcholine receptors in human transfected cells. Eur J Neurosci 10:172-8.

Galzi JL, Revah F, Bessis A, Changeux JP (1991). Functional architecture of the nicotinic acetylcholine receptor: from electric organ to brain. Annu Rev Pharmacol Toxicol 31:37-72.

Gerlai R (1996). Gene-targeting studies of mammalian behaviour: is it the mutation or the background genotype? [see comments] [published erratum appears in Trends Neurosci 1996 Jul;19(7):271]. Trends Neurosci 19:177-81.

Giacobini E (1991). Nicotinic cholinergic receptors in human brain: effects of aging and Alzheimer. Adv Exp Med Biol 296:303-15.

Gilbert DG (1979). Paradoxical tranquilizing and emotion-reducing effects of nicotine. Psychol Bull 86:643-61.

Gilbert DG, Robinson JH, Chamberlin CL, Spielberger CD (1989). Effects of smoking/nicotine on anxiety, heart rate, and lateralization of EEG during a stressful movie. Psychophysiology 26:311-20.

Gioanni Y, Rougeot C, Clarke PB, Lepouse C, Thierry AM, Vidal C (1999). Nicotinic

    receptors in the rat prefrontal cortex: increase in glutamate release and

    facilitation of mediodorsal thalamo-cortical transmission. Eur J Neurosci, 11:18-

    30.

Giorguieff MF, Le Floc'h ML, Westfall TC, Glowinski J, Besson MJ (1976). Nicotinic

    effect of acetylcholine on the release of newly synthesized (3H)dopamine in rat

    striatal slices and cat caudate nucleus. Brain Res 106:117-31.

Giorguieff-Chesselet MF, Kemel ML, Wandscheer D, Glowinski J (1979). Regulation

    of dopamine release by presynaptic nicotinic receptors in rat striatal slices: effect

    of nicotine in a low concentration. Life Sci 25:1257-62.

Goddard GV, McIntyre DC, Leech CK (1969). A permanent change in brain function

    resulting from daily electrical stimulation. Exp Neurol 25:295-330.

Gopalakrishnan M, Buisson B, Touma E, Giordano T, Campbell JE, Hu IC, Donnelly-

    Roberts D, Arneric SP, Bertrand D, Sullivan JP (1995). Stable expression and

    pharmacological properties of the human alpha 7 nicotinic acetylcholine

    receptor. Eur J Pharmacol 290:237-46.

Gopalakrishnan M, Monteggia LM, Anderson DJ, Molinari EJ, Piattoni-Kaplan M,

    Donnelly-Roberts D, Arneric SP, Sullivan JP (1996). Stable expression,

    pharmacologic properties and regulation of the human neuronal nicotinic

    acetylcholine alpha 4 beta 2 receptor. J Pharmacol Exp Ther 276:289-97.

Grady S, Marks MJ, Wonnacott S, Collins AC (1992). Characterization of nicotinic

    receptor-mediated [3H]dopamine release from synaptosomes prepared from

    mouse striatum. J Neurochem 59:848-56.

Groot-Kormelink PJ, Luyten WH, Colquhoun D, Sivilotti LG (1998). A reporter mutation approach shows incorporation of the "orphan" subunit beta3 into a functional nicotinic receptor. J Biol Chem 273:15317-20.

Hanley MR, Eterovic VA, Hawkes SP, Hebert AJ, Bennett EL (1977). Neurotoxins of Bungarus multicinctus vernom. Purification and partial characterization. Biochemistry 16:5840-9.

Happe HK, Peters JL, Bergman DA, Murrin LC (1994). Localization of nicotinic cholinergic receptors in rat brain: autoradiographic studies with [3H]cytisine. Neuroscience 62:929-44.

Hasty P, Rivera-Perez J, Bradley A (1991). The length of homology required for gene targeting in embryonic stem cells. Mol Cell Biol 11:5586-91.

Hauser WA, Annegers JF, Kurland LT (1993). Incidence of epilepsy and unprovoked seizures in Rochester, Minnesota: 1935-1984. Epilepsia 34:453-68.

Hill JA, Jr., Zoli M, Bourgeois JP, Changeux JP (1993). Immunocytochemical localization of a neuronal nicotinic receptor: the beta 2-subunit. J Neurosci 13:1551-68.

Hilleman DE, Mohiuddin SM, Del Core MG and Sketch MH, Sr. (1992) Effect of buspirone on withdrawal symptoms associated with smoking cessation. Arch Intern Med 152:350-352.

Hirose S, Iwata H, Akiyoshi H, Kobayashi K, Ito M, Wada K, Kaneko S, Mitsudome A (1999). A novel mutation of CHRNA4 responsible for autosomal dominant nocturnal frontal lobe epilepsy. Neurology 53:1749-53.

Hosford DA, Clark S, Cao Z, Wilson WA, Jr., Lin FH, Morrisett RA, Huin A (1992). The role of GABAB receptor activation in absence seizures of lethargic (lh/lh) mice. Science 257:398-401.

Hughes JR (1992) Tobacco withdrawal in self-quitters. J Consult Clin Psychol 60:689-697.

Hughes JR, Gust SW, Skoog K, Keenan RM and Fenwick JW (1991) Symptoms of tobacco withdrawal. A replication and extension. Arch Gen Psychiatry 48:52-59.

Hughes JR and Hatsukami D (1986) Signs and symptoms of tobacco withdrawal. Arch Gen Psychiatry 43:289-294.

Hughes JR, Higgins ST and Bickel WK (1994) Nicotine withdrawal versus other drug withdrawal syndromes: similarities and dissimilarities. Addiction 89:1461-1470.

Hussy N, Ballivet M, Bertrand D (1994). Agonist and antagonist effects of nicotine on chick neuronal nicotinic receptors are defined by alpha and beta subunits. J Neurophysiol 72:1317-26.

Hutchinson RR, Emley GS (1973). *In "Smoking Behaviour: Motives and Incentives"*. Washington, DC: Winston & Sons.

Ishida N, Kasamo K, Nakamoto Y, Suzuki J (1993). Epileptic seizure of El mouse initiates at the parietal cortex: depth EEG observation in freely moving condition using buffer amplifier. Brain Res 608:52-7.

Iwamoto ET (1989). Antinociception after nicotine administration into the mesopontine tegmentum of rats: evidence for muscarinic actions. J Pharmacol Exp Ther 251:412-21.

Iwamoto ET (1991). Characterization of the antinociception induced by nicotine in the pedunculopontine tegmental nucleus and the nucleus raphe magnus. J Pharmacol Exp Ther 257:120-33.

Jones GM, Sahakian BJ, Levy R, Warburton DM, Gray JA (1992). Effects of acute subcutaneous nicotine on attention, information processing and short-term memory in Alzheimer's disease. Psychopharmacology 108:485-94.

Jorenby DE, Hatsukami DK, Smith SS, Fiore MC, Allen S, Jensen J and Baker TB
(1996) Characterization of tobacco withdrawal symptoms: transdermal nicotine
reduces hunger and weight gain. Psychopharmacology (Berl) 128:130-138.

Joyner AL (2000). *Gene Targeting: A practical approach.* Oxford: Oxford, University
Press.

Joyner AL, Guillemot F (1994). Gene targeting and development of the nervous system.
Curr Opin Neurobiol 4:37-42.

Kandel ER, Schwartz, JH, Jessell T.M. (1991). *Principles of Neural Science*: Appleton
& Lange.

Kawase E, Suemori H, Takahashi N, Okazaki K, Hashimoto K, Nakatsuji N (1994).
Strain difference in establishment of mouse embryonic stem (ES) cell lines. Int J
Dev Biol 38:385-90.

Kayadjanian N, Retaux S, Menetrey A, Besson MJ (1994). Stimulation by nicotine of
the spontaneous release of [3H]gamma-aminobutyric acid in the substantia nigra
and in the globus pallidus of the rat. Brain Res 649:129-35.

Keyser KT, Britto LR, Schoepfer R, Whiting P, Cooper J, Conroy W, Brozozowska-
Prechtl A, Karten HJ, Lindstrom J (1993). Three subtypes of alpha-
bungarotoxin-sensitive nicotinic acetylcholine receptors are expressed in chick
retina. J Neurosci 13:442-54.

Koller BH, Smithies O (1992). Altering genes in animals by gene targeting. Annu Rev
Immunol 10:705-30.

Kuhn R, Schwenk F, Aguet M, Rajewsky K (1995). Inducible gene targeting in mice.
Science 269:1427-9.

Kulak JM, Nguyen TA, Olivera BM, McIntosh JM (1997). Alpha-conotoxin MII blocks nicotine-stimulated dopamine release in rat striatal synaptosomes. J Neurosci 17:5263-70.

Kurokawa M, Naruse H, Kato M (1966). Metabolic studies on ep mouse, a special strain with convulsive predisposition. Prog Brain Res 21:112-29.

Kuryatov A, Gerzanich V, Nelson M, Olale F, Lindstrom J (1997). Mutation causing autosomal dominant nocturnal frontal lobe epilepsy alters Ca2+ permeability, conductance, and gating of human alpha4beta2 nicotinic acetylcholine receptors. J Neurosci 17:9035-47.

Lader M (1990). Drug development optimization--benzodiazepines. Agents Actions Suppl 29:59-69.

Le Novere N,Changeux JP (1995). Molecular evolution of the nicotinic acetylcholine receptor: an example of multigene family in excitable cells. J Mol Evol 40:155-72.

Le Novere N, Zoli M, Changeux JP (1996). Neuronal nicotinic receptor alpha 6 subunit mRNA is selectively concentrated in catecholaminergic nuclei of the rat brain. Eur J Neurosci 8:2428-39.

Ledermann B, Burki K (1991). Establishment of a germ-line competent C57BL/6 embryonic stem cell line. Exp Cell Res 197:254-8.

Lena C, Changeux JP, Mulle C (1993). Evidence for nicotinic receptors on GABAergic axons in the rat interpeduncular nucleus. J Neurosci 13:2680-8.

Leonard RJ, Labarca CG, Charnet P, Davidson N, Lester HA (1988). Evidence that the M2 membrane-spanning region lines the ion channel pore of the nicotinic receptor. Science 242:1578-81.

Levin ED, Briggs SJ, Christopher NC, Rose JE (1992). Persistence of chronic nicotine-

induced cognitive facilitation. Behav Neural Biol 58:152-8.

Lister RG (1987). The use of a plus-maze to measure anxiety in the mouse.

Psychopharmacology 92:180-5.

Loring RH, Aizenman E, Lipton SA, Zigmond RE (1989). Characterization of nicotinic

receptors in chick retina using a snake venom neurotoxin that blocks neuronal

nicotinic receptor function. J Neurosci 9:2423-31.

Lothman EW, Collins RC (1981). Kainic acid induced limbic seizures: metabolic,

behavioural, electroencephalographic and neuropathological correlates. Brain Res,

218:299-318.

Lothman EW, Collins RC, Ferrendelli JA (1981). Kainic acid-induced limbic seizures:

electrophysiologic studies. Neurology, 31:806-12.

Luetje CW, Patrick J (1991). Both alpha- and beta-subunits contribute to the agonist

sensitivity of neuronal nicotinic acetylcholine receptors. J Neurosci 11:837-45.

Luetje CW, Wada K, Rogers S, Abramson SN, Tsuji K, Heinemann S, Patrick J (1990).

Neurotoxins distinguish between different neuronal nicotinic acetylcholine

receptor subunit combinations. J Neurochem 55:632-40.

Macdonald RL, McLean MJ (1986). Anticonvulsant drugs: mechanisms of action. Adv

Neurol, 44:713-36.

Malin DH, Lake JR, Carter VA, Cunningham JS, Wilson OB (1993). Naloxone

precipitates nicotine abstinence syndrome in the rat. Psychopharmacology

112:339-42.

Mansour SL, Thomas KR, Capecchi MR (1988). Disruption of the proto-oncogene int-2

in mouse embryo-derived stem cells: a general strategy for targeting mutations

to non-selectable genes. Nature 336:348-52.

Marescaux C, Micheletti G, Vergnes M, Depaulis A, Rumbach L, Warter JM (1984). A model of chronic spontaneous petit mal-like seizures in the rat: comparison with pentylenetetrazol-induced seizures. Epilepsia, 25:326-31.

Marien M, Brien J, Jhamandas K (1983). Regional release of [3H]dopamine from rat brain in vitro: effects of opioids on release induced by potassium, nicotine, and L-glutamic acid. Can J Physiol Pharmacol 61:43-60.

Marks MJ, Pauly JR, Gross SD, Deneris ES, Hermans-Borgmeyer I, Heinemann SF, Collins AC (1992). Nicotine binding and nicotinic receptor subunit RNA after chronic nicotine treatment. J Neurosci 12:2765-84.

Marks MJ, Stitzel JA, Romm E, Wehner JM, Collins AC (1986). Nicotinic binding sites in rat and mouse brain: comparison of acetylcholine, nicotine, and alpha-bungarotoxin. Mol Pharmacol 30:427-36.

Marley RJ, Gaffney D, Wehner JM (1986). Genetic influences on GABA-related seizures. Pharmacol Biochem Behav 24:665-72.

Marley RJ, Wehner JM (1987). Correlation between the enhancement of flunitrazepam binding by GABA and seizure susceptibility in mice. Life Sci 40:2215-24.

Marshall E (1997). The mouse that prompted a roar [news] [see comments]. Science 277:24-5.

Martin TJ, Suchocki J, May EL, Martin BR (1990). Pharmacological evaluation of the antagonism of nicotine's central effects by mecamylamine and pempidine. J Pharmacol Exp Ther 254:45-51.

Marubio LM, del Mar Arroyo-Jimenez M, Cordero-Erausquin M, Lena C, Le Novere N, de Kerchove d'Exaerde A, Huchet M, Damaj MI, Changeux JP (1999). Reduced antinociception in mice lacking neuronal nicotinic receptor subunits. Nature 398:805-10.

Mash DC, Flynn DD, Potter LT (1985). Loss of M2 muscarine receptors in the cerebral cortex in Alzheimer's disease and experimental cholinergic denervation. Science 228:1115-7.

Mason CR, Cooper RM (1972). A permanent change in convulsive threshold in normal and brain-damaged rats with repeated small doses of pentylenetetrazol. Epilepsia 13:663-74.

Mason WT (1985). Staining of the magnocellular nuclei of the rat hypothalamus by a monoclonal antibody directed against the alpha-subunit of the nicotinic cholinergic receptor. Neurosci Lett 59:89-95.

McCarrick JWd, Parnes JR, Seong RH, Solter D, Knowles BB (1993). Positive-negative selection gene targeting with the diphtheria toxin A-chain gene in mouse embryonic stem cells. Transgenic Res 2:183-90.

McGehee DS, Role LW (1995). Physiological diversity of nicotinic acetylcholine receptors expressed by vertebrate neurons. Annu Rev Physiol 57:521-46.

McKenna JP and Cox JL (1992) Transdermal nicotine replacement and smoking cessation. Am Fam Physician 45:2595-2602.

McMahon AP, Bradley A (1990). The Wnt-1 (int-1) proto-oncogene is required for development of a large region of the mouse brain. Cell 62:1073-85.

McMahon LL, Yoon KW, Chiappinelli VA (1994). Nicotinic receptor activation facilitates GABAergic neurotransmission in the avian lateral spiriform nucleus. Neuroscience 59:689-98.

Medvedev A, Mackenzie L, Hiscock JJ, Willoughby JO (2000). Kainic acid induces distinct types of epileptiform discharge with differential involvement of hippocampus and neocortex. Brain Res Bull, 52:89-98.

Meyer EM, Tay ET, Papke RL, Meyers C, Huang GL, de Fiebre CM (1997). 3-[2,4-
Dimethoxybenzylidene] anabaseine (DMXB) selectively activates rat alpha7
receptors and improves memory-related behaviours in a mecamylamine-
sensitive manner. Brain Res 768:49-56.

Mori N, Singer-Sam J, Lee CY, Riggs AD (1986). The nucleotide sequence of a cDNA
clone containing the entire coding region for mouse X-chromosome-linked
phosphoglycerate kinase. Gene 45:275-80.

Mulle C, Sailer A, Perez-Otano I, Dickinson-Anson H, Castillo PE, Bureau I, Maron C,
Gage FH, Mann JR, Bettler B, Heinemann SF (1998). Altered synaptic
physiology and reduced susceptibility to kainate-induced seizures in GluR6-
deficient mice. Nature 392:601-5.

Nadler JV (1981). Minireview. Kainic acid as a tool for the study of temporal lobe
epilepsy. Life Sci, 29:2031-42.

Nagy A, Rossant J, Nagy R, Abramow-Newerly W, Roder JC (1993). Derivation of
completely cell culture-derived mice from early-passage embryonic stem cells.
Proc Natl Acad Sci U S A 90:8424-8.

Nanri M, Kasahara N, Yamamoto J, Miyake H, Watanabe H (1998). A comparative
study on the effects of nicotine and GTS-21, a new nicotinic agonist, on the
locomotor activity and brain monoamine level. Jpn J Pharmacol 78:385-9.

Nebert DW, Duffy JJ (1997). How knockout mouse lines will be used to study the role
of drug- metabolizing enzymes and their receptors during reproduction and
development, and in environmental toxicity, cancer, and oxidative stress.
Biochem Pharmacol 53:249-54.

Nef P, Oneyser C, Alliod C, Couturier S, Ballivet M (1988). Genes expressed in the brain define three distinct neuronal nicotinic acetylcholine receptors. Embo J 7:595-601.

Newhouse PA, Sunderland T, Tariot PN, Blumhardt CL, Weingartner H, Mellow A, Murphy DL (1988). Intravenous nicotine in Alzheimer's disease: a pilot study. Psychopharmacology 95:171-5.

Nickel E, Potter LT (1973). Ultrastructure of isolated membranes of Torpedo electric tissue. Brain Res 57:508-17.

Noebels JL (1996). Targeting epilepsy genes. Neuron 16:241-4.

Noebels JL, Qiao X, Bronson RT, Spencer C, Davisson MT (1990). Stargazer: a new neurological mutant on chromosome 15 in the mouse with prolonged cortical seizures [published erratum appears in Epilepsy Res 1992 Mar;11(1):72]. Epilepsy Res 7:129-35.

Noebels JL, Sidman RL (1979). Inherited epilepsy: spike-wave and focal motor seizures in the mutant mouse tottering. Science 204:1334-6.

Nordberg A, Winblad B (1986). Reduced number of [3H]nicotine and [3H]acetylcholine binding sites in the frontal cortex of Alzheimer brains. Neurosci Lett 72:115-9.

Nowakowska E, Chodera A and Kus K (1997) Pharmacological aspects of withdrawal from certain benzodiazepines. Pol J Pharmacol 49:89-95.

Olney JW, Rhee V, Ho OL (1974). Kainic acid: a powerful neurotoxic analogue of glutamate. Brain Res 77:507-12.

Olsen RW (1981). GABA-benzodiazepine-barbiturate receptor interactions. J Neurochem 37:1-13.

O'Neill AB, Brioni JD (1994). Benzodiazepine receptor mediation of the anxiolytic-like effect of (-)- nicotine in mice. Pharmacol Biochem Behav 49:755-7.

Orr-Urtreger A, Goldner FM, Saeki M, Lorenzo I, Goldberg L, De Biasi M, Dani JA, Patrick JW, Beaudet AL (1997). Mice deficient in the alpha7 neuronal nicotinic acetylcholine receptor lack alpha-bungarotoxin binding sites and hippocampal fast nicotinic currents. J Neurosci 17:9165-71.

Papke RL (1993). The kinetic properties of neuronal nicotinic receptors: genetic basis of functional diversity. Prog Neurobiol 41:509-31.

Papke RL, Boulter J, Patrick J, Heinemann S (1989). Single-channel currents of rat neuronal nicotinic acetylcholine receptors expressed in Xenopus oocytes. Neuron 3:589-96.

Pauly JR, Stitzel JA, Marks MJ, Collins AC (1989). An autoradiographic analysis of cholinergic receptors in mouse brain. Brain Res Bull 22:453-9.

Perry DC, Kellar KJ (1995). [3H]epibatidine labels nicotinic receptors in rat brain: an autoradiographic study. J Pharmacol Exp Ther 275:1030-4.

Perry EK, Tomlinson BE, Blessed G, Bergmann K, Gibson PH, Perry RH (1978). Correlation of cholinergic abnormalities with senile plaques and mental test scores in senile dementia. Br Med J 2:1457-9.

Picciotto MR, Caldarone BJ, King SL and Zachariou V (2000) Nicotinic receptors in the brain. Links between molecular biology and behaviour. Neuropsychopharmacology 22:451-465.

Picciotto MR, Zoli M, Lena C, Bessis A, Lallemand Y, LeNovere N, Vincent P, Pich EM, Brulet P, Changeux JP (1995). Abnormal avoidance learning in mice lacking functional high-affinity nicotine receptor in the brain. Nature 374:65-7.

Picciotto MR, Zoli M, Rimondini R, Lena C, Marubio LM, Pich EM, Fuxe K, Changeux JP (1998). Acetylcholine receptors containing the beta2 subunit are involved in the reinforcing properties of nicotine. Nature 391:173-7.

Pinel JP, Rovner LI (1978). Experimental epileptogenesis: kindling-induced epilepsy in rats. Exp Neurol 58:190-202.

Pomerleau OF (1986). Nicotine as a psychoactive drug: anxiety and pain reduction. Psychopharmacol Bull 22:865-9.

Porter JT, Cauli B, Tsuzuki K, Lambolez B, Rossier J, Audinat E (1999). Selective excitation of subtypes of neocortical interneurons by nicotinic receptors. J Neurosci, 19:5228-35.

Porter RJ, Cereghino JJ, Gladding GD, Hessie BJ, Kupferberg HJ, Scoville B, White BG (1984). Antiepileptic Drug Development Program. Cleve Clin Q 51:293-305.

Potter H, Weir L, Leder P (1984). Enhancer-dependent expression of human kappa immunoglobulin genes introduced into mouse pre-B lymphocytes by electroporation. Proc Natl Acad Sci USA 81:7161-5.

Purpura DP, Penry, JK Woodbury, DM, Tower DB, Walter, RD (1972). *Experimental models of epilepsy - A manual for the laboratory worker*. New York: Raven.

Qian C, Li T, Shen TY, Libertine-Garahan L, Eckman J, Biftu TI (1993). Epibatidine is a nicotinic analgesic. Eur J Pharmacol 250:R13-4.

Radcliffe KA, Dani JA (1998). Nicotinic stimulation produces multiple forms of increased glutamatergic synaptic transmission. J Neurosci, 18:7075-83.

Raiteri M, Cerrito F, Cervoni AM,Levi G (1979). Dopamine can be released by two mechanisms differentially affected by the dopamine transport inhibitor nomifensine. J Pharmacol Exp Ther 208:195-202.

Ramanjaneyulu R, Ticku MK (1984). Interactions of pentamethylenetetrazole and tetrazole analogues with the picrotoxinin site of the benzodiazepine-GABA receptor-ionophore complex. Eur J Pharmacol, 98:337-45.

Ramirez-Latorre J, Yu CR, Qu X, Perin F, Karlin A, Role L (1996). Functional contributions of alpha5 subunit to neuronal acetylcholine receptor channels. Nature 380:347-51.

Rao TS, Correa LD, Reid RT, Lloyd GK (1996). Evaluation of anti-nociceptive effects of neuronal nicotinic acetylcholine receptor (NAChR) ligands in the rat tail-flick assay. Neuropharmacology 35:393-405.

Rapier C, Lunt GG, Wonnacott S (1988). Stereoselective nicotine-induced release of dopamine from striatal synaptosomes: concentration dependence and repetitive stimulation. J Neurochem 50:1123-30.

Rapier C, Lunt GG, Wonnacott S (1990). Nicotinic modulation of [3H]dopamine release from striatal synaptosomes: pharmacological characterisation. J Neurochem 54:937-45.

Rise ML, Frankel WN, Coffin JM, Seyfried TN (1991). Genes for epilepsy mapped in the mouse. Science 253:669-73.

Robertson EJ (1987). *In teratocarcinomas and embryonic stem cells : a practical approach.* Oxford: IRL Press.

Robinson TE, Becker JB (1986). Enduring changes in brain and behaviour produced by chronic amphetamine administration: a review and evaluation of animal models of amphetamine psychosis. Brain Res 396:157-98.

Rogers DT, Iwamoto ET (1993). Multiple spinal mediators in parenteral nicotine-induced antinociception. J Pharmacol Exp Ther 267:341-9.

Rogers SW, Gahring LC, Collins AC, Marks M (1998). Age-related changes in neuronal nicotinic acetylcholine receptor subunit alpha4 expression are modified by long-term nicotine administration. J Neurosci 18:4825-32.

Role LW, Berg DK (1996). Nicotinic receptors in the development and modulation of CNS synapses. Neuron 16:1077-85.

Ross SA, Wong JY, Clifford JJ, Kinsella A, Massalas JS, Horne MK, Scheffer IE, Kola I, Waddington JL, Berkovic SF, Drago J (2000). Phenotypic characterization of an alpha 4 neuronal nicotinic acetylcholine receptor subunit knock-out mouse. J Neurosci, 20:6431-41.

Rupniak NM, Patel S, Marwood R, Webb J, Traynor JR, Elliott J, Freedman SB, Fletcher SR, Hill RG (1994). Antinociceptive and toxic effects of (+)-epibatidine oxalate attributable to nicotinic agonist activity. Br J Pharmacol 113:1487-93.

Sachin N. Pradhan RPM, Samar N. Dutta (1986). *Pharmacology in Medicine: Principles and Practice*. Maryland: SP Press International.

Sahley TL, Berntson GG (1979). Antinociceptive effects of central and systemic administrations of nicotine in the rat. Psychopharmacology (Berl) 65:279-83.

Sakurai Y, Takano Y, Kohjimoto Y, Honda K,Kamiya HO (1982). Enhancement of [3H]dopamine release and its [3H]metabolites in rat striatum by nicotinic drugs. Brain Res 242:99-106.

Sambrook J, Fritsch, EF and Maniatis, T. (1989). *Molecular cloning: A laboratory manual,*. New York: Cold Spring Habour Laboratory Press.

Sargent PB (1993). The diversity of neuronal nicotinic acetylcholine receptors. Annu Rev Neurosci 16:403-43.

Scheffer IE, Bhatia KP, Lopes-Cendes I, Fish DR, Marsden CD, Andermann E, Andermann F, Desbiens R, Keene D, Cendes F (1995a). Autosomal dominant nocturnal frontal lobe epilepsy. A distinctive clinical disorder. Brain 118:61-73.

Scheffer IE, Bhatia KP, Lopes-Cendes I, Fish DR, Marsden CD, Andermann F, Andermann E, Desbiens R, Cendes F, Manson J! (1994). Autosomal dominant frontal epilepsy misdiagnosed as sleep disorder. Lancet 343:515-7.

Scheffer IE, Jones L, Pozzebon M, Howell RA, Saling MM, Berkovic SF (1995b). Autosomal dominant rolandic epilepsy and speech dyspraxia: a new syndrome with anticipation. Ann Neurol 38:633-42.

Schneider NG, Olmstead RE, Steinberg C, Sloan K, Daims RM and Brown HV (1996) Efficacy of buspirone in smoking cessation: a placebo-controlled trial. Clin Pharmacol Ther 60:568-575.

Schoepfer R, Conroy WG, Whiting P, Gore M, Lindstrom J (1990). Brain alpha-bungarotoxin binding protein cDNAs and MAbs reveal subtypes of this branch of the ligand-gated ion channel gene superfamily. Neuron 5:35-48.

Schroder H, Zilles K, Maelicke A, Hajos F (1989). Immunohisto- and cytochemical localization of cortical nicotinic cholinoceptors in rat and man. Brain Res 502:287-95.

Schulz DW, Loring RH, Aizenman E, Zigmond RE (1991). Autoradiographic localization of putative nicotinic receptors in the rat brain using 125I-neuronal bungarotoxin. J Neurosci 11:287-97.

Schulz DW, Zigmond RE (1989). Neuronal bungarotoxin blocks the nicotinic stimulation of endogenous dopamine release from rat striatum. Neurosci Lett 98:310-6.

Schwartz RD, Lehmann J, Kellar KJ (1984). Presynaptic nicotinic cholinergic receptors labeled by [3H]acetylcholine on catecholamine and serotonin axons in brain. J Neurochem 42:1495-8.

Sedivy JM, Joyner, A.L (1992). *Gene targeting*. New York: W.H. Freeman and Company.

Seguela P, Wadiche J, Dineley-Miller K, Dani JA, Patrick JW (1993). Molecular cloning, functional properties, and distribution of rat brain alpha 7: a nicotinic cation channel highly permeable to calcium. J Neurosci 13:596-604.

Seyfried TN, Glaser GH (1985). A review of mouse mutants as genetic models of epilepsy. Epilepsia 26:143-50.

Seyfried TN, Yu RK, Glaser GH (1980). Genetic analysis of audiogenic seizure susceptibility in C57BL/6J X DBA/2J recombinant inbred strains of mice. Genetics 94:701-18.

Shader RI, Greenblatt DJ (1993). Use of benzodiazepines in anxiety disorders [see comments]. N Engl J Med 328:1398-405.

Shin C, McNamara JO (1994). Mechanism of epilepsy. Annu Rev Med 45:379-89.

Shiffman S, Johnston JA, Khayrallah M, Elash CA, Gwaltney CJ, Paty JA, Gnys M, Evoniuk G and DeVeaugh-Geiss J (2000) The effect of bupropion on nicotine craving and withdrawal. Psychopharmacology (Berl) 148:33-40.

Smith AG, Heath JK, Donaldson DD, Wong GG, Moreau J, Stahl M, Rogers D (1988). Inhibition of pluripotential embryonic stem cell differentiation by purified polypeptides. Nature 336:688-90.

Spande TF, Garraffo HM, Yeh HJ, Pu QL, Pannell LK, Daly JW (1992). A new class of alkaloids from a dendrobatid poison frog: a structure for alkaloid 251F. J Nat Prod 55:707-22.

Squires RF, Saederup E, Crawley JN, Skolnick P, Paul SM (1984). Convulsant

potencies of tetrazoles are highly correlated with actions on

GABA/benzodiazepine/picrotoxin receptor complexes in brain. Life Sci

35:1439-44.

Steinlein OK, Magnusson A, Stoodt J, Bertrand S, Weiland S, Berkovic SF, Nakken

KO, Propping P, Bertrand D (1997). An insertion mutation of the CHRNA4

gene in a family with autosomal dominant nocturnal frontal lobe epilepsy. Hum

Mol Genet 6:943-7.

Steinlein OK, Mulley JC, Propping P, Wallace RH, Phillips HA, Sutherland GR,

Scheffer IE, Berkovic SF (1995). A missense mutation in the neuronal nicotinic

acetylcholine receptor alpha 4 subunit is associated with autosomal dominant

nocturnal frontal lobe epilepsy. Nat Genet 11:201-3.

Stolerman IP, Fink R, Jarvik ME (1973). Acute aшd chronic tolerance to nicotine

measured by activity in rats. Psychopharmacologia 30:329-42.

Sugaya E, Ishige A, Sekiguchi K, Iizuka S, Ito K, Sugimoto A, Aburada M, Hosoya E

(1986). Pentylenetetrazol-induced convulsion and effect of anticonvulsants in

mutant inbred strain El mice. Epilepsia 27:354-8.

Sullivan JP, Decker MW, Brioni JD, Donnelly-Roberts D, Anderson DJ, Bannon AW,

Kang CH, Adams P, Piattoni-Kaplan M, Buckley MJ (1994). (+/-)-Epibatidine

elicits a diversity of in vitro and in vivo effects mediated by nicotinic

acetylcholine receptors. J Pharmacol Exp Ther 271:624-31.

Suzuki J (1976). Paroxysmal discharges in the electroencephalogram of the El mouse.

Experientia 32:336-8.

Swanson LW, Simmons DM, Whiting PJ, Lindstrom J (1987). Immunohistochemical
    localization of neuronal nicotinic receptors in the rodent central nervous system.
    J Neurosci 7:3334-42.

Takano Y, Sakurai Y, Kohjimoto Y, Honda K, Kamiya HO (1983). Presynaptic
    modulation of the release of dopamine from striatal synaptosomes: differences
    in the effects of high K+ stimulation, methamphetamine and nicotinic drugs.
    Brain Res 279:330-4.

Thomas KR, Capecchi MR (1987). Site-directed mutagenesis by gene targeting in
    mouse embryo-derived stem cells. Cell 51:503-12.

Tripathi HL, Martin BR, Aceto MD (1982). Nicotine-induced antinociception in rats
    and mice: correlation with nicotine brain levels. J Pharmacol Exp Ther 221:91-
    6.

Tsien JZ, Chen DF, Gerber D, Tom C, Mercer EH, Anderson DJ, Mayford M, Kandel
    ER, Tonegawa S (1996). Subregion- and cell type-restricted gene knockout in
    mouse brain. Cell 87:1317-26.

Tybulewicz VL, Crawford CE, Jackson PK, Bronson RT, Mulligan RC (1991).
    Neonatal lethality and lymphopenia in mice with a homozygous disruption of
    the c-abl proto-oncogene. Cell 65:1153-63.

Upchurch M, Wehner JM (1988). Differences between inbred strains of mice in Morris
    water maze performance. Behav Genet 18:55-68.

Vernino S, Amador M, Luetje CW, Patrick J, Dani JA (1992). Calcium modulation and
    high calcium permeability of neuronal nicotinic acetylcholine receptors. Neuron
    8:127-34.

Vibat CR, Lasalde JA, McNamee MG and Ochoa EL (1995) Differential desensitization properties of rat neuronal nicotinic acetylcholine receptor subunit combinations expressed in Xenopus laevis oocytes. Cell Mol Neurobiol 15:411-425.

Wada E, McKinnon D, Heinemann S, Patrick J, Swanson LW (1990). The distribution of mRNA encoded by a new member of the neuronal nicotinic acetylcholine receptor gene family (alpha 5) in the rat central nervous system. Brain Res 526:45-53.

Wada E, Wada K, Boulter J, Deneris E, Heinemann S, Patrick J, Swanson LW (1989). Distribution of alpha 2, alpha 3, alpha 4, and beta 2 neuronal nicotinic receptor subunit mRNAs in the central nervous system: a hybridization histochemical study in the rat. J Comp Neurol 284:314-35.

Wada K, Ballivet M, Boulter J, Connolly J, Wada E, Deneris ES, Swanson LW, Heinemann S, Patrick J (1988). Functional expression of a new pharmacological subtype of brain nicotinic acetylcholine receptor. Science 240:330-4.

Wahlsten D, Bulman-Fleming B (1994). Retarded growth of the medial septum: a major gene effect in acallosal mice. Brain Res Dev Brain Res 77:203-14.

Wahlsten D, Schalomon PM (1994). A new hybrid mouse model for agenesis of the corpus callosum. Behav Brain Res 64:111-7.

Waldman AS, Liskay RM (1988). Dependence of intrachromosomal recombination in mammalian cells on uninterrupted homology. Mol Cell Biol 8:5350-7.

Wang F, Gerzanich V, Wells GB, Anand R, Peng X, Keyser K, Lindstrom J (1996). Assembly of human neuronal nicotinic receptor alpha5 subunits with alpha3, beta2, and beta4 subunits. J Biol Chem 271:17656-65.

Warpman U, Nordberg A (1995). Epibatidine and ABT 418 reveal selective losses of alpha 4 beta 2 nicotinic receptors in Alzheimer brains. Neuroreport 6:2419-23.

Weiland S, Witzemann V, Villarroel A, Propping P, Steinlein O (1996). An amino acid exchange in the second transmembrane segment of a neuronal nicotinic receptor causes partial epilepsy by altering its desensitization kinetics. FEBS Lett 398:91-6.

Westfall TC (1974). Effect of nicotine and other drugs on the release of 3H-norepinephrine and 3H-dopamine from rat brain slices. Neuropharmacology 13:693-700.

Westfall TC, Anderson GP (1967). Influence of nicotine on catecholamine metabolism in the rat. Arch Int Pharmacodyn Ther 169:421-8.

Westfall TC, Perry H (1986). The nicotinic-induced release of endogenous dopamine from rat striatal slices from animals chronically exposed to dimethylphenylpiperazinium (DMPP). Neurosci Lett 71:340-4.

White HS (1999). Comparative anticonvulsant and mechanistic profile of the established and newer antiepileptic drugs. Epilepsia 40:S2-10.

Whitehouse PJ, Martino AM, Antuono PG, Lowenstein PR, Coyle JT, Price DL, Kellar KJ (1986). Nicotinic acetylcholine binding sites in Alzheimer's disease. Brain Res 371:146-51.

Whiting P, Lindstrom J (1987). Purification and characterization of a nicotinic acetylcholine receptor from rat brain. Proc Natl Acad Sci USA 84:595-9.

Whiting PJ,Lindstrom JM (1986). Purification and characterization of a nicotinic acetylcholine receptor from chick brain. Biochemistry 25:2082-93.

Whiting PJ, Lindstrom JM (1988). Characterization of bovine and human neuronal nicotinic acetylcholine receptors using monoclonal antibodies. J Neurosci 8:3395-404.

Whiting PJ, Schoepfer R, Swanson LW, Simmons DM, Lindstrom JM (1987).

Functional acetylcholine receptor in PC12 cells reacts with a monoclonal

antibody to brain nicotinic receptors. Nature 327:515-8.

Wiles MV, Keller G (1991). Multiple hematopoietic lineages develop from embryonic

stem (ES) cells in culture. Development 111:259-67.

Williams RL, Hilton DJ, Pease S, Willson TA, Stewart CL, Gearing DP, Wagner EF,

Metcalf D, Nicola NA, Gough NM (1988). Myeloid leukaemia inhibitory factor

maintains the developmental potential of embryonic stem cells. Nature 336:684-

7.

Willoughby JO, Mackenzie L, Medvedev A, Hiscock JJ (1997). Fos induction following

systemic kainic acid: early expression in hippocampus and later widespread

expression correlated with seizure. Neuroscience, 77:379-92.

Wisden W, Seeburg PH (1993). A complex mosaic of high-affinity kainate receptors in

rat brain. J Neurosci, 13:3582-98.

Wong ET, Holstad SG, Mennerick SJ, Hong SE, Zorumski CF, Isenberg KE (1995).

Pharmacological and physiological properties of a putative ganglionic nicotinic

receptor, alpha 3 beta 4, expressed in transfected eucaryotic cells. Brain Res Mol

Brain Res 28:101-9.

Wong JY, Liberatore GT, Donnan GA and Howells DW (1997) Expression of brain-

derived neurotrophic factor and TrkB neurotrophin receptors after striatal injury

in the mouse. Exp Neurol 148:83-91.

Wonnacott S (1997). Presynaptic nicotinic ACh receptors. Trends Neurosci 20:92-8.

Xu W, Gelber S, Orr-Urtreger A, Armstrong D, Lewis RA, Ou CN, Patrick J, Role L,

De Biasi M and Beaudet AL (1999) Megacystis, mydriasis, and ion channel

defect in mice lacking the alpha3 neuronal nicotinic acetylcholine receptor. Proc
Natl Acad Sci USA 96:5746-5751.

Yaksh TL (1997). Pharmacology and mechanisms of opioid analgesic activity. Acta
Anaesthesiol Scand 41:94-111.

Yang DD, Kuan CY, Whitmarsh AJ, Rincon M, Zheng TS, Davis RJ, Rakic P, Flavell
RA (1997). Absence of excitotoxicity-induced apoptosis in the hippocampus of mice
lacking the Jnk3 gene. Nature, 389:865-70.

Zarrindast MR, Farzin D (1996). Nicotine attenuates naloxone-induced jumping
behaviour in morphine- dependent mice. Eur J Pharmacol 298:1-6.

Zarrindast MR, Nami AB, Farzin D (1996). Nicotine potentiates morphine
antinociception: a possible cholinergic mechanism. Eur Neuropsychopharmacol
6:127-33.

Zoli M, Picciotto MR, Ferrari R, Cocchi D, Changeux JP (1999). Increased
neurodegeneration during ageing in mice lacking high-affinity nicotine
receptors. Embo J 18:1235-44.